Utilizing 3-D and 4-D ultrasound systems to improve radiation treatment of cervix and prostate cancer patients.

Baker, Mariwan

Publication date:
2015

Document Version
Publisher's PDF, also known as Version of record

PhD Thesis

Utilizing 3-D and 4-D ultrasound systems to improve radiation treatment of cervix and prostate cancer patients

Mariwan Baker

Supervised by: Senior Researcher, PhD. Claus E. Andersen, Honorary Assoc. Prof., PhD. Claus F. Behrens, and Prof., PhD. Jørgen Arendt Jensen.

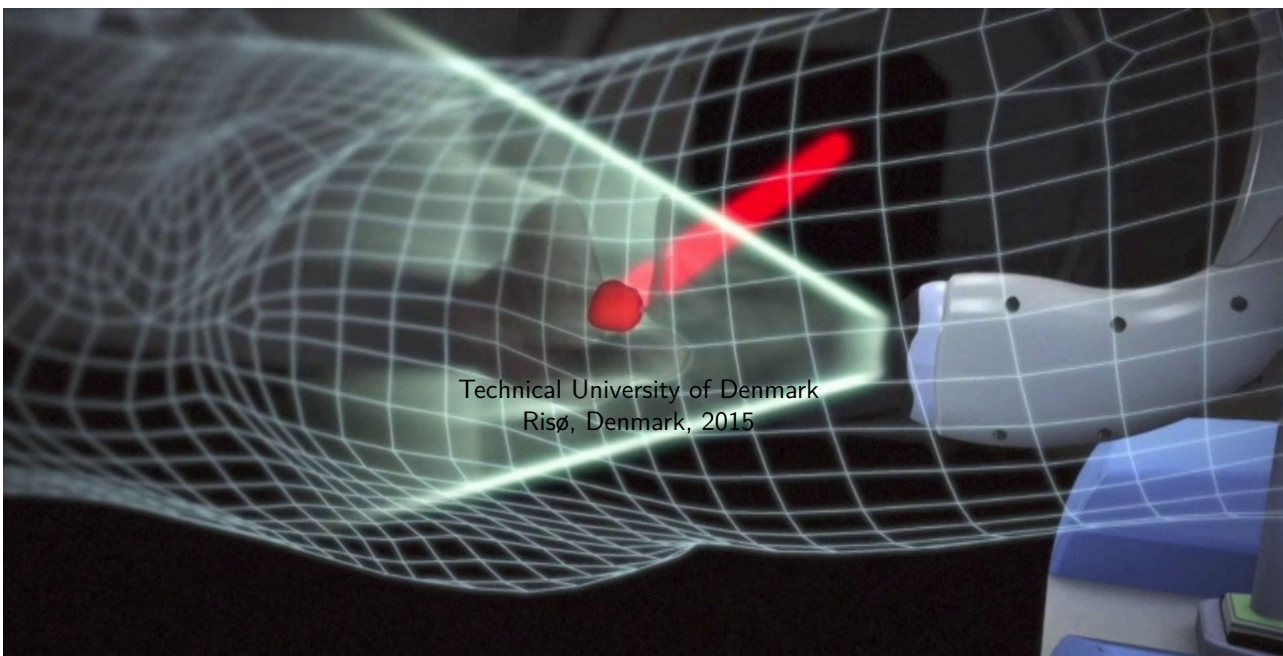

Technical University of Denmark
Risø, Denmark, 2015

Cover image: Ultrasound autoscan probe monitoring prostate. By Elekta Ltd.

Technical University of Denmark (DTU)
Center for Nuclear Technologies
Risø Campus, Build. 201
DK-4000 Roskilde
DENMARK
Author e-mail: baker@dtu.dk
Tel: (+46) 76 190 9108

Herlev Hospital, University of Copenhagen
Department of Oncology (R)
Radiotherapy Research Unit (52AA)
Herlev Ringvej 75
DK-2730 Herlev
DENMARK

Contents

Summary

Radiotherapy plays an important role in modern treatment for cancer, such as cervical and prostate radiation treatment. One of the major issue in radiotherapy is that the target should be aligned to the planned target volume prior to each treatment fraction, for which different kilovoltage (kV) and megavoltage (MV) image guided radiotherapy (IGRT) methods are developed. However, these ionization systems provide poor visualization of soft tissue, and therefore the bone matching is frequently applied as a daily tumor alignment method in cervical radiotherapy. In this project, the Clarity 3D ultrasound system, non-invasive, non-ionizing, and good in visualization soft tissue, was used to apply uterine matching for determining the uterine shifts relative to the bone structure. The main purpose was to investigate the reliability of the Clarity system as a possible IGRT method. We found that the conventional probe (C-probe) has limitations, while applying transabdominal US (TAUS) scan, when it came to capturing the entire uterus owing to the difficulty in probe handling. Contrarily, the novel autoscan-probe (A-probe) was shown to be capable of capturing the entire uterus in almost all of the scans. The operators found the A-probe to be more user-friendly, and image acquisition was also performed more smoothly. In conclusion the A-probe is a more reliable IGRT tool, and it might replace the kV- and the MV IGRT systems.

In prostate radiotherapy, the movement of the prostate during radiation delivery (intrafractional prostate motion) remains challenging. To determine the intrafractional prostate motion, various imaging techniques have been introduced, such as kV, and MV imaging, CineMRI, implanted markers and transponders. Most of the systems are based on acquiring pre- and posttreatment images, which has limitations in addressing real-time prostate motion, and includes inter-observer variations while matching image to image.
In this project, the recently developed transperineal ultrasound 4D autoscan probe is used to investigate the real-time prostate monitoring. The purpose of this study was to investigate the feasibility of the 4D autoscan in tracking the prostate for a duration of 2 to 2.5 minutes.
We found that most of the intrafractional prostate motion is less than 2 mm, which was in concordance with previously reported data. Thus, during a RapidArc/VMAT plan delivery with a beam-on time of approximately 2.5 minutes, the intrafractional prostate motion is negligible. But, since the prostate motion increases with monitoring time, the prostate

displacement during 3D conformal and IMRT plans must be taken into consideration. Additionally, we conducted a prostate probe pressure study, in which TAUS scan was simulated, using a C-probe, while the prostate was continuously monitored using the TPUS autoscan. We found that the TAUS induced pressure displacement of the prostate, in most cases, was clinically irrelevant. Since this conclusion was in opposition to most of the previously published results, which reported displacements of up to 7 mm, we discovered that 4D real-time monitoring is the most reliable method for determining the pressure displacement compared to US/US or US/CT matching methods, in which the considerable inter-observer variability, due to variations in applied probe pressure and image/image match, limits the accuracy of the readings.

Resumé

(Summary in Danish)

Stråleterapi spiller en vigtig rolle i kræftbehandling. I moderne stråleterapi, kan der opnås en høj dosis i tumor. Det er derfor vigtigt, at man kender den eksakte placering af kræftknuden og de omkringliggende risikoorganer i forbindelse med behandlingen. For at kunne identificere tumorens beliggenhed præcist og for at reducere medbestrålingen af raskt normalvæv, bruges daglig billedvejledt strålebehandling, "Image Guided Radiation Therapy" (IGRT). IGRT kan fx være et sæt ortogonale kilovolt (kV) eller megavolt (MV), 2D kontrolbilleder. Men disse billed-metoder har begrænset visualisering af bløddelsvæv, såsom livmoder, blære eller rektum. Således udføres ofte dagligt match på knoglestrukturer i stedet for direkte match på tumorvæv. Der er derfor et ønske at tilføje ultralyd som et nyt IGRT system, hvilket nu er muligt med Clarity systemet. Clarity systemet, som hverken er invasivt eller ioniserende, er et relativt billigt billedverifikations system, som er velegnet til bl.a. visualisering af bløddelsvæv i det kvindelige bækken. Der er dog forskellige udfordringer med brugen af ultralyd-systemet, såsom transducer-tryk, billedtolkning og inter-operatør variabilitet.
Hovedformålet med dette projekt er at undersøge muligheden for at bruge Clarity som IGRT-metode for at identificere den daglige positionelle variation af livmoderen.
Vi fandt, at den konventionelle probe (C-proben) har begrænsninger således at det er svært at skanne hele livmoderen ved anvendelse af transabdominal ultralydsskanning (TAUS), på grund af vanskeligheder med probe håndteringen. Autoscan-transduceren (A-probe) viste sig imidlertid at være i stand til at skanne hele livmoderen i næsten alle skanningsforsøg. Operatørerne fandt at A-proben var mere brugervenlig, og at billedoptagelse også udføres mere smidigt, med brug af mindre transducer-tryk. Afslutningsvis: A-proben er et mere pålideligt IGRT værktøj end C-proben, og den kan formentligt erstatte kV- og MV IGRT systemer.

Ved prostata strålebehandling er bevægelighed af prostata under bestråling (intrafraktionelle prosata bevægelse) stadig en udfordring. For at bestemme den intrafraktionelle bevægelse har forskellige IGRT systemer været indført, såsom røntgenbilleder (kV og MV), CineMRI, "in-room" CT og implanterede markører og "transponders". De fleste af disse systemer er baseret på før- og efter behandling billedtagning, som har begrænsninger i at identificere prostatabevægelse i "real time". En anden ulempe er inter-observatør variationer ved billed-match.

For nyligt udviklede Clarity et produkt (transperineal ultralyd 4D autoscan probe (TPUS)) til at kunne overvåge prostata under bestråling. Prostataforskydning har vist sig at øges med strålingsvarigheden, hvilket betyder at størrelsen af forskydningen afhænger af behandlingstiden. På Herlev hospital, får alle prostata patienter RapidArc behandling, hvilket indebærer en bestrålingstid på ca. 2,5 minutter sammenlignet med op til 10 minutter ved anvendelse af en konventionel ”konform” plan eller en IMRT behandling. Formålet med dette studie er at undersøge gennemførligheden af Clarity 4D autoscan til at følge prostata i 2 til 2,5 minut.
Vi fandt, at de fleste intrafraktionelle prostatabevægelser er mindre end 2 mm, hvilket var i god overensstemmelse med tidligere rapporterede data. Dette betyder at, ved brug af RapidArc er den intrafraktionelle prostata bevægelse ofte ubetydelig. Hvis man behandler med konventionel stråleterapi eller IMRT , bør der tages hensyn til prostataforskydningen. Desuden gennemførte vi et transducer-tryk-studie, hvor TAUS skanning blev simuleret ved hjælp af en C-probe, mens prostata kontinuert blev overvåget ved hjælp af TPUS autoscan.
Vi fandt, at froskydningen af prostate som følge af C-probens tryk i de fleste tilfælde er klinisk ubetydelig. Dette resultat var i modsætning til de tidligere offentliggjorte resultater, hvor der er rapporteret forskydninger på op til 7 mm. Vi konkluderede at 4D autoscan overvågning er en pålidelig metode til at bestemme forskydning som følge af probe-tryk.

Preface

This PhD thesis has been submitted to the Department of Nuclear Technologies, Technical University of Denmark, DTU Risø in fulfillment of the requirements for acquiring the PhD degree.

The research work has carried out at the department of Radiotherapy Research Unit (R.R.U.), Herlev Hospital (HH), University of Copenhagen from September 2012 to November 2015. Research has also conducted at the Center for Fast Ultrasound Imaging (CFU), Department of Electrical Engineering, located at the Technical University of Denmark (DTU), Lyngby. This thesis deals with the implementation of three dimensional (3D) ultrasound imaging to determine inter-fractional uterine displacement of cervical cancer patients, and acquiring real-time four dimensional (4D) imaging of prostate cancer patients to investigate the extent of the prostate motion during radiation delivery (intra-fractional motion). The research described herein was conducted under the supervision of Senior Researcher, PhD, Claus E. Andersen, DTU, and co-supervised by Honorary Associate Professor, PhD, Medical Physicist, Claus F. Behrens, HH, and Professor, PhD, Jørgen Arendt Jensen, DTU.

The project was funded by HH, which was granted by Elekta, according to the Elekta Research Grant Program.

Mariwan Baker
Copenhagen, November 2015

Acknowledgements

First and foremost I want to thank my supervisor Claus E. Andersen at DTU Nutech. It has been an honor to be his PhD student. Claus has been very supportive, and has given me the freedom to pursue various projects. He has also provided insightful discussions about the research. I am also very grateful to PhD supervisor Claus F. Behrens at Herlev hospital for his scientific advice and knowledge and many insightful discussions and suggestions. He is my primary resource for getting my science questions answered and was instrumental in helping me complete this thesis. I will forever be thankful to my co-supervisor Jørgen Arendt Jensen at DTU CFU. I would like to thank him for encouraging my research and for allowing me to be a part of his group. I was lucky to be a part of their valuable Wednesday meetings.

I would especially like to thank our nurses; Lisa Gullander. (RTT), Stina K. Pedersen (RTT), Tina Zarp (RTT), Susanne Jacobsson (RTT), Siavash Pazhang (radiographer) and Vibe K. Lynnerup (radiographer) in the R.R.U. at Herlev Hospital. All of them were available to support me while they simultaneously recruited patients, planned imaging schedules, and gave me a continuous supply of information. Without their efforts I would not have been able to collect all the valuable patient data for my PhD thesis. THANK YOU!

I would also like to take the opportunity to give a heartfelt, special thanks to Brian Kristiansen for giving me the chance of winning a research position at Herlev hospital. I would like to express my special appreciation and thanks to my colleagues; Trine Juhler-Nøttrup and Henriette Lindberg, two oncologists in the oncology department (R) at Herlev hospital. They were a great help in preparing the protocols for this research project.

A special thanks is due to my family. Words cannot express how grateful I am to my wife, Karin Baker. Thank you for supporting me through everything, and in particular I cannot thank you enough for supporting me through this experience. I would like to express my thanks to my beloved daughters Hanna and Sara for being such good girls and always cheering me up. I also have to thank the other members of my family; my brothers, sisters, and mother. Thank you for your encouragement, support and most of all for your humor. You all kept things light-hearted and kept me smiling.

I gratefully acknowledge the financial support for this project from Elekta Ltd, Stockholm, Sweden.

I also thank my colleagues at Herlev hospital (too many to list here but you know who you are!) for providing the support and friendship that I needed. My gratitude is also extended to my colleagues at DTU, Lyngby and Risø. Thank you for your encouragement, support and most of all your humor.
Last, but certainly not least, I must acknowledge with tremendous and deep thanks my PhD colleagues with whom I shared offices at Herlev hospital.

List of Figures

List of Tables

Abbreviations

2-D	Two-Dimensional
3-D	Three-Dimensional
4-D	Real-time three-dimensional
I/S	Inferior Superior
A/P	Anterior Posterior
L/R	Left Right
AAPM	American Association of Physicists in Medicine
A-probe	Autoscan probe
CBCT	Cone Beam Computed Tomography
CI	Confidence Interval
COM	Center of Mass
CT	Computed Tomography
CTV	Clinical Target Volume
C-US probe	Conventional Ultrasound probe
DRRs	Digitally Reconstructed Radiographs
DTU	Danmarks Tekniske Universitet (Technical University of Denmark)
EPID	electronic portal imaging device
GYN	Gynaecology
HH	Herlev Hospital
IGRT	Image Guided Radiation Therapy
IMRT	Intensity-Modulated Radiotherapy
IRMER	The British Ionising Radiation Medical Exposure Regulations
kV	Kilo-Voltage
LINAC	Linear Accelerator
MHz	Mega Hertz
MRI	Magnetic Resonance Imaging
MV	Mega-Voltage
OARs	Organs At Risk
R.R.U.	Radiotherapy Research Unit
RTTs	Radiation Therapy Technologist
PRV	Position Reference Volume

PTV	Planning Target Volume
SD	Standard Deviation
TAUS	Transabdominal Ultrasound
TPUS	Transperineal Ultrasound
US	Ultrasound
VMAT	Volumetric Modulated Arc Therapy

CHAPTER 1

Introduction

1.1 Radiotherapy

Radiotherapy mainly uses high-energy photon or electron beams to kill tumor cells, by damaging the DNA chain, disabling the cells from reproducing themselves. Cancer cells are usually more sensitive to radiation since they divide more quickly than normal cells. The intention behind the application of radiation is either curative, curing the disease by eradicating the cancer cells, or palliative, relieving symptoms, such as pain or seizures, when the cancer has developed or spread (metastases). Radiotherapy, often in combination with either surgery or chemotherapy, or both, is an effective treatment method to eradicate the cancer cells. For instance, treatment of prostate and cervical cancer patients requires often external radiation, using linear accelerator machines (LINAC) (Fig. 1.1) and/or internal (Brachy) radioactive sources, to achieve an optimal outcome.

Since the cancer sites are usually surrounded by healthy tissues and normal organs (Organs at risk (OARs)), it is of the utmost importance that the OARs are protected from the prescribed radiation dose while the tumor is adequately covered, in order to minimize radiation complications, such as gastrointestinal toxicity in cervical radiotherapy (Salama et al. 2006). Since a course of treatment for cervical radiation can include 25 fractions, while for prostate cancer patients the sessions include up to 39 fractions, daily target positional variations (interfractional displacement) due to organ motion, tumor regressions, and setup variations, may occur. This positional uncertainty, for example for uterine position, can be as large as some centimeters (Chan et al. 2008). To minimize this uncertainty, daily target alignment is a necessity, and for this reason different daily pre-treatment verification imaging (Image Guided Radiation Therapy (IGRT)) modalities have been introduced into radiotherapy (Beadle et al. 2009; Chan et al. 2008; Kupelian et al. 2008; Langen and Jones 2001; Scarbrough et al. 2006), which makes it possible to correct misalignment, thereby improving the precision of the radiation treatment (Mackie et al. 2003).

Another challenge in radiotherapy is that during treatment delivery target displacement might occur (intrafractional displacement)(Ghilezan et al. 2005; Huang et al. 2002), which may lead to underdosage of the target (Kitamura 2002; H. Li et al. 2008). For instance, large prostate positional shifts have been observed, due to bladder filling variations, rectal volume changes, and respiratory motions (Dawson 2000; Herk 1995; Padhani 1999). To address the intrafractional uncertainty, different imaging modalities have been developed.

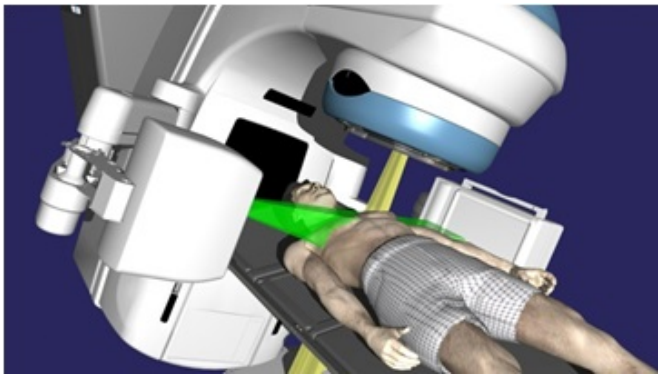

Figure 1.1: Linear accelerator (LINAC); Using high energy photon and electron beams (illustrated in yellow color) to irradiate the planned target, but verification imaging (illustrated in green color) prior to treatment delivery is necessary to correct for daily positional variations.

1.2 Image Guided Radiation Therapy (IGRT) of cervical cancer patients

In adaptive conformal radiotherapy with tight margins and steep dose gradients, such as intensity-modulated radiotherapy (IMRT), and volumetric modulated arc therapy (VMAT)/RapidArc, it is essential that the position of the clinical target volume (CTV) is precisely defined prior to each treatment fraction throughout the entire course of treatment. Recent technical innovations have enabled the direct integration of various image verification methods into clinical practice in radiotherapy. This allows uncertainty with patient and tumor positioning to be addressed and corrected. Different kilovoltage (kV) and megavoltage (MV) planar radiographic imaging (electronic portal imaging device (EPID)), and kV volumetric cone beam CT (CBCT) imaging are standard IGRT methods. However, these ionizing radiation systems have poor soft tissue visualization of the uterus of gynecological (GYN) cancer patients (Fig. 1.2). As a result, bone matching is frequently applied as a daily tumor alignment method in cervical cancer treatment. However, the weakness of employing bone-match is that it cannot take the relative uterine shift to the bone structure into consideration. Additionally, tumor regression might occur, with up to 80 % volume-reduction by the end of the treatment course (Beadle et al. 2009; Lim et al. 2008; Nam et al. 2007), which adversely impacts the precision of the target coverage and increment of the dose to the healthy tissues.

For GYN cancer patients, large margins are applied around the delineated gross tumor volume (GTV), to ensure target radiation dose coverage. The large margin is due to the complexity of the pelvis with its tumor and normal organ motion as well as deformational dynamics, which adversely impacts on the irradiated healthy tissues (Chan et al. 2008).

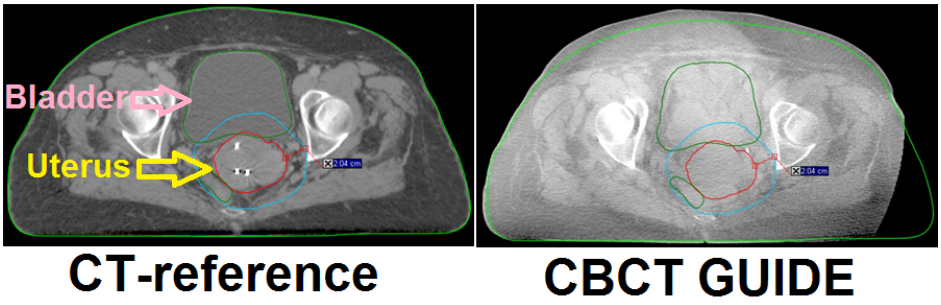

Figure 1.2: CT and CBCT images; CT-reference image, where soft tissue structures of uterus and bladder are easily recognizable, but in the acquired CBCT verification image the organs are barely identifiable.

Another method involves using implanted fiducial markers, readily identifiable in kV and MV verification imaging, as a surrogate (Heide et al. 2007; Litzenberg et al. 2002). Implanting fiducial markers in GYN radiotherapy has been found to be a substantial challenge (Kaatee et al. 2002; Lee et al. 2007; X. Li et al. 2007), because implanted fiducial markers can fall out, or be displaced due to tumor shrinkage and organ deformation. Another disadvantage of implanted fiducial markers is that they necessitate an invasive procedure, with an inherent risk of infection and discomfort to the patient, as well as a risk of fiducial migration, with consequent risk of misalignment during the course of treatment. On the other hand, MR imaging provides outstanding visualization of the uterus and cervix, enabling distinguishing them from other organs (Bunt et al. 2008). The application of MRI as IGRT requires MRI/LINAC accessibility, which is costly and rarely used clinically (Kerkhof et al. 2008; Lagendijk et al. 2008). Therefore, various 3D ultrasound (US) systems have been developed, such as the Clarity® Soft Tissue Visualization system (Clarity® Model 310C00, Elekta, Stockholm, Sweden) and the NOMOS B-mode Acquisition and Targeting (BAT) ultrasound system (Boda-Heggemann et al. 2008; Feigenberg et al. 2007). Both of these systems are based on 3D transabdominal US (3D-TAUS) scanning (Fig. 1.3). The Clarity system, for instance, is non invasive, non ionizing and cheap medical imaging technology. However, different uncertainty factors such as probe handling, image quality, and inter-operator variability are involved in the use of a US system.

1.3 Prostate monitoring

The movements of internal organs are one of the most challenging and unpredictable factors in delivering the prescribed radiation dose to the target in prostate cancer radiotherapy (Graham, Gee, and S.Hilton 2003; Meijer et al. 2003). This is mostly due to

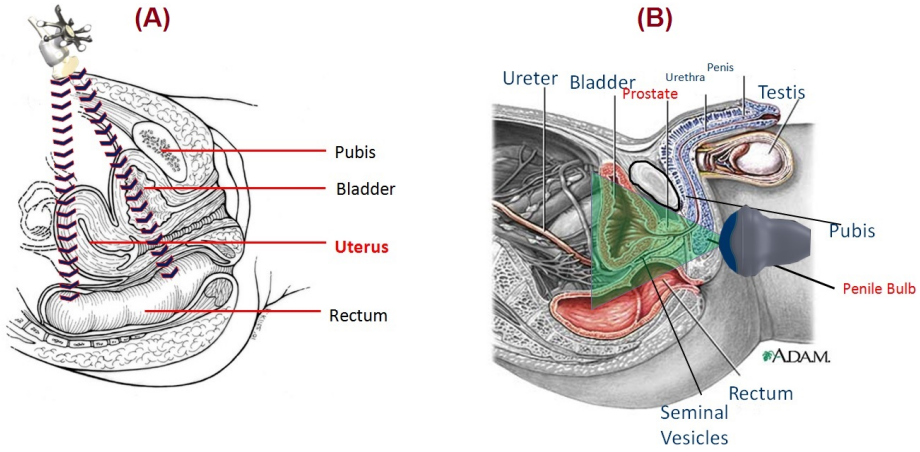

Figure 1.3: The Clarity 3D ultrasound imaging system; Based on **(A)** transabdominal uterine IGRT, and **(B)** transpernieal prostate monitoring.

variations in the volume and shape of rectum and bladder between consecutive fractions (interfractional) and during the delivery of radiation (intrafractional). Thus, interfractional movements emphasize the significance of accurate prostate localization prior to the delivery of radiation, and intrafractional prostate motion, on the other hand, refers to internal prostate displacement occurring during the actual delivery of treatment.

To determine the intrafractional prostate motion, various imaging techniques have been investigated in different studies, such as X-ray imaging, kilovoltage (kV) CBCT and megavoltage (MV) imaging, CineMRI, in-room CT, implanted markers and transponders, and ultrasound (Chan et al. 2008; Ghilezan et al. 2005; Mayyas et al. 2013; Tong et al. 2015). Most of the studies are based on acquiring pre- and post-treatment images (Adamson and Wu 2009; Kron et al. 2010). Furthermore, various techniques are developed to enable real-time online prostate localization and monitoring, such as: tracking implanted electromagnetic transponders (Calypso Medical Technologies, Seattle, WA), and tracking fiducial markers or implanted radioactive seeds (in Brachytherapy) using real-time X-ray imaging.
Recently, transperineal ultrasound (TPUS) auatoscan (Clarity®, Elekta, Stockholm, Sweden) (Fig. 1.3 B) has been developed to allow real-time prostate tracking (Lachaine and Falco 2013).
The relevance of addressing prostate motion during treatment delivery is dependent on the treatment time. With faster treatment techniques, such as VMAT or RapidArc® Radiotherapy Technology, as used at our institution, the magnitude of intrafractional prostate motion are reduced (J. Li et al. 2013; Mutanga et al. 2012).

1.4 Motivation and Objective

The overall objective of this project is to investigate the feasibility of the ultrasound systems to identify daily uterine positional variations, and to address the prostate motion during treatment delivery.

1.4.1 Clarity 3D ultrasound system as cervical IGRT system

The main purpose of the current study is to implement and evaluate the potential benefit of the new 3D ultrasound system during daily radiation treatment fractions of gynecological cancer patients.
The objective of the thesis is to confirm or deny its working hypothesis, that the Clarity 3D-TAUS, as a soft tissue uterine IGRT system, is a reliable method.

1.4.2 Clarity 4D ultrasound system as prostate tracking system

The aim is to investigate the feasibility of the clarity 4D ultrasound system for real-time prostate tracking during radiation delivery.
We hypothesize that prostate motion can be tracked with the 4D ultrasound probe, hence recording the magnitude and direction of prostate displacement in real time. As a result, the clinical consequences of this motion can be determined during VMAT/RapidArc radiation delivery.

1.5 Publications in the Thesis

This thesis is based on the 6 papers listed below, covering two main subjects: Interfractional uterine displacement, and intrafractional prostate motion. In the printed version of the thesis, the publications are included as separate appendix collection. The publication letters (A to F) refer to the appendix containing the corresponding paper.

Interfractional uterine displacement

Two conference papers and two journal papers cover implementing the 3D-US imaging of the cervix, focusing on phantom, volunteer, and patient studies.

Paper A

M. Baker, J. A. Jensen, and C. F. Behrens
"Inter-operator Variability in Defining Uterine Position Using Three-dimensional Ultrasound Imaging".
Published in: *Proceedings of IEEE Ultrason. Symp.*, pp. 848-851 (2013).

Paper B

M. Baker, J. A. Jensen, and C. F. Behrens
"Determining inter-fractional motion of the uterus using 3D ultrasound imaging during radiotherapy for cervical cancer".
Published in: *Proceedings of SPIE, the Medical Imaging 2014: Ultrasonic Imaging and Tomography.*,Vol. 9040 90400Y-1, (2014).

Paper C

M. Baker, T. Juhler-Nøttrup, and C. F. Behrens
"Impact of ultrasound probe pressure on uterine positional displacement in gynecologic cancer patients".
Published in: *Future Medicine Women's Health.*, Vol. , pp. 583-590, (2014).

Paper E

M. Baker, D. T. Cooper, and C. F. Behrens
"Evaluation of uterine ultrasound imaging in cervical radiotherapy; a comparison of autoscan and conventional probe".
Submitted (2015).

Intrafractional prostate motion

Two journal papers cover inrafractional prostate motion, using 4D TPUS system, and the prostate induced displacement during TAUS simulation, using 4D TPUS autoscan for real-time prostate monitoring.

Paper D

M. Baker, and C. F. Behrens
"Prostate displacement during transabdominal ultrasound image-guided radiotherapy assessed by real-time four-dimensional transperineal monitoring".
Published in: *Acta Oncologica* (2015).

Paper F

M. Baker, and C. F. Behrens
"Determining intrafractional prostate motion using four dimensional ultrasound system".
Submitted (2015).

1.6 Thesis Outline

In this work, the Clarity 3D-TAUS and 4D-TPUS systems are used as a platform to determine the daily displacements of the uterus, as well as intrafractional prostate motion.

Chapter 2 describes the Clarity ultrasound system, and provides details of the system's characteristics.

Chapter 3 covers interfractional uterine displacement during cervical radiotherapy. After a brief literature review, the principle behind using ultrasound as a new IGRT method is described. Initially, the implementation of the conventional 3D-TAUS probe is explained and the advantages and disadvantages of this probe are highlighted. Furthermore, the challenges in terms of image acquisition and image interpretation are discussed. Moreover, the potential utility of the system relative to other IGRT systems is debated. In addition, the obstacles to implementing the conventional probe in cervical radiotherapy are explained, based on phantom, volunteer and patient studies.
The chapter also covers the novel 3D-TAUS autoscan probe. The advantage of this probe over conventional ones is reported based on a volunteer study. Moreover, the capacity of this probe as cervical IGRT imaging modality is clarified according to feedback from the operators during a clinical study.

In Chapter 4, the focus is shifted towards the intrafractional prostate motion using 4D TPUS autoscan system. Firstly, a literature review shows previously used prostate tracking systems. Secondly, the magnitude of the intrafraction prostate motion, based on a clinical study, is determined for a monitoring duration of 2-2.5 minutes, a typical beam-on time required to deliver a VMAT/RapidArc fraction.
The chapter encompasses also the challenges in using conventional 3D TAUS probe, in the term of impact of probe pressure in prostate displacement. The magnitude of the induced prostate displacement is addressed based on a clinical paper.

The thesis is concluded in Chapter 5, where suggestions for future research are also provided.

The aim with the chapters is to highlight basic information of the Clarity system and key results from the project. Additional details can be found in the original paper manuscripts, which are provided in the appendix section.

CHAPTER 2

The Clarity 3D-TAUS and 4D-TPUS systems

The division of radiotherapy at Herlev hospital is a large site, where over 3 000 cancer patients receiving radiation treatment annually, using nine LINACs and a superficial kilovoltage apparatus. The site is provided with two CT units and one MR imaging device. Over 100 RTTs and radiographers are among the clinical staff directly involved in the treatment of the patients. For the cervical IGRT, daily EPID-imaging are acquired to align the patient based on bone-matching. For prostate IGRT daily fiducial markers' matching is performed, using daily EPID verification imaging. The treatment of prostate and cervical cancer patients is based on RapidArc plans. The Clarity ultrasound system was installed in 2012, and Herlev is a pioneer in implementing the ultrasound imaging as cervical IGRT.

The clarity system consists of two US units - one located in the CT-room, and one in the treatment room. These units are connected through a workstation/server located at an independent location on site. Each US unit is equipped with a convex array probe for 3D TAUS scanning of the cervix, and an autoscan probe for 4D prostate monitoring. After our feedback regarding the limitation of the 3D TAUS probe, the Clarity provided us with a novel 3D TAUS autoscan probe (Fig. 2.1).

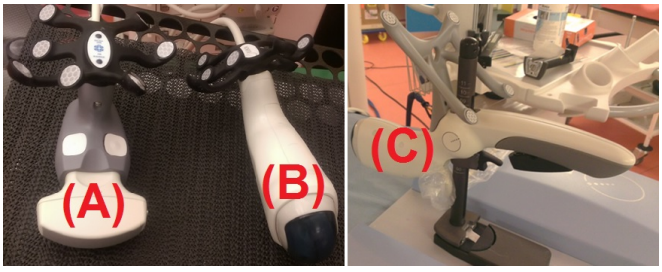

Figure 2.1: The Clarity ultrasound probes; (A) the 3D TAUS probe for cervical scanning, (B) the 3D TAUS autoscan probe for cervical scanning, and (C) the 4D TPUS probe for prostate monitoring.

Each unit consists of a ceiling-mounted infrared (IR) camera that can track the US-

Figure 2.2: The Clarity ultrasound components; (A) Ultrasound unit in the CT-simulation room, (B) The Clarity guide in the treatment room (LINAC-room), (C) The ultrasound alignment phantom for probe-, and room-calibration, and (D) The Clarity workstation, in which all acquired images are stored.

probe by monitoring the IR-reflectors/emitters are permanently mounted on each probe. This is central for determining the geographical position of the reconstructed anatomical structures. To enable superimposing the acquired CT images over the 3DUS-image-sets, the 3D-US system is calibrated to the same coordinate system as the CT and treatment rooms, respectively (Fig. 2.2). The calibration procedure is accomplished by means of a delivered alignment phantom. Quality assurance checks confirm system calibration each day of use.

2.1 Physics of Ultrasonic Wave

Ultrasound imaging is basically about sending acoustic waves into the body and measuring the reflective of waves at the interfaces between tissue. Comparing to the x-rays, that penetrates through the body to the detector, and is dependent on the tissue through which the beams passes, the ultrasound behaves very differently. Many of the objects and artifacts seen in ultrasound images are due to the physical properties of the ultrasonic beams, such as reflection, refraction and attenuation (Fig. 2.3 A) (Weyman 1994). As a beam of ultrasound passes through a media, it can be reflected, called for echo, at the boundary between two materials with different acoustic impedance (impedance is a

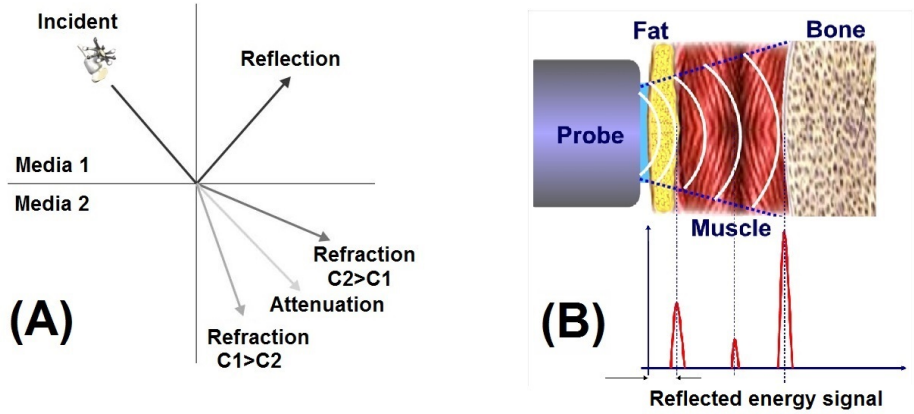

Figure 2.3: The ultrasound acoustic waves; (A) Ultrasonic beams reflects, refracts, and attenuates when it travels through tissues in different speed (C); (B) The strength of the echo (reflected waves) is dependent on the tissues' impedance (modified from http://coreten.ca/wp-content/uploads/2012/01/BX-Tissue-Graphic.png).

product of the material's density and propagation speed) (Middleton, Kurtz, and Hertzberg 2004). The speed of sound is [m/s] approximately 343, 1 480, 4 080, for air, tissue and bone, respectively. The strength of the reflected echo is dependent on the difference of the impedance. When the acoustic impedance is very large, as in bone, the ultrasound will be totally reflected, and tissues beyond them cannot be imaged (Fig. 2.3 B). This is where the technique of the operator becomes important, since the operator should avoid such structures or regions.
Just as there are infrared, visible, and ultraviolet ranges in the electromagnetic spectrum, so there are infrasound (< 20 Hz), audible (20 Hz to 20 kHz), and ultrasound (> 20 kHz). The frequency of an ultrasound wave, which determines by the transducer, consists of the number of cycles or pressure changes that occur in one second. The frequency used in diagnostic imaging is in the range of 1 - 5 MHz.

2.2 The 3D-TAUS scan of the cervical cancer patients

2.2.1 The conventional 3D-TAUS probe (C-probe) and the 3D-TAUS autoscan probe (A-probe)

The 3D TAUS probe consists of a transducer array of 128 elements, using a central frequency of 3.4 MHz. The probe is provided with IR reflectors fixed so that they can be detected by the ceiling-mounted IR camera. The camera cannot detect the reflectors

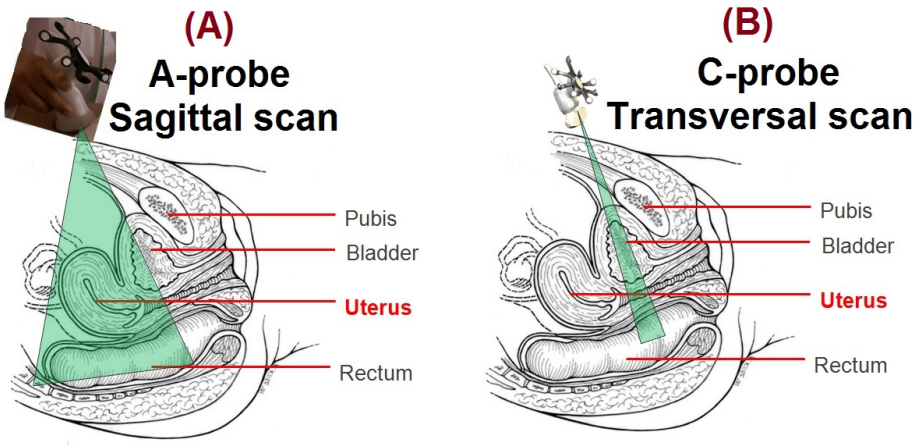

Figure 2.4: The 3D TAUS scan of the uterus; (A) The autoscan probe (A-probe) acquires images in the sagittal paln, (B) The conventional probe (C-probe) acquires images in the transversal plane.

if the probe, for instance, is rotated 90 degrees, thus restricting image acquisition to the transversal plane. Initially, the probe is tilted backwards to localize the vaginal region, followed by sweeping to the vertical position. Approximately half of the uterine volume can be captured by the sweep, thus a cranial slide technique is required to cover the rest of the uterus (Fig. 2.4 B).

The A-US probe comprises the similar type of transducer, but with a central frequency of 5 MHz. Initially, and prior to acquiring the scan, the desired uterine structure is identified in the sagittal plane. The semiautomatic transabdominal scan is achieved by localizing the central slice of the uterus and then allowing the motorized head to automatically sweep over the uterine volume (Fig. 2.4 A).

2.2.2 Image acquisition and structure contouring

2.2.2.1 CT SIMULATION ROOM

At CT simulation, all patients are CT scanned in a supine position, according to a standard cervix protocol. The acquired CT-data sets are used for treatment planning (Eclipse, Varian Medical System). After the CT scan, all the GYN patients undergo a standard MR-scan. Eventually, the CT-MR fusion is carried out by the radiographers using the Eclipse planning system. The fusion is based on bone-matches.

The uterine target and OARs are delineated in the CT-MR fusion data sets. Initially, the specialized GYN oncologist outlines the CTV after the CT-MR fusion is performed. The planning target volume (PTV) is then obtained by an additional margin to CTV in

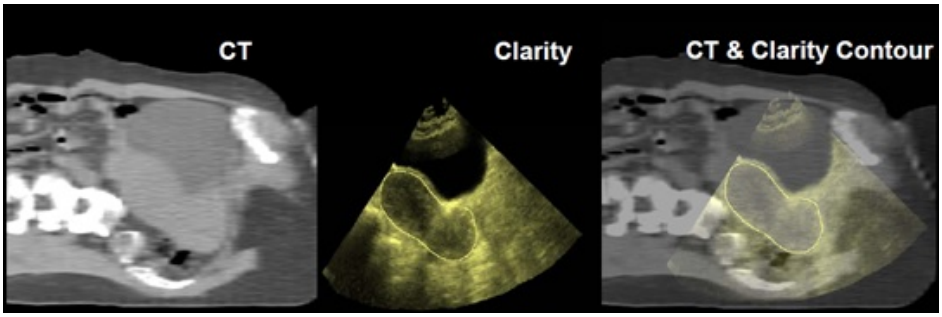

Figure 2.5: CT-US fusion process; Fusion of acquired US-scan to CT-image dataset, in which the positioning reference volume (PRV) of the uterus is contoured, is performed in US workstation.

anterior-posterior (A/P), and left-right (L/R), and inferior-superior (I/S) directions. The treatment is administered in a total of 25 fractions, at 2Gy/fraction. A CT image and digitally reconstructed radiographs (DRRs) are created of the anterior and left lateral treatment fields in order to provide planned bone position for daily IGRT.

In this project, immediately after the CT scan, the patient is prepared for the trans-abdominal US-scan. The US-scans are performed using the C-probe by one of the six experienced radiation therapists (RTTs). (Note that the A-probe was implemented after we confirmed that the C-probe has limitations as cervical IGRT). Each RTT has participated in an extensive two week training provided by the Clarity's manufacturer, and participated in several practice sessions before commencement of the study. Furthermore, the patients were instructed to follow a moderate bladder filling protocol, which involved not urinating after leaving their home on their way to their daily radiation treatment. The bladder-rectal protocol is important for daily reproducibility of the uterine position. A moderately full bladder also provides better propagation of US waves and hence enhances image quality by sharpening the outlines of the bladder and uterus interface. Further, the acquired CT datasets, delineated structures, and the planning treatment fields can be exported from Eclipse to the US workstation. Hence, co-registering and superimposition of US and CT can be performed, in which the positioning reference volume (PRV) of the uterus is contoured (Fig. 2.5). Thus the PRV defines uterine position at the time of planning. Moreover, the PRV is later used as an initial reference for the consecutive US-guide-scans acquired in the treatment room.

2.2.2.2 Treatment room

Initially, the patient is aligned to the room lasers by means of skin marks (setup tattoos from CT-scan alignment). For each patient, daily IGRT is performed by acquiring verification IGRT images, either using the EPID-image, or weekly CBCT-imaging, in

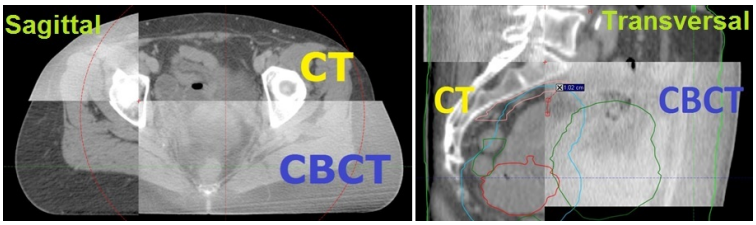

Figure 2.6: Bone match process; Alignment of bony structure landmarks from verfication CBCT image to the DRR-images from planned CT, in both sagittal and transversal planes.

order to adjust for bone misalignment, i.e. interfractional setup uncertainties. The images are used to align bony structure landmarks to DRR-images from planned CT (Fig. 2.6). Consequently, any possible daily bone positional displacement is addressed and corrected for through applying a set of orthogonal shifts to the therapy treatment couch prior to radiation delivery. After the uterine positional correction, the radiation treatment is delivered.

Immediately after the delivery of each radiotherapy fraction, a US scan is acquired. Instantly, the outlined uterus is superimposed on the initial reference PRV from the CT room. The intramodal comparison reveals couch shifts in three dimensions that can be recorded and compared to the actual clinical couch shift performed prior to the treatment delivery. Hence, the deviation of interfractional uterine displacement, based on bony alignment and US, can be statistically represented and evaluated. And thus, the possible shift between the US-guide uterus (red) and the US-reference (PRV) (green) can be observed as in (Fig. 2.7).

2.3 The 4D-TPUS tracking system of the prostate cancer patients

The Clarity 4D-TPUS unit system is identical to the 3D-TAUS system, except for using a 4D autoscan probe for transperineal monitoring of the prostate.

2.3.1 The 4D TPUS autoscan probe

The autoscan-US probe consists of a one dimensional (1D) sector array of 128 elements, and a radius of curvature of 40 mm, using a frequency bandwidth from 3.2 to 5.8 MHz (center frequency of 5 MHz) and a penetration depth of 17 cm. The transducer is motorized, offering automatic scanning over the region of interest.
The probe is provided with IR reflectors fixed so that they can be detected by the ceiling-mounted IR camera. Initially, the probe is affixed to a TPUS base, placed over the coach under the patient's knees, and pushed gently to the patient for transperineal scanning (Fig. 2.8). The motorized head is capable of real-time online scanning of the prostate.

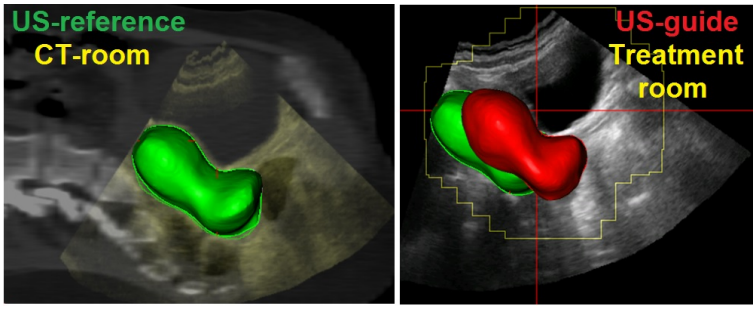

Figure 2.7: Uterine match process; Alignment of uterus from the US-guide (red) to the US-reference (green).

2.3.2 CT-simulation and autoscan imaging

In this study, after the CT scan acquisition, the patient was prepared for the US scan using vendor provided knee cushions (immobilization devices) resting over the autoscan base, implying a different setup in comparison to the CT position. The aim of this study was to determine intrafractional prostate motion during a certain period of time (2.0 - 2.5 minutes), corresponding to the beam-on time required to deliver a RapidArc fraction. Therefore differences in setup were not considered to have a significant impact on the acquired results. First the operator mounts the autoscan probe on the base and gently attaches the probe head to the patient until the prostate, bladder, and rectum are visually identified on the US console. The patient was instructed to remain motionless during image acquisition and US monitoring.

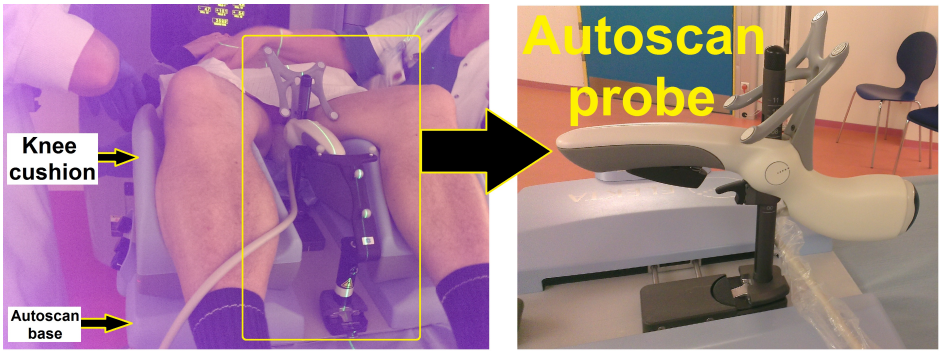

Figure 2.8: Transperineal prostate 4D monitoring: the autoscan is attached to the base, before being gently pushed to the patient, whose legs are resting on the vendor provided cushions.

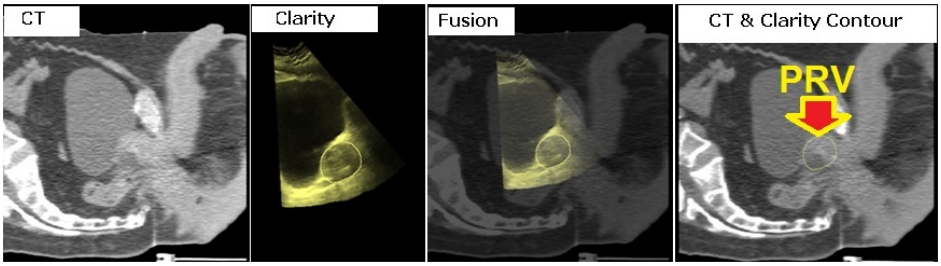

Figure 2.9: CT-US fusion process; Using the Clarity workstation, the positioning reference volume (PRV) of the prostate is contoured after performing CT-US fusion.

After repositioning of the patient, a TPUS image was acquired by radiographers. Furthermore, the acquired CT datasets, delineated structures and planning treatment fields can be exported from Eclipse to the US workstation. Hence co-registration and superimposition of US and CT can be performed (Fig. 2.9), in which the positioning reference volume (PRV) of the prostate gland is contoured. Thus the PRV defines prostate position at the time of planning. In this study, the assisted segmentation in the Clarity workstation was utilized for prostate delineation. Export/import from the treatment planning system to the Clarity workstation, CT/US fusion and prostate delineation were carried out by two radiographers and one physicist.

2.3.3 Image acquisition and prostate tracking in the treatment room

Initially, the patient is fixed in accordance with the CT set-up in the CT room. The patient is then aligned to the room lasers by means of the skin marks (set-up tattoos from the CT scan alignment). For each patient daily IGRT is performed by acquiring an EPID image in order to adjust for prostate gland misalignment, i.e. interfractional set-up uncertainties. The EPID images are used to align the prostate with DRR-images from planned CT by means of fiducial markers' matching. Consequently, any possible daily prostate positional displacement is addressed and corrected for through applying a set of orthogonal shifts to the therapy treatment couch prior to the delivery of radiation. After the prostate positional correction, the radiation treatment is delivered.

Immediately after the delivery of each fraction, the patient is fixed in accordance with the US setup in the CT room, where the autoscan-base is positioned under the patient's legs. The patient is then aligned to the room lasers using the same setup tattoos that were used for the actual treatment alignment. Thereafter the autoscan probe is mounted on the base and carefully attached to the patient (transperineally). Meanwhile, the 3D-US guide scan is performed. Afterwards a copy of the PRV-contour was aligned to the acquired prostate. Instantly, the outlined (the copy of the PRV) prostate is superimposed over the initial reference PRV from the CT room. Finally the 4D-US scan is performed. Thus

the magnitude and direction of prostate motion is quantified and recorded. Henceforth, the intrafractional uncertainty, i.e. the motion of the prostate during the corresponded radiation treatment time, can be retrospectively evaluated.

2.4 Statistical analysis

The phantom, volunteer, and clinical patient data (cervix and prostate patients) were mostly evaluated by one observer (MB). Interfractional and intrafractional COM shifts, in the I/S, L/R, and A/P directions, of uterine and prostate were retrospectively retrieved using the Clarity workstation. Furthermore, the Euclidean distance (3D vector) was computed and the maximal 3D vector was recorded for each fraction. Finally, the means ($\pm$ 1 standard deviation (SD)) of the displacements in each direction and for the 3D vector were calculated.
For the data and statistical analysis the statistical program R (version 2.15.3) was used.

CHAPTER 3

Interfractional uterine displacement

In this chapter, the implementation of the Clarity 3D probe at Herlev hospital is described in detail. After a brief literature review, the procedure from day one to the US scanning of the last patient is explained in three phases. Before starting this study, ethical approval was obtained from "De Videnskabsetiske Komiteer" Appendix C

Phase I (Phantom study): Six operators, with no previous experience of US scanning, were acquainted with the Clarity system by implementing the conventional 3D probe (C-probe) to acquire images of a phantom, mimicking the female pelvic region. Based on the phantom US scan, the impact of probe pressure, and inter-operator variability was investigated, papers A and C.

Phase II (Volunteer study): Firstly, a volunteer study (a case study) was designed to investigate daily uterine shifts, paper C.

In a clinical study, paper B, we concluded that, using the C-probe for transabdominal uterine scan, the operators faced practical challenges when applying a sweep slide technique. A volunteer study was conducted to compare a new prototype autoscan probe that had been received from the vendor (A-probe) with the C-probe, paper E.

Phase III (Clinical study): A clinical study, for which five patients were enrolled, was carried out to evaluate the C-probe for determining interfractional shifts of the uterus, paper B. But, after concluding that the C-probe had limitations when used for uterine TAUS-scanning, the new A-probe was applied instead in a clinical study. The results of using of the A-probe are presented here. These results have not been submitted for publication.

3.1 Phantom study

The research project was initiated by installing the Clarity soft tissue visualization system at Herlev hospital. The Clarity system in radiotherapy differs from other US scanning systems, since it is integrated into radiotherapy by calibrating it to the same coordinate system as in the CT and treatment room. The calibration is performed using a vendor provided phantom (Fig. 2.2 C). The operators participated in two weeks of theoretical and practical training arranged by a Clarity specialist. The practical training included prostate and uterus transabdominal scanning using the C-probe to scan the volunteers. First and foremost, all the operators found the system challenging, since US scanning has not previously been implemented at our site. Secondly, the scanning of the uterus, by applying a sweep-slide technique to capture the larger volume of the uterus, was perceived to be cumbersome (Fig. 3.1). In addition, image interpretation was found to be difficult, in terms of image orientation and organ identification. It is well-known that US probe handling and recognition of the anatomical structures are serious issues for inexperienced operators, due to difficulties with correct probe positioning and variable image quality. To overcome these obstacles, we initiated the research study by scanning a commercial phantom.

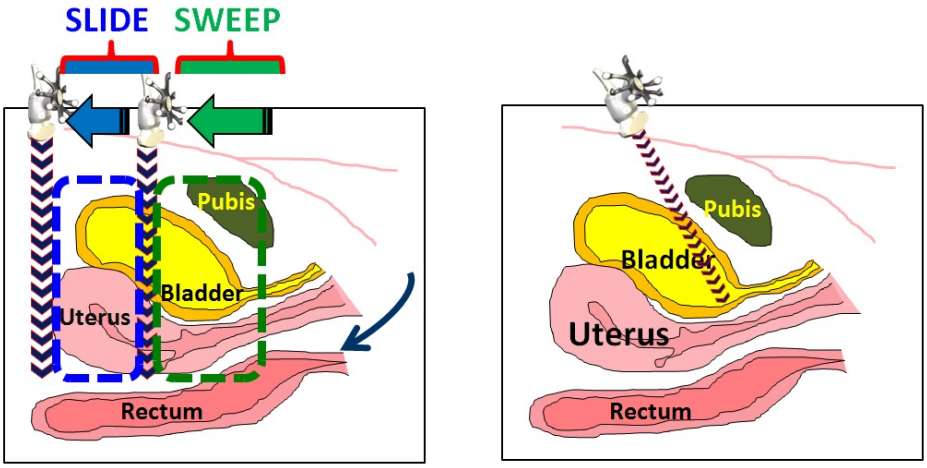

Figure 3.1: The TAUS scan of the uterus; Illustrates the sweep-slide technique required to capture the uterus.

The ultrasound training phantom (CIRS 404, Universal Medical, Norwood, USA) mimics the female pelvic region and contains a uterus, bladder and rectum representing the standard female pelvic organs (Fig. 3.2). The organs are subjected to displacement by

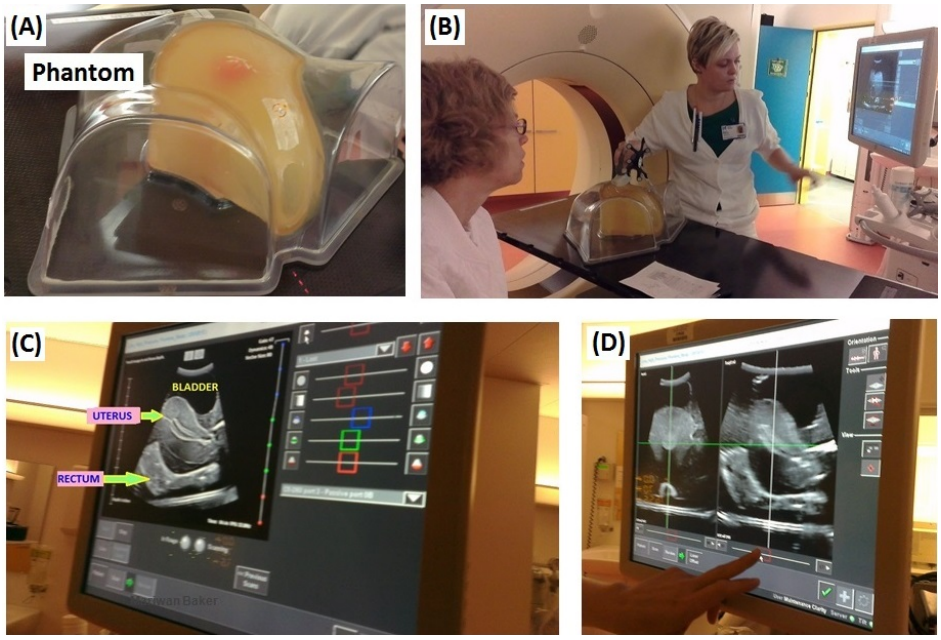

Figure 3.2: The Clarity ultrasound system; (A) The uterine phantom. (B) Phantom US scanning by means of a C-probe in the CT room. (C) Clarity US console, in which the phantom organs (bladder, uterus, and rectum) are easily identifiable. (D) The console is utilized to optimize image contrast and brightness before acquiring the US images.

the exerted probe pressure. The phantom does not contain any skeletal structure, such as the head of the femur or pelvic bone. The phantom is constructed of material that is intended for ultrasound scans, thus all organs are easily defined in the acquired US-images. Initially, the phantom was marked with small spherical ball bearings (laser alignment markers), used to aid reproducibility of the daily set-up prior to each US-scan session. Use of this technique requires acquisition of a reference US image data-set, and therefore during an initial session the best possible US-scan was selected as the reference position for the following sessions.

The aim of the initial study was to; (A) quantify the inter-operator variability, (B) determine the uterine positional displacement induced by the probe pressure.

3.1.1 Inter-operator variability

Different US imaging systems have been introduced into radiotherapy to visualize the soft tissue sites such as the prostate, GYN, and the postoperative lumpectomy cavity in breast cancer patients, (Boda-Heggemann et al. 2008; Cury et al. 2006; Pinkawa et al. 2008; Scarbrough et al. 2006; Serago, Buskirk, et al. 2006). However, to our knowledge, very few published papers have reported the application of 3D US in GYN patients (Ahmad, et al. 2008). As with all other systems, there are some limitations to the implementation of US imaging in radiotherapy. For instance, some challenges in terms of probe handling difficulties and inter-observer variability have previously been reported (McGahan, Ryu, and Fogata 2004; Serago, Chungbin, et al. 2002). In the current study, the inter-operator variability was investigated through 21-US scans of the phantom by seven operators over four sessions in different days (Fig. 3.3).

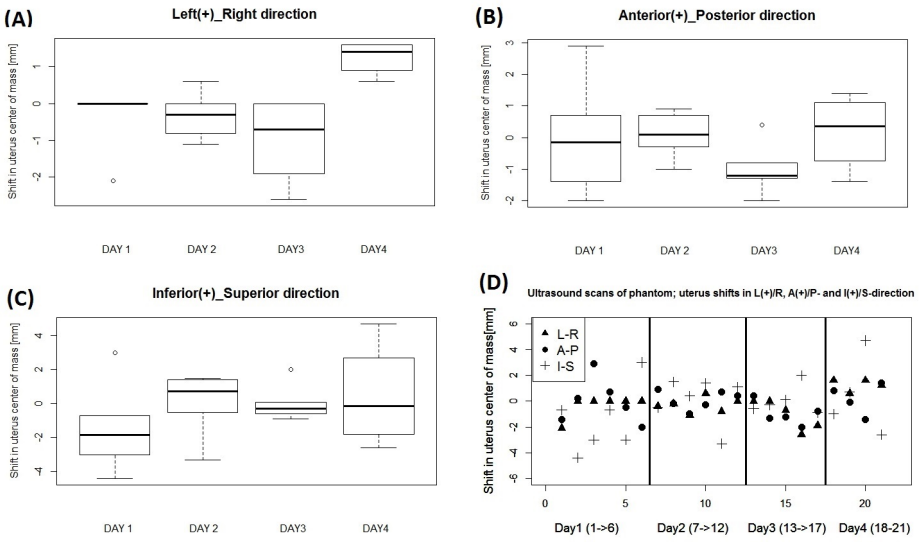

Figure 3.3: Positional uterine center of mass (COM) shifts of a phantom; The plot shows uterine COM shifts in the L/R (A), A/P (B), and I/S (C) directions for daily scans (D) (Day 1: 6 operators, Day 2: 6 operators, Day 3: 5 operators, and Day 4: 4 operators).

Positional uterine shifts in the L/R, A/P, and I/S directions demonstrates that there are no statistically significant differences compared to the mean of COM shifts, i.e. mean of the session scans for each day (Table. 3.1). All the acquired US-scans indicated that uterine COM displacements are in the vicinity of zero, with a daily mean value of less than 2 mm in all three cardinal directions. Since the interfractional positional variations of the cervical region, vaginal canal, and the head of the uterus (fundus) can vary by

Table 3.1: Tabulates values of one sample t.test of obtained uterine shifts using ultrasound scans of a phantom

Day	*Directions*	N	SD[1] [mm]	Mean [mm]	df[2]	t	95% CI[3] (Lower/upper)	P-value
DAY 1	L/R	6	0.86	-0.35	5	-1.00	-1.25/0.55	0.36
	A/P	6	1.74	-0.02	5	-0.02	-1.84/1.81	0.98
	I/S	6	2.62	-1.47	5	-1.37	-4.22/1.28	0.23
DAY 2	L/R	6	0.60	-0.32	5	-1.29	-0.95/0.31	0.25
	A/P	6	0.71	0.08	5	0.29	-0.67/0.83	0.79
	I/S	6	1.83	0.10	5	0.13	-1.82/2.02	0.90
DAY 3	L/R	5	1.17	-1.04	4	-1.99	-2.49/0.41	0.12
	A/P	5	0.88	-0.98	4	-2.48	-2.08/0.12	0.07
	I/S	5	1.15	0.06	4	0.12	-1.36/1.348	0.91
DAY 4	L/R	4	0.47	1.25	3	5.29	0.50/2.00	0.01
	A/P	4	1.22	0.18	3	0.29	-1.76/2.11	0.79
	I/S	4	3.14	0.45	3	0.29	-4.54/5.44	0.79

[1] Standard Deviations; [2] Degree of Freedom; [3] Confidence Interval

more than 2 cm (Chan et al. 2008; Jurgenliemk-Schulz et al. 2011), these day to day variations outweigh the magnitude of our inter-operator variability. In summary, the present US-phantom study suggests that inter-operator variability in determining uterine position is clinically irrelevant.

3.1.2 Probe pressure displacement

While the inter-operator variability in use of the phantom was shown to be clinically irrelevant, we conducted a new study to investigate the positional impact of probe pressure on the uterine COM. The aim of the study was to compare the magnitude of the pressure displacement with the daily uterine motion in a healthy volunteer. Variations in the transducer probe pressure applied have previously been documented during 3D US on prostate patients (Serago, Chungbin, et al. 2002; Taylor and Powell 2008), but, to our knowledge, there is no published paper on the cervix.

The study was initiated by US scanning of the phantom (transabdominal US scan using the C-probe) by seven operators in four sessions on different days. Each operator performed two scans per session, one without pressure (WOP) or light probe pressure, and one with maximum pressure (WP). A total of 42 scans were acquired.

In each phantom scan the US probe was performed on the first occasion with minimal pressure and on the second with firm pressure in the region corresponding to the pubic symphysis and rotated, after which it was swept cranially.

Positional shifts of the phantom uterus center of mass (COM) in the three orthogonal directions WP (depicted as circles) and WOP (depicted as triangles) are presented (Fig. 3.4). No statistically significant differences in any direction can be seen when comparing the shifts between WP and WOP (Table 3.2). The largest recorded shift is in the I/S-direction; +5 mm (WOP) and -5 mm (WP). The mean of the COM shifts in all three directions (L/R, A/P, I/S) for WP and WOP are centered around zero (Fig. 3.4 D).

Table 3.2: Paired t-test values of the mean uterine shifts using ultrasound scans of the phantom with pressure, and without pressure.

Directions	Number of scans	SD[1] [mm]	Difference between the means [mm]	95 % CI[2] (lower/upper)	p-value
Left-Right	21	0.93	-0.29	-1.03/0.45	0.43
Anterior-posterior	21	2.13	0.10	-0.99/1.18	0.86
Inferior-superior	21	1.87	0.50	-0.85/1.85	0.45

[1] Standard Deviations; [2] Confidence Interval

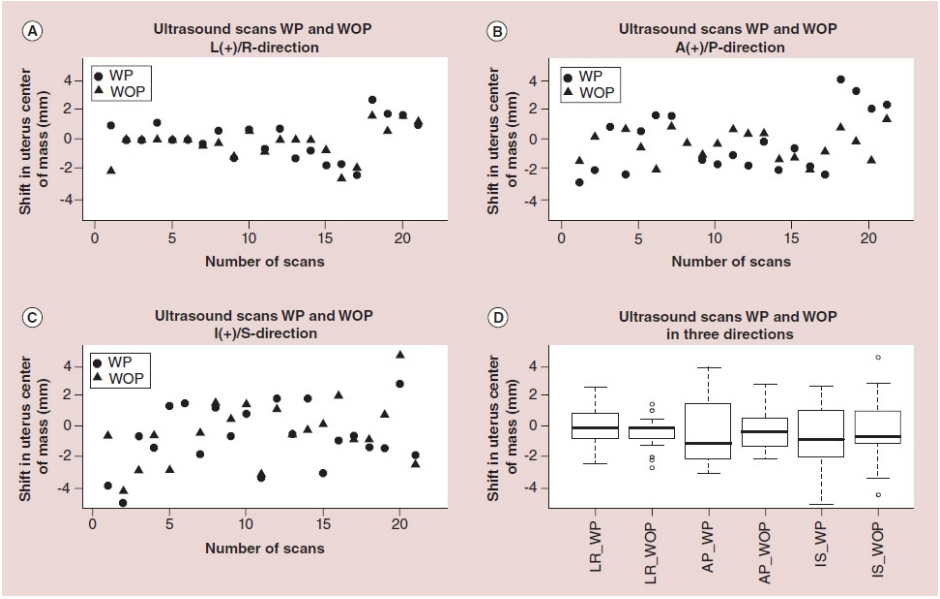

Figure 3.4: Plots of the COM shifts based of ultrasound scans of the phantom uterus; WP & WOP in (A) L/R, (B) A/P and (C) I/S directions. (D) Boxplot for WP and WOP for all three cardinal directions (L/R, A/P, I/S). A: Anterior; I: Inferior; L: Left; P: Posterior; R: Right; S: Superior; WOP: Without pressure; WP: With pressure.

3.1.3 Limitations and benefits of the current approach

The phantom study has limitations since it is not necessarily representative of a real GYN patient. Daily bladder and rectal filling variations might induce large uterine positional variations, which cannot be simulated by a phantom. However, each operator scanned this phantom several times, and also the possibility of acquiring images of a volunteer facilitated acquaintance with the Clarity system. The initial procedure with phantom scanning was perceived by each operator as an effective method obtaining experience in probe handling, image orientation, and ultrasound image interpretation. The American Association of Physics in Medicine (AAPM) emphasizes that the clinical US training is of the utmost importance, especially for inexperienced operators (Molloya et al. 2011). Experienced US-users are reported to be more consistent in image acquisition and have easier to recognize anatomical structures, leading to less inter-operator variability (Fuss 2003). In brief, a solid US training program is a necessity before implementing the TAUS scan method as an IGRT system in cervical radiotherapy. Additionally, it is highly recommended that an experienced ultrasound radiologist or oncologist are involved in implementing a new ultrasound IGRT system, since they can be a major support for the

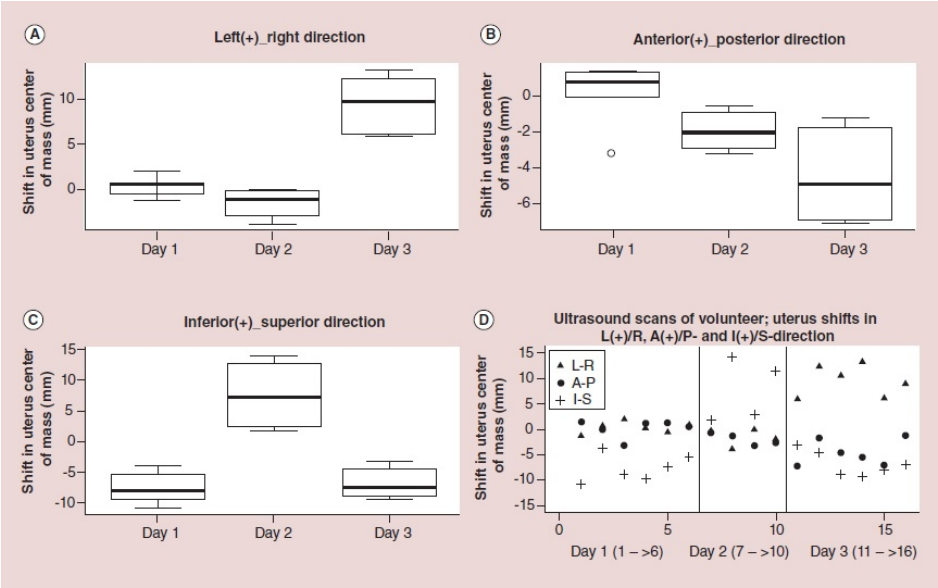

Figure 3.5: Omnidirectional shifts of uterine center of mass of a volunteer; (A–C)COM shifts for the volunteer on 3 days in the three cardinal directions. (D) Uterine COM shifts; the daily ultrasound scans.

RTTs in terms of image interpretation. Unfortunately, we lacked this essential support while conducting this project.

3.2 Case study (volunteer)

A healthy young volunteer was scanned by six operators in three sessions, leading to a total of 16 scans, over a period of 3 weeks (one session per week). During the first session the best scan, in which the organs were clearly definable, was selected as a reference for the following three sessions. Prior to the scanning, the volunteer was asked to have an empty rectum and full bladder prior to each US scan. The fixation was in supine position by means of a Vac Fix fixation system to ensure position reproducibility between sessions. Consistent positioning of the volunteer was enabled by the alignment of natural skin markers to the isocenter lasers of the CT room. A US transabdominal scan of the pelvic region was performed repeatedly by each operator until adequate image quality was achieved. Initially, a best scan, in which the organs were clearly definable, was selected as a reference for the following three sessions. No firm pressure was applied on the volunteer,

Table 3.3: Mean values with standard deviations of the uterine shifts in the volunteer scanned by six operators.

Day	*Directions*	Nr. of scans	Mean [mm]	SD [mm]
DAY 1	Left-Right	6	0.27	1.09
	Anterior-posterior	6	0.18	1.71
	Inferior-superior	6	-7.65	2.64
DAY 1	Left-Right	4	-1.58	1.74
	Anterior-posterior	4	-1.95	1.21
	Inferior-superior	4	7.55	6.12
DAY 1	Left-Right	6	9.48	3.08
	Anterior-posterior	6	-4.47	2.53
	Inferior-superior	6	-6.85	2.47

as the focus was on obtaining clear images, where the complex pelvic structure could be identified.

For the volunteer, the recorded mean COM shift on day three in the L/R direction is approximately 10 mm relative to the reference, while on days 1 and 2 the lateral shift is less than 2 mm (Fig. 3.5). The largest interfractional displacement is observed in the I/S direction, with a mean value of -7.7 mm, +7.6 mm and -6.9 mm on days 1, 2 and 3, respectively (Table 3.3), which is a clinically significant. This major divergence in the shifts was mainly due to the bladder volume variation, especially from Day 1 to Day 2 (Fig. 3.6). Previous reports have confirmed that uterine positional changes are strongly correlated with daily variation in bladder–rectum filling (Ahmad et al. 2011; Lee et al. 2007). The challenge experienced by most of our operators during 3D US acquisition was to find an appropriate probe handling technique that captured the entire uterus from the cervical os to the fundus, as the image quality was poor in some cases. Obviously, poor image quality has an adverse influence on uterine delineation, thus leading to uncertainty in COM shifts. Our experience of suboptimal image quality is confirmed by a previous study, where assisted segmentation (employed in the present study) was compared to manual segmentation of prostate patients using the Clarity 3D US system (Johnston et al. 2008). During quality classification of the acquired US images, they found that up to 33% were of bad quality, which hinders accurate outlining of the target. One limitation of this study is that the statistical evaluation of the interfractional uterine positional changes based on a single volunteer must be considered with caution, and a clinical study is needed to validate the present result.

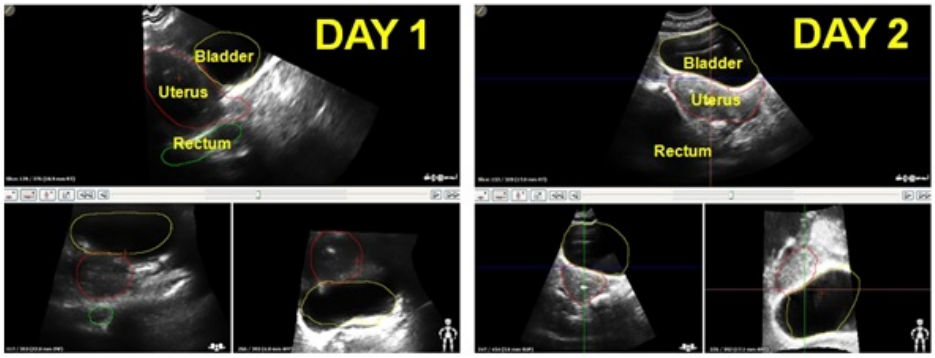

Figure 3.6: Outlined organs (bladder, uterus and rectum), sagittal, transversal and frontal cross-sections; The uterine positional shift is obvious from days 1 to 2.

3.3 Volunteer study to compare C-probe to A-probe

The implementation of 3D TAUS imaging, using the C-probe, on the GYN patients was experienced as a challenge, since all the operators faced difficulty in applying the sweep-slide technique. After conducting a clinical study of five cervical cancer patients, paper B, we confirmed that using the C-probe is cumbersome and might lead to undesired inter-operator variability in terms of variations in capturing the uterine volume, and difficulty in identifying the uterine structure in the transversal plane, although normally it is easily recognizable in the sagittal plane. Consequently, the Clarity manufacturer provided us with a new suggested prototype autoscan probe (A-probe). A volunteer study was designed to evaluate a novel A-probe by comparing it to the C-probe.

The semiautomatic A-probe inherits a mechanically motorized head, enabling automatic transabdominal sweep scans after manual positioning of the probe above the pubis symphysis. The A-probe is a modification of an autoscan probe (Lachaine and Falco 2013) that was initially designed for transperineal prostate scanning and real-time tracking of the prostate, to address intrafractional prostate motion. The hypothesis of the volunteer study was that the novel A-probe may be a better IGRT alternative than the C-probe in cervical radiotherapy. In this approach, nine healthy volunteers were US scanned by seven operators, using C-probe followed by an A-probe scan (Fig. 3.7). The volunteers were asked to remain motionless, and instructed to follow a moderate bladder filling protocol. After the superimposing reconstructed image sets from the C-probe over the A-probe images, two observers (OBS 1 and OBS 2) delineated the uterine organ in the 72 acquired scans; 36 from C-probe and 36 from A-probe. Thus, the outlined uterine structures served to determine inter-observer contouring variability. OBS 1 delineated the same scans after two weeks, to investigate intra-observer variations. Furthermore, the delineated uterine structures were classified into two groups: one with all scans and the other with the best

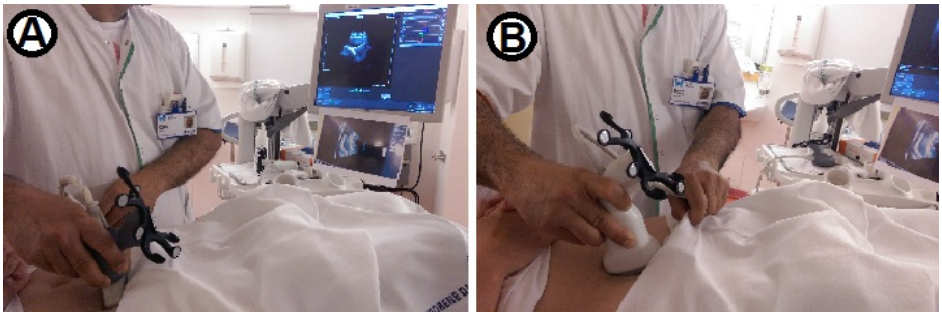

Figure 3.7: Transabdominal ultrasound imaging; (A) Using the C-probe, and (B) using the A-probe.

scans. In the best scans, both C-probe and A-probe images showed the whole uterus.

We found out that A-probe images were slightly better in spatial resolution, the reason being the higher transducer frequency (Fig. 3.8 A & B). Additionally, figure 3.8 C & D exemplifies a uterine scan, where the image is incomplete using the C-probe, due to difficulty identifying the uterus in the transversal plane while manually scanning the pelvic region. As a result, the whole uterus was captured in only 19 (53 %) scans using the C-probe, whereas the corresponding figure for the A-probe was 32 (89 %).

When comparing the C-probe to the A-probe, the calculated SD of inter-observer (OBS 1- OBS 2) and intra-observer (OBS 1 - OBS 1) differences were smaller for the A-probe in all three directions, the only exception being intra-observer delineations in the A/P-direction (Table. 3.4). Application of the F-test showed that the reduction was statistically significant, verifying better inter-observer concordance while employing the A-probe

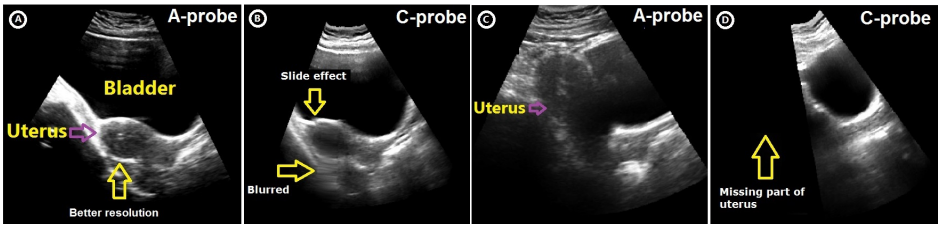

Figure 3.8: Ultrasound (US) images using C-probe, and A-probe; (A) Volunteer 1 ultrasound image of bladder and uterus using the A-probe. (B) The same volunteer but using the C-probe, where image distortion and lower image quality can be observed. (C) Volunteer 2 using the A-probe, where the whole uterus is captured. (D) The same volunteer but using the C-probe, where only half of the uterus is imaged.

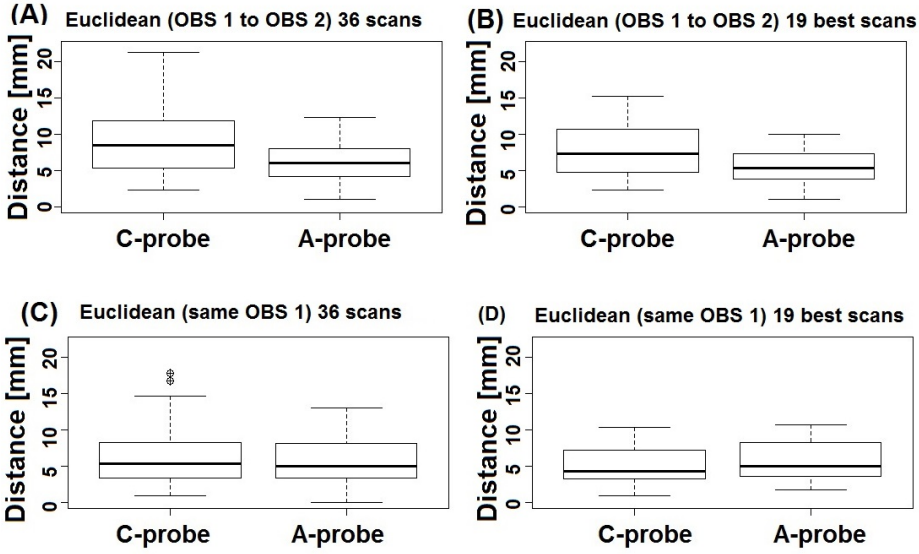

Figure 3.9: Median (horizontal line), 25th and 75th percentiles (box), and range (whiskers) of Euclidean distances between uterine center of Mass (COM) delineated by OBS 1 and OBS 2, and the same observer twice (OBS 1); (A, B) Distance differences (OBS 1 minus OBS 2) for the C-probe and A-probe using all 36 scans and best 19 scans, respectively. (C, D) Distance differences (two delineations by the same observer (OBS 1)) for the C-probe and A-probe using all 36 scans and best 19 scans, respectively.

While investigating set of all scans compared with the best scans, an F-test revealed that the different SD for inter-observer COM, while using all scans and comparing the C-probe with the A-probe, was statistically significant. In contrast, the corresponding F-test on the best 19 scans indicated no significant differences, except for a weak difference in the A/P-direction ($p < 0.04$) (Table. 3.5), yet again confirming that there is better agreement in delineating the target when the entire uterus is captured (best scans). This was verified by studying the Euclidean distance, where applying the F-test to the inter-observer differences was revealed to be statistically significant, but not for the intra-observer distance (last two rows in Table. 3.5).

Furthermore, the median of the Euclidean COM distances for inter-observer scans was reduced by 2.5 mm (all scans) while using the A-probe instead of the C-probe, compared with only 0.4 mm (best scans) (Fig. 3.9). However, the intra-observer graphs (Fig. 3.9 C & D) illustrate that for all scans and for the best scans, the median distance is around 5.0 mm, irrespective of whether the the C-probe or A-probe was employed. The smaller

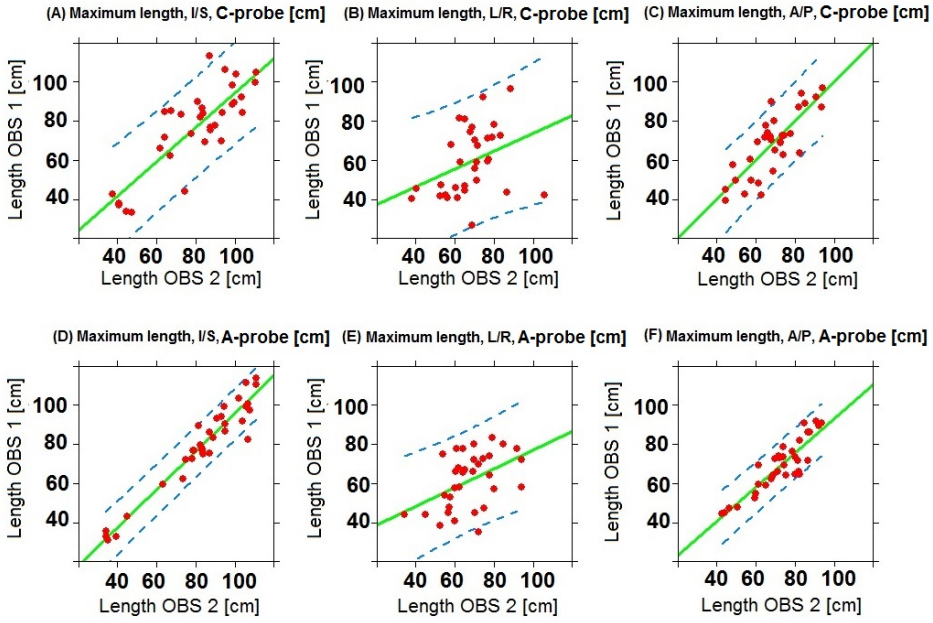

Figure 3.10: Comparison of the maximum uterine length by OBS 1 and OBS 2 on C-probe and A-probe scans in Inferior-Superior (I/S); Left-Right (L/R); Anterior-Posterior (A/P)-directions); Regression line fit (solid line) and predicted interval (dashed lines) for 95 % confidence interval (CI) are indicated.

reduction in the best scans indicates that there is better target delineation concordance when the entire uterus is captured, which is the case with the "best scan". Moreover, the dice coefficient index (the volume overlap of the delineated uterus by the OBS1 and OBS2) was calculated as 0.67 and 0.75 for the C-probe and A-probe scans, respectively, verifying that there is good concordance using the A-probe but only modest concordance with the C-probe. The highest inter-observer discordance stems from inaccurate uterine segmentation in the missing part of the imaged uterus using the C-probe.

As one uterine COM point did not reveal substantial data on the outlined large uterine volume, the maximum uterine length in all three directions was examined. The predictive interval indicated better inter-observer concordance when applying the A-probe compared to the C-probe (Fig. 3.10). However, the benefit was limited in the L/R-direction, which can be attributed to the poor lateral image resolution in both the C-probe and the A-probe scans. Yet again, this result suggests that the A-probe might be a better IGRT method than using the C-probe in cervical radiotherapy.

In summary, all the operators in the current study reported that it was easier to handle

Table 3.4: Mean inter and intra-observer differences in uterine COM for the three directions, using C- and A-probes.

	Mean ± 1SD[1] [mm]			
	Inter-observer[2]		Intra-observer	
Directions	C-probe	A-probe	C-probe	A-probe
I(+)/S	3.2 ± 6.3	1.8 ± 3.9	-0.9 ± 6.1	-1.3 ± 3.2
L(+)/R	0.9 ± 5.5	0.0 ± 3.6	0.2 ± 5.8	-2.1 ± 3.8
A(+)/P	-0.4 ± 6.6	0.4 ± 3.6	-0.7 ± 3.5	0.8 ± 3.5

[1]Standard deviations [2]Inter-observer: the differences between two observers; Intra-observer: the differences between two delineations by the same observer.

Table 3.5: F-test of the SD for inter-observer uterine COM differences as well as inter and intra-observer Euclidean COM distances in all the three orthogonal directions. The test is done for all scans and the best scans.

	All scans (n = 36)			Best scans[1] (n = 19)		
Directions	Ratio of variances	95 % CI[2] Upper/Lower	p-value	Ratio of variances	95 % CI Upper/Lower	p-value
I(+)/S	2.61	(1.33 to 5.22)	0.006	1.16	(0.45 to 3.01)	0.7571
L(+)/R	2.38	(1.21 to 4.67)	0.012	1.84	(0.71 to 4.77)	0.2067
A(+)/P	3.29	(1.68 to 6.45)	0.001	2.83	(1.09 to 7.35)	0.0331
Euclidean (inter-observer)	4.90	(2.50 to 9.61)	0.000006			
Euclidean (intra-observer)	1.83	(0.93 to 3.59)	0.077			

[1]Best scans: The US scans where the whole uterus is captured both with the A-probe and the C-probe
[2] Confidence Interval

the A-probe, particularly when identifying the uterus and bladder in the sagittal plane. Furthermore, image acquisition was quicker and less probe pressure was exerted during A-probe scanning. Moreover the image detail of the A-probe scan was slightly better than that of the C-probe. Additionally, the study revealed that the A-probe is superior to the C-probe for capturing the whole uterine volume.

Briefly, in this study we confirmed that A-probe imaging might be a better modality than C-probe imaging in terms of better spatial resolution, facilitating capture of the whole uterus, and requiring less applied probe pressure. While the sweep-slide technique in using the C-probe was a challenge, the A-probe scans were performed faster and more smoothly. As a result, the A-probe demonstrated less inter-operator variability and consequently less contouring variations. In conclusion, the A-probe is confirmed to be

a better IGRT system, with less uncertainties, than the C-probe for correcting for daily uterine positional changes in cervical radiotherapy. As this conclusion was evident, we changed the C-probe to the A-probe in our continuous clinical study for applying TAUS scans of cervical cancer patients. The next section is a clinical comparison of the two probes.

Table 3.6: Uterine center of mass shifts (C-probe and A-probe)[2] realtive to bony structures (CBCT).

		Mean ± 1SD[1] [mm]		
	Maximum shift [mm]	Overall uterine match US	C-probe	A-probe
Directions	(11 pts, 38 fractions)	(11 pts, 38 fractions)	(6 pts, 25 fractions)	(5 pts, 13 fractions)
A(+)/P	-19.7	-1.3 ± 7.4	-0.5 ± 8.2	-3.0 ± 6.3
I(+)/S	-23.0	-2.5 ± 7.1	-4.1 ± 7.7	0.6 ± 4.5
L(+)/R	12.5	1.8 ± 4.3	1.6 ± 4.5	2.2 ± 3.8

[1]Standard deviations, [2]Conventional and autoscan probes .

3.4 Clinical study using C-probe and A-probe

After several phantom and volunteer C-probe TAUS scans, clinical scans of cervical cancer patients were initiated. First of all we conducted a clinical study of five patients, paper B. Three more patients were incorporated in the TAUS C-probe study before the conclusion that there were uncertainties in implementing the C-probe as an IGRT method. Our feedback to the Clarity manufacturer, suggesting that they design a new automatic probe that should be able to acquire US images in the sagittal plane rather than the C-probe's transversal plane, resulted in designation of a novel autoscan probe (A-probe). The A-probe was implemented to determine the interfractional uterine displacements of the cervical cancer patients through the TAUS scanning. In this section we will take up some results from the first published paper, and also compare the C-probe results (six patients) with the A-probe results (five patients).

The overall positional uterine COM shifts (± 1SD, 38 scans by C-probe and A-probe) relative to the bone structure, was [mm]; ±7.4, ±7.1, and ±4.3, in A/P, I/S, and L/R, respectively (Table. 3.6). When the uterine shifts of the C-probe was compared to the shifts using the A-probe, we found that the standard deviations of the C-probe was larger than of the A-probe (columns 4 & 5 in the table. 3.6). This can be due to the fact that when using the C-probe there are challenges to identifying the pelvic structures, and also to capturing the entire uterus, leading to larger inter-operator and inter-observer variability, which was confirmed in the comparison volunteer study in the previous section. The largest interfractional displacements using US were 19.7 mm, 23 mm, and 12.5 mm in the posterior, superior, and left directions, respectively.

Generally, we showed that US-imaging is capable of identifying soft tissue structures, especially on the bladder-uterus interface, which otherwise were difficult to distinguish using CBCT imaging. At the same time, a comparison of the uterine shifts between the C-probe and the A-probe confirmed the results of the previous volunteer study in that there is greater uncertainty in using the C-probe as uterine IGRT method. The operators experienced the A-probe as easier to employ, and the uterus, bladder and rectum could

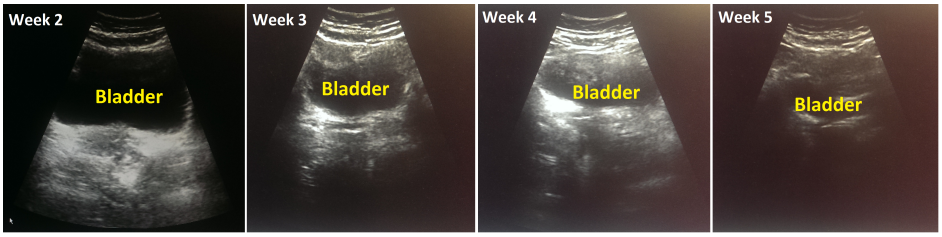

Figure 3.11: The bladder volume reduction; Showing that the bladder volume decreases during the treatment course, due to radiation induced sideeffect.

easily be recognized, thus leading to a reduction of image acquisition time. Moreover, we observed a bladder volume reduction during the treatment course, despite the fact that the patients were following a moderate bladder filling protocol (Fig. 3.11). Bladder volume reduction presents a challenge as it affects the daily uterine and bladder position as well as making the use of ultrasound as a daily IGRT modality more difficult. The bladder volume reduction might be attributed to the radiation induced urinary adverse effects.

CHAPTER 4

Probe pressure and intrafractional prostate motion

In this chapter, the probe induced prostate displacement and intrafractional prostate motion are addressed based on the two papers D & F.

In the probe pressure displacement study, the Clarity TPUS system was utilized to monitor the prostate in real-time. During the prostate tracking, a TAUS scan was simulated, using the C-probe. The aim of this study was to determine the magnitude of prostate displacement while the probe simulation was being applied.

In the clinical study of intrafractional prostate motion, the prostate was tracked in real time for about 2 to 2.5 minutes, a typical beam-on time required to deliver a RapidArc plan in our site. The aim of the study was to investigate whether the intrafractional motion is within 2.0 mm. 2 mm is a tolerance value recommended by the British Ionization Radiation Medical Exposure Regulations 2000 (IRMER 2000).

4.1 Probe pressure displacement of the prostate during TAUS scan

TAUS imaging has previously been used in prostate IGRT at different sites (Heuvel et al. 2003; Johnston et al. 2008; McNair et al. 2006; Scarbrough et al. 2006; Serago, Buskirk, et al. 2006). There are two models for US IGRT systems, a intramodal Clarity system and an intermodal BAT system (Cury et al. 2006; Feigenberg et al. 2007; Meer et al. 2013; Peng et al. 2008; Pinkawa et al. 2008). In intermodal US, the US images from the treatment room are matched to computed tomography (CT)-reference images, whilst in intramodal US the US images are matched to the US-reference images from the simulation room. Both systems are based on 3D TAUS scanning, using a 2D US probe. One of the challenges in acquiring the TAUS imaging is variations in transducer probe pressure (McGahan, Ryu, and Fogata 2004; Serago, Chungbin, et al. 2002). In different phantoms, volunteers, and clinical studies, the pressure induced shift of the prostate has been investigated (Artignan et al. 2004; Fargier-Voiron et al. 2014; McGahan, Ryu, and Fogata 2004). The limitation of a phantom study is that a phantom cannot reflect the patient's organs. In the volunteer study by Artignan et al. (2004), the probe was affixed to a robotic arm, capable of only vertical movement, which might not reflect the sweep technique required to perform a TAUS scan. The most recently published paper by Fargier-Viron et al. shows that the prostate displacement can be up to 8 mm, due to

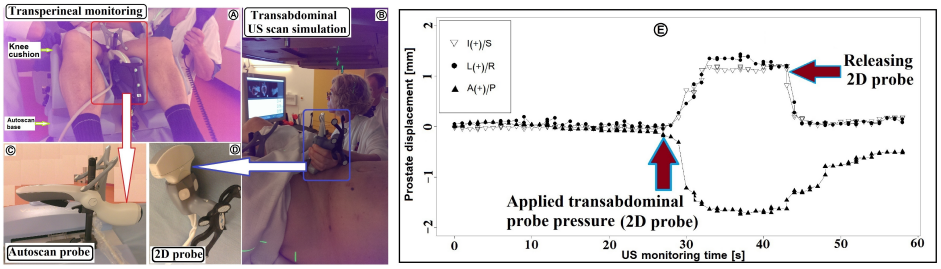

Figure 4.1: The TAUS simulation during TPUS monitoring of the prostate; (A) 4D monitoring autoscan attached to the patient, (B) TAUS simulation using 2D probe, (C) 4D autoscan probe, (D) The 2D probe, (E) The prostate monitoring graph, indicating the impact of applied probe pressure.

exerted vertical "strong pressure", but it was not possible to observe displacements during the exertion of "soft pressure" adequate for acquiring sufficient image quality. Thus, a study to simulate the daily in-room TAUS IGRT while, in real-time, recording the induced prostate displacement is required, and this was the motive for our probe pressure study. The aim of this study was to determine prostate displacement, due to applied TAUS probe pressure, by continuously 4D monitoring the prostate utilizing the TPUS 4D real-time autoscan.

4.1.1 Clinical study

Nine prostate cancer patients were US scanned weekly by two of our six experienced RTTs, using the TPUS autoscan. The patients were instructed to follow a moderate bladder-filling protocol. After the CT scan, a US scan was acquired. Afterwards, the CT-US fusion was performed and the prostate gland was delineated as a reference for subsequent weekly US scans in the treatment room. In this study, the US monitoring images were used for research purposes only and not applied clinically. Immediately after the treatment delivery, the patient was repositioned in preparation for autoscan monitoring. A total of 42 US scans were acquired. The TAUS scan was simulated, using a C-probe, while the prostate was continuously monitored using the TPUS autoscan (Fig. 4.1). The figure shows an example of prostate displacements in I/S, L/R, and A/P directions during the probe simulation. The simulation duration applying the TAUS probe was from 15 to 20 seconds. During the simulation, no US images were acquired with the C-probe, i.e. the probe was used as a dummy. However, the trained RTTs were instructed to reproduce the sweeping technique and associated applications of pressure required to acquire adequate US image quality. Furthermore, the RTTs were asked to avoid observing the impact of the pressure on the console screen.

The TPUS auatoscan was capable of tracking the prostate in real time. The TAUS

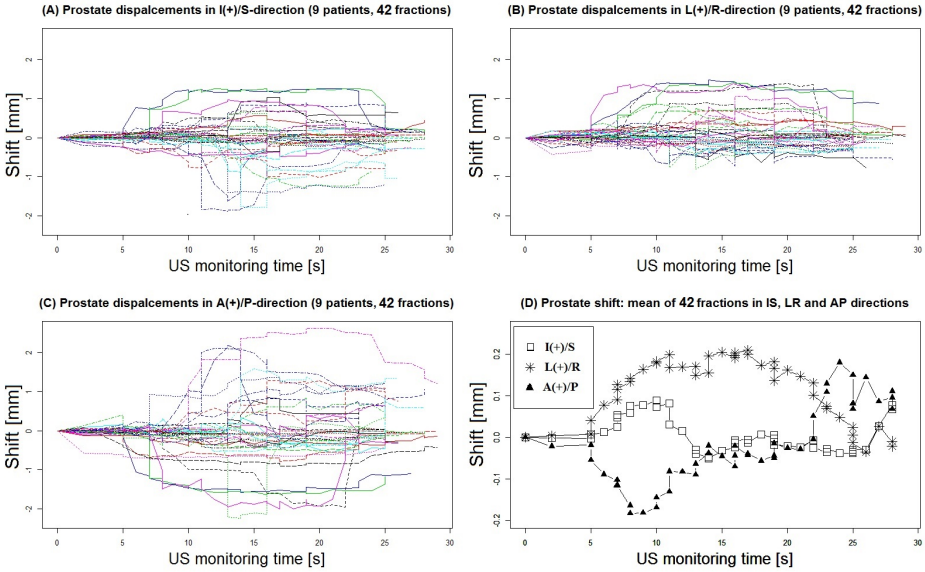

Figure 4.2: The prostate displacement; (A-C) Monitoring graphs show the prostate displacements due to applied probe pressure for total 42 US scans in I/S, L/R, and A/P directions, (D) The graph over mean of the 42 scans in I/S, L/R, and A/P directions.

simulation was performed for all the patients, although some variations in probe handling were observed. Results of the data analysis of the 42 scans, means and SDs of the prostate displacements and the mean of the maximum Euclidean distance, are tabulated in Table 4.1. Most of the displacements were observed to be smaller than 2 mm in all three directions (Fig. 4.2). Furthermore, figure 4.2 D, reveals that the mean displacements are within $\pm$ 0.2 in all three directions. Only 5 % (two scans in A/P direction), and 16 % of the Euclidean distance were larger than 2 mm. In many cases, we observed a permanent displacement of the prostate after releasing the probe.

Individual boxplots of all nine patients demonstrated some variations in prostate displacements between them, and even for individual patients (Fig. 4.3). Additionally, the boxplot of the overall displacements revealed that the first and the third quartiles were within 1.0 mm in all three directions. Finally, the last boxplot in the figure indicates that the median Euclidean distance is about 1.3 mm.

The TPUS autoscan was shown to be an excellent tool for real-time prostate tracking. The uncertainty of the autoscan probe had previously been validated as less than 0.2 mm in all three directions (Lachaine and Falco 2013). For some fractions (6 of 48 scans), identification of the prostate was difficult, and therefore those 6 scans were excluded. Surprisingly, the prostate displacements from our study were less than all previous

Table 4.1: Mean, standard deviations (SD), max of prostate displacement, and displacements larger than 0.5, 1.0, 2.0 mm in all three directions, including Euclidean distance Max(D(t)).

	Directions			
	I(+)/S[1]	L(+)/R	A(+)/P	MaxD(t)[1]
Mean ± SD [mm]	-0.1 ± 0.8	0.2 ± 0.7	-0.1 ± 1.0	1.3 ± 0.7
Max displacement [mm]	1.2/-1.8	1.6/-1.1	2.6/-2.2	2.9
Displacement > 0.5 mm	49 %	47 %	58 %	81 %
Displacement > 1.0 mm	16 %	14 %	33 %	60 %
Displacement > 2.0 mm	0 %	0 %	5 %	16 %

[1]A/P, anterior-posterior; I/S, inferior-superior; L/R, left-right;
[2]Max(D(t)): maximum Euclidean distance

reported displacements in all directions, except for one study (Dobler et al. 2006). The reason might be that Dobler et al. were using a similar method as in our approach, i.e. observing the pressure displacements in real-time (They tracked the inserted seeds in Brachy therapy using the X-ray simulation, while applying TAUS probe) and, importantly, not using a US scan with minimal pressure as reference. Most of the other studies were implementing either US/US (Clarity system) or US/CT (BAT system) image matching in order to measure the prostate COM displacements (Artignan et al. 2004; Fargier-Voiron et al. 2014; Meer et al. 2013). For instance, in this study, the mean Euclidean distance of the prostate COM displacement was 1.3 mm, compared to Fargier-Voiron et al. (3.3 mm), Van der meer et al. (3.0 mm), and Artignan et al. (3.1 mm). Apart from the uncertainty of not applying real-time prostate monitoring in these studies, there are two other factors that might explain the greater Euclidean distances. Firstly, the US/US- and US/CT-matching is inter-operator dependent. For example, Van der Meer et al. investigated the US/US matching procedure to determine intra-, and inter-operator matching variability, and discovered the intra-operator/inter-operator variability (1 SD) to be 0.8 mm/1.8 mm (I/S), 0.7 mm/1.3 mm (L/R), and 1.0 mm/1.4 mm (A/P), respectively. In another study (Langen et al. 2008), the inter-operator variability in US/CT matching, among eight observers, was found to be larger than 2.0 mm in 50 % of the matches (difference between any two matches). Secondly, in these three studies they applied maximum pressure, not soft pressure, perceived to be sufficient to achieve adequate image quality. Additionally, Artignan et al. applied vertical pressure, using a rigid arm, enabling it to move towards the prostate i graded steps, which cannot reflect a real sweep technique, required in acquiring US images of the prostate.

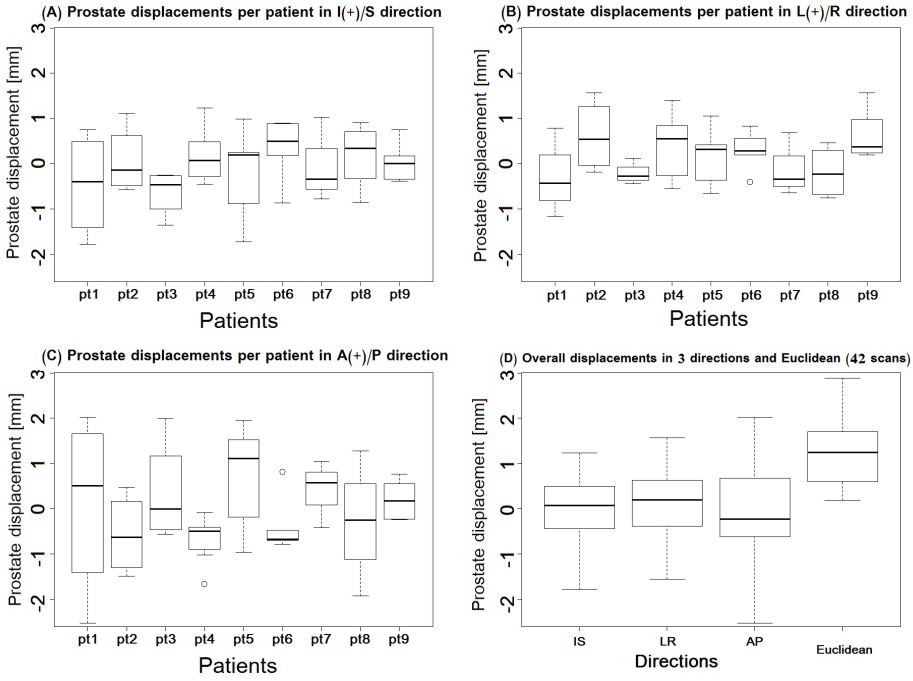

Figure 4.3: Boxplots of the prostate displacements; (A – C) Boxplots of the prostate displacements for nine patients in I/S, L/R, and A/P directions (D) Boxplot of overall prostate displacements in I/S, L/R, and A/P directions, including Euclidean distance. The horizontal band indicates the median, the lower and the upper edges of the box explain the first (25th), and third (75th) quartiles. The lower and the upper extremes of the whiskers, display the minimum and maximum values in absence of single data point outliers.

4.1.2 Limitations and Conclusion

Despite that our results were considered to have less uncertainties than the previously published studies, there are some limitations with the current study. First of all, it is desirable to acquire real US images, using the C-probe during TPUS prostate monitoring rather than using only a C-probe simulation. The question always remains as to whether the operators had used enough pressure to acquire good images, or how one operator can reproduce the same magnitude of pressure among the patients, or for different fractions of the same patient. In the present study, we were unable to simultaneously acquire TAUS images while TPUS monitoring, using the same US unit, since another Clarity system was required to do this. Moreover, although a gentle transperineal attach of the autoscan was carried out with caution, a counter-effect of the probe's head might influence the

position of the prostate, and hence changing the magnitude and likewise the direction of the prostate displacements during TAUS simulation.

In summary, the 4D TPUS autoscan is able to track prostate motion during C-probe TAUS simulation. We demonstrated that the probe pressure induces displacement of the prostate mostly is less than 2 mm in all three directions, which is perceived to be clinically irrelevant in prostate radiotherapy.

4.2 Intrafractional prostate motion

In prostate radiotherapy, it is important that the dose is delivered to the prostate, while minimizing the dose to the OARs. To achieve this, different reliable prostate IGRT methods are available, enabling positional correction for daily interfractional motion, such as surrogate implanted fiducial markers (Johnston et al. 2008; McNair et al. 2006; Scarbrough et al. 2006; Serago, Buskirk, et al. 2006). But, prostate displacement during treatment delivery (intrafractional) remains a challenge (Dawson 2000; Padhani 1999). Therefore, different real-time tracking methods are developed to monitor the prostate during radiotherapy (Bittner et al. 2010; Chan et al. 2008; Curtis et al. 2013; Tong et al. 2015; Wilbert et al. 2013). In this project the Clarity 4D TPUS autoscan was utilized to determine intrafractional prostate motion for approximately 2 to 2.5 minutes. To our knowledge, there is only one previously published paper based on the Clarity autoscan, in which six prostate patients were involved (Ballhausen et al. 2015).

The objective of the present study is to explore whether the intrafractional prostate motion is smaller than 2 mm, for a period of approximately 2-2.5 minutes, corresponding to the beam-on time for RapidArc delivery. The aim is also to investigate if there is any correlation between the patients' BMI-value and the magnitude of the displacement.

Ten prostate cancer patients were US scanned in the CT room (after CT scanning) and once a week in the treatment room (after treatment delivery) using the Clarity TPUS autoscan. The patients were aligned to the external lasers in the supine position, and asked to remain motionless during image acquisition and prostate monitoring. They were instructed to follow a moderate bladder-filling protocol. After CT scan and treatment delivery the patient was repositioned in preparation for the autoscan monitoring using the vendor provided autoscan base (Fig. 2.8), implying a different setup. The different setup is assumed not to have adverse impact on the results, since the aim of this study was to monitor the prostate during a certain time, corresponding to the duration of the treatment delivery. Initially, the autoscan probe is attached to the TPUS base, fixation cushions placed over the bases just under the patient's knees, and the probe, transperineally, pushed gently to the patient for scanning. The prostate monitoring was recorded for retrospective statistical analysis.

The patients were cooperative, despite the extra time of about 10 minutes, needed for patient repositioning in preparation to prostate monitoring. None of the patients showed any discomfort during the US prostate tracking. The overall mean values (51 TPUS curves) of the maximal intrafractional prostate displacements ($\pm$ 1SD [mm]) in three directions were; I(+)/S: (-0.2 $\pm$ 0.9); L(+)/R: (-0.2 $\pm$ 0.8); and A(+)/P: (-0.2 $\pm$ 1.1) (Table 4.2). The largest prostate displacement was 2.8 mm in posterior direction, and the percentage of sessions with displacements larger than 2.0 mm was 4 % (I/S), 2 % (L/R), and 10 % (A/P), respectively. The percentage of fractions with a Euclidean distance (3D vector) larger than 2.0 mm was 12 %. We found no correlation between BMI-value and the magnitude of the displacement.

We found pattern variations of the monitoring curves for different fractions, and we

Table 4.2: Intrafraction prostate motion in three directions and 3D vector; a comparison of the present study with previously published data using different systems.

Investigator year	N fractions	System	Time [min]	Mean of max prostate shifts (± SD) [mm] I(+)/S	L(+)/R	A(+)/P	% 3D vector shift	3D vector [mm]
Lometti et al., 2005[32]	11(133)	MV fluoroscopy: real-time FM tracking	1				> 2 mm 4 %	0.7 ± 0.5
Li. HS et al., 2008[4]	35(1267)	Calypso	12	0.3 ± 0.7	0.0 ± 0.3	0.4 ± 0.6		
Kupelian et al., 2008[2]	17(550)	Calypso	10				> 3 mm 14 %	
Langen et al., 2008[18]	17(550)	Calypso	2				> 3 mm 3 %	
Li et al., 2009[19]	20(157)	Calypso	11.4				> 3 mm 19 %	
Vargas et al., 2010[28]	7(68)	Cine-MRI	4					0.41 ± 1.2
Wang et al., 2011[33]	29(1061)	Calypso	3				> 3 mm 9 %	
Smeenk et al., 2011[29]	15(576)	Calypso	2.5				> 3 mm 1.4 %	
Ng et al., 2012[18]	10(268)	Real-time kV FM tracking	3-4				> 3 mm 5.6 %	
Mayyas et al., 2013[9]	8	pre- post treatment kV images		0.8 ± 2.7	0.2 ± 2.1	-0.3 ± 2.4		
Mayyas et al., 2013[9]	19	Calypso		0.0 ± 1.5	0.0 ± 0.6	0.0 ± 1.3		
Tong et al., 2015[8]	236(8660	Calypso	2				> 2 mm 13 %	
Choi et al., 2015[27]	17(550)	Transrectal US/3FMs	4.5	0.6 ± 0.6	-0.3 ± 0.3	-0.7 ± 0.6	> 2 mm 11 %	1.1 ± 0.8
Present study	**10(51)**	**Clarity real-time TPUS**	**2-2.5**	**0.2 ± 0.9**	**-0.2 ± 0.8**	**-0.2 ± 1.1**	**> 2 mm 12 %**	**0.9 ± 0.6**

Intrafractional motion of prostate patients (N) in 3D vector, I/S, inferior-superior, L/R, left-right, and A/P, anterior-posterior directions, using TPUS transperineal Clarity ultrasound (US) system, Calypso system, implanted fiducial markers, CINE-MRI, and endorectal balloon.

also observed larger prostate displacement with longer monitoring time (Fig. 4.4). This is obvious in figure 4.4 D, in which the 3D vector distance shows the larger displacement with monitoring time. Some of the fractions show that the prostate motion can be reversed, in a certain direction, to the initial position. Furthermore, the boxplot graph, analysis of maximal prostate displacements of 4-6 scans, displays variations between the patients and in the different directions (Fig. 4.5). The overall maximal prostate displacement in three directions and the Euclidean distances were shown to be less than 2.0 mm for most of the fractions (Fig.4.5 D).

Previously, many researchers have struggled to determine intrafrational prostate motion using pre- and post-treatment imaging methods (Adamson and Wu 2009; Kron et al. 2010), but the disadvantage of this method is inter-observer matching variability (Deegan et al. 2013). Another drawback with this method is that the prostate displacement might revert back to the initial position, which cannot be detected by using the pre- and post-treatment (Kotte et al. 2007). Therefore, a more favorable method is real-time prostate monitoring, in which the entire 3D prostate volume can be tracked. Our results are compared to other previously published data from different studies based on the utilization of different techniques (Table 4.2). The Calypso 4D localization electromagnetic tracking system has previously been confirmed to deliver precise and accurate tumor tracking, using the surrogate implanted tiny transponders in the cancerous tissues, which sends a signal to a station which tracks the 3D localization of the transponders (Shah et al. 2011). In a previous phantom study, a group found good agreement between the TPUS autoscan and Calypso system in tracking the embedded prostate-like sphere (Abramowitz et al. 2012).

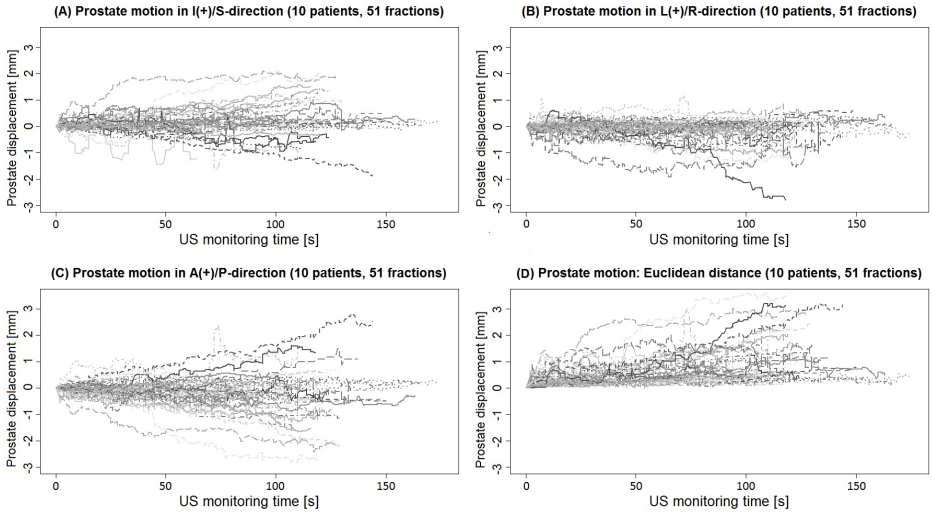

Figure 4.4: Intrafractional prostate displacement; (A-C) Monitoring graphs show the prostate motion for the total 51 US scans in I/S, L/R, and A/P directions, (D) The 3D vector displacement of the prostate center of mass.

In the current study, we observed that the prostate is not stationary during the tracking time, and displacements tend to increase with elapsed monitoring time (2-2.5 minutes), which is in line with the findings of other papers (Ballhausen et al. 2015). Furthermore, we noticed that, for most of the fractions, the intrafractional prostate motion was mostly smaller than 2 mm, and only 12 % of the 3D vector distances were larger than 2 mm, which is comparable to a study (using transrectal ultrasound scans to track three implanted fiducial markers) by (Choi et al. 2015), which observed that only 11 % of the 336 fractions the 3D vector displacement was larger than 2 mm during 4-5 minutes of monitoring. Similarly, in a Calypso study (35 patients and 1267 fractions) (Li et al. 2008), a research group reported that the intrafractional prostate motion is predominantly below 2 mm. Furthermore, in another study based on Cine-MRI imaging (Vargas et al. 2010), it was shown that the intrafractional prostate motion is smaller during supine fixation than in the prone position. In this project, all the US scans were carried out while the patients were in the supine position. Moreover, in a Calypso tracking study (15 patients and 576 fractions) (Smeenk et al. 2012), the prostate motion was shown to be larger than 3 mm in 1.4 % of the fractions during 2.5 minutes monitoring, but the percentage increased up to 18 % for a monitoring duration of 10 minutes. This increment of the prostate displacement was also observed in another recently published Calypso study (236 patients and 8660 fractions) (Tong et al. 2015), in which prostate motion was confirmed to be larger than

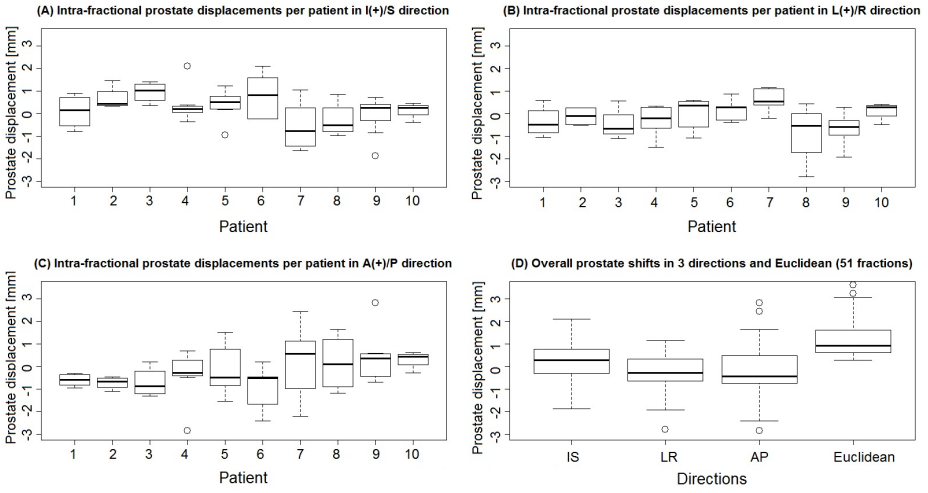

Figure 4.5: Boxplots of the intrafractional prostate displacements; (A-C) Boxplots of the prostate displacements for ten patients in I/S, L/R, and A/P directions. (D) Boxplot of overall prostate displacements in I/S, L/R, and A/P directions, including Euclidean (3D vector) distance.

3 mm in 20 % of the fractions, for a tracking time of 12 minutes. But they ascertained motion for the first three minutes is mostly smaller than 2 mm. Similarly, a research group conducted a study (37 patients and 1332 fractions) (Shelton et al. 2011), once again using the Calypso system, and concluded that the overall mean value of the 3D vector displacement is less than 3 mm for three minutes monitoring, but grew to up to 6.5 mm in the fourteenth minute. Likewise, once more in a Calypso study (17 patients and 550 fractions) (Kupelian et al. 2008), they detected that the prostate motion can be larger than 3 mm in 14 % of the scans for a time of 10 minutes. Furthermore, in a study of 11 patients and 133 fractions (Ng et al. 2012), using a real-time tracking of the fiducial markers, it was observed that in 62 % of the scans (3-4 minutes monitoring), the 3D vector displacement of the prostate was less than 1 mm, and only 6 % of the shifts were larger than 3 mm. In addition, Lometti et al. (32), using MV fluoroscopy and real-time fiducial marker tracking (11 patients and 133 fractions), confirmed that in only 4 % of the fractions was the displacement of the prostate larger than 2 mm while tracking for only one minute. Last, Mayyas et al. (9), in a comparison study of four different systems (27 patients and 1100 fractions), found that the percentage of intrafractional prostate shifts within $\pm$ 1.5 mm was 76 %, 94 %, and 82 % in the I/S, L/R, and A/P directions.

In short, the previously published results, in combination with our study, confirm that the intrafractional motion of the prostate is mostly less than 2 mm during the first 2

to 2.5 minutes of monitoring, and thus has insignificant adverse impact on the clinical outcome of prostate radiotherapy while employing advanced VMAT/ RapidArc. However, for conformal 3D planning and IMRT plans, the treatment delivery might last for up to 10 minutes, within which the prostate displacement grow to up to 7 mm. This large displacement might adversely affects the treatment response and outcome, and therefore should be taken into consideration.

CHAPTER 5

Conclusion and Perspectives

First and foremost, all the operators found the entire system to be cumbersome, especially performing the sweep-slide technique. Phantom scanning followed by volunteer imaging was perceived to be a good practical tool to acquaint the user with the system. As a result of several phantom scans, including two phantom studies, we recommend that if implementing the US system in a radiotherapy center, without previous experience, one should conduct similar phantom and volunteer scans to provide the responsible staff sufficient knowledge and confidence, before implementing it clinically. We recommend also that a US specialist (radiologist or oncologist) should be involved during the commencement phase to assist with image interpretation. Unfortunately, we lacked the involvement of a specialist while implementing the Clarity system in this project, resulting in frustrations among the operators while struggling to identify anatomical structures.

In the phantom pressure study, we concluded that the uterine COM displacement due to TAUS probe pressure is minimal and statistically insignificant. But, since a phantom cannot represent a real patient, the conclusion must be taken with caution.
In another phantom study to determine inter-operator variability, we found that variability in addressing the uterine position is small, thus clinically irrelevant. Once again, because the phantom does not reflect the real patients' pelvic structures, the employment of a clinical study is a necessity.

In the interfractional study of the US-IGRT (uterine match) relative to the bone structures, we found that the C-probe is capable of identifying daily uterine positional variations, but with limitations when it came to capturing the entire uterus owing to the difficulty of the sweep-slide technique. Consequently, this uncertainty impedes utilizing the C-probe as a reliable cervical IGRT method. For this reason, we suggested that the manufacturer design a prototype autoscan probe (A-probe), capable of automatic sweeping over the uterus, acquiring images in the sagittal plane rather than C-probe's transversal plane.
In a comparison study between the C-probe and A-probe, based on US-scanning of volunteers, the operators found the A-probe to be more user-friendly, and they realized that it was easier to identify the anatomical structures in the sagittal plane, and image acquisition was also performed smoothly, with less applied probe pressure. The results were promising, since the A-probe was capable of capturing the entire uterus in almost all of the scans. After this study we changed the C-probe to the A-probe for further uterine scans.
While comparing A-probe patient results to the C-probe patient study, we found large

delineation variability in C-probe images, yet again, confirming that the A-probe is a more reliable IGRT tool than the C-probe.
In brief, the C-probe is not a recommended cervical IGRT method. In contrast, the A-probe might replace the kV and MV IGRT systems, since it is capable of identifying the daily uterine shifts relative to the bone structures.

In the probe pressure study, we found that during prostate TAUS scanning the prostate displacement is, in most cases, clinically irrelevant. Since this conclusion was in opposition to most of the previously published results, which reported displacements of up to 7 mm, we discovered that 4D real-time monitoring is the most reliable method for determining pressure displacement compared to US/US or US/CT matching methods, in which the considerable inter-observer variability, due to variations in applied probe pressure and image/image match, limits the accuracy of the readings. Despite this clear conclusion, the limited number of patients and fractions reduces the generalizability of our statistical analysis.
In the intrafractional study, we confirmed that most intrafractional prostate motion is less than 2 mm with a duration of monitoring of 2 to 2.5 minutes, which was in concordance with previously reported data. Thus, during a RapidArc/VMAT plan delivery, the intrafractional prostate motion is negligible. But, since the motion increases with longer monitoring time, prostate displacement during 3D conformal and IMRT plans must be taken into consideration.

In short, our research demonstrated that there is a potential for applying ultrasound IGRT in cervical radiotherapy, especially using the A-probe. Despite our promising results regarding the A-probe, the question still remains open as to whether this would have any dosimetric advantages. Therefore, a study investigating the impact of uterine positional shifts on dosimetric outcomes is recommended.
The autoscan probe was also shown to be a good tracking tool capable of addressing prostate motion during treatment delivery. But a similar study based on the enrollment of greater numbers of patients and longer monitoring time is recommended. Moreover, we realized that the use of the US system in large radiotherapy centers will be a challenge, since it must involve a solid training program to give adequate practical experience, in order that the staff gain sufficient confidence before applying the system clinically.
Specifically, our conclusion in the probe pressure study with a phantom justifies a future clinical study, based on TAUS scanning of real cervical cancer patients engaged in real-time monitoring of the uterus, to observe the impact of probe pressure. One challenge of such a study might be the difficulty of conducting the 4D real-time tracking.
In addition, we recommend that a study similar to our interfractional uterine study should be conducted based on the enrollment of patient volunteers in greater numbers. Since we do not have more than one or two cervical cancer patients a month at our site, we could not perform a larger patient based study. But the principal question still remains, whether US IGRT, like many other IGRT methods, survive clinically if the real-time MRI guide, integrated into the MRI-LINAC, is in clinical use, unless the high cost of MRI is an obstacle. Finally, conducting adaptive radiation treatment to investigate the dosimetric

impact of interfractional uterine shifts (offline between fractions), and intrafractional prostate motion (in real time during the fraction) always remains as an optimal goal for further research.

Combined Bibliography

References from Chapter 1

Adamson, J. and Q. Wu (2009). "Inferences about prostate intrafraction motion from pre- and posttreatment volumetric imaging." In: *International journal of radiation oncology, biology, physics* 75.1, pp. 260–267 (cit. on p. 4).

Beadle, B. M., A. Jhingran, M. Salehpour, M. Sam, R. B. Iyer, and P. J. Eifel (2009). "Cervix regression and motion during the course of external beam chemoradiation for cervical cancer." In: *International journal of radiation oncology, biology, physics* 73.1, pp. 235–241 (cit. on pp. 1, 2).

Boda-Heggemann, J., F. M. Köhler, B. Kü, D. Wolff, H. H. Wertz, S. Mai, J. Hesser, F. Lohr, and F. Wenz (2008). "Accuracy of ultrasound-based (BAT) prostate-repositioning: a three-dimensional on-line fiducial-based assessment with cone-beam computed tomography". In: *IJROBP* 70.4, pp. 1247–1255 (cit. on p. 3).

Bunt, L. van de, I. M. J. Schulz, G. A. de Kort, J. M. Roesink, R. J. H. A. Tersteeg, and U. A. van der Heide (2008). "Motion and deformation of the target volumes during IMRT for cervical cancer: what margins do we need?" In: *Radiotherapy and oncology* 88.2, pp. 2233–2240. DOI: 10.1016/j.radonc.2007.12.017 (cit. on p. 3).

Chan, P., R. Dinniwell, M. Haider, Y. B. Cho, D. Jaffray, G. Lockwood, W. Levin, L. Manchul, A. Fyles, and M. Milosevic (2008). "Inter- and intrafractional tumor and organ movement in patients with cervical cancer undergoing radiotherapy: a cinematic-MRI point-of-interest study". In: *International journal of radiation oncology, biology, physics* 70.5, pp. 1507–1515 (cit. on pp. 1, 2, 4).

Dawson, L. (2000). "A comparison of ventilatory prostate movement in four treatment positions". In: *International journal of radiation oncology, biology, physics* 48.2, pp. 319–323 (cit. on p. 1).

Feigenberg, S. J., K. Paskalev, S. McNeeley, E. M. Horwitz, A. Konski, L. Wang, C. Ma, and A. Pollack (2007). "Comparing computed tomography localization with daily ultrasound during image-guided radiation therapy for the treatment of prostate cancer: a prospective evaluation". In: *Journal of applied clinical medical physics* 8.3, pp. 99–110 (cit. on p. 3).

Ghilezan, M., D. Jaffray, J. Siewerdsen, M. V. Herk, A. Shetty, M. Sharpe, S. Z. J. F.A., A. Vicini, R. Matter, C. Richard, D. Brabbins, and A. Martinez (2005). "Prostate gland motion assessed with cine-magnetic resonance imaging (cine-MRI)." In: *International journal of radiation oncology, biology, physics* 62.2, pp. 406–417 (cit. on pp. 1, 4).

Graham, J., A. Gee, and S.Hilton (2003). *Geometric uncertainties in radiotherapy of the prostate and bladder. In: Geometric uncertainties in radiotherapy.* London: British Institute of Radiology (cit. on p. 3).

Heide, U. van der, A. Kotte, H. Dehnad, P. Hofman, J. Lagenijk, and M. van Vulpen (2007). "Analysis of fiducial marker-based position verification in the external beam radiotherapy of patients with prostate cancer." In: *RO* 82.1, pp. 38–45 (cit. on p. 3).

Herk, M. V. (1995). "quantification of organ motion during conformal radiotherapy of the prostate by three dimensional image registration." In: *International journal of radiation oncology, biology, physics* 33.5, pp. 1311–1320 (cit. on p. 1).

Huang, E., L. Dong, A. Chandra, D. Kuban, I. I. Rosen, A. Evans, and A. Pollack (2002). "Intrafraction prostate motion during IMRT for prostate cancer". In: *International journal of radiation oncology, biology, physics* 53.2, pp. 261–268 (cit. on p. 1).

Kaatee, R., M. O. MJ, M. Venstraate, S. Quint, and B. Heijmen (2002). "DETECTION OF ORGAN MOVEMENT IN CERVIX CANCER PATIENTS USING A FLUOROSCOPIC ELECTRONIC PORTAL IMAGING DEVICE AND RADIOPAQUE MARKERS". In: *International journal of radiation oncology, biology, physics* 54.2, pp. 576–583 (cit. on p. 3).

Kerkhof, E. M., B. W. Raaymakers, U. A. van der Heide, L. van de Bunt, I. M. J. S. J. J. W., and Lagendijk (2008). "Online MRI guidance for healthy tissue sparing in patients with cervical cancer: an IMRT planning study." In: *Radiotherapy and oncology* 88.2, pp. 241–249 (cit. on p. 3).

Kitamura, K. (2002). "Three-dimensional intrafractional movement of prostate measured during real-time tumor-tracking radiotherapy in supine and prone treatment positions". In: *International journal of radiation oncology, biology, physics* 53.5, pp. 1117–1123 (cit. on p. 1).

Kron, T., J. Thomas, C. Fox, A. Thompson, R. Owen, A. Herschtal, A. Haworth, K. Tai, and F. Foroudi (2010). "Intra-fraction prostate displacement in radiotherapy estimated from pre- and post-treatment imaging of patients with implanted fiducial markers." In: *RO* 95.2, pp. 191–197 (cit. on p. 4).

Kupelian, P., K. Langen, T. Willoughby, O. Zeidan, and S. Meeks (2008). "Image-Guided Radiotherapy for Localized Prostate Cancer: Treating a Moving Target". In: *Semin. Radiat. Oncol.* 18.1, pp. 58–66 (cit. on p. 1).

Lachaine, M. and T. Falco (2013). "Intrafractional prostate motion management with the Clarity Autoscan system". In: *Med. Phys. Int.* 1.1, pp. 72–80 (cit. on p. 4).

Lagendijk, J. J. W., B. W. Raaymakers, A. J. E. Raaijmakers, J. Overweg, K. J. Brown, E. M. Kerkhof, R. W. van der Put, B. Haardemark, M. van Vulpen, and U. A. van der Heide (2008). "MRI/linac integration." In: *Radiotherapy and oncology* 86.1, pp. 25–29 (cit. on p. 3).

Langen, K. M. and D. Jones (2001). "Organ motion and its management". In: *International journal of radiation oncology, biology, physics* 50.1, pp. 265–278 (cit. on p. 1).

Lee, J. E., Y. Han, S. J. Huh, W. Park, M. G. Kang, Y. C. Ahn, and D. H. Lim (2007). "Interfractional variation of uterine position during radical RT: weekly CT evaluation." In: *Gynecologic oncology* 104.1, pp. 145–151 (cit. on p. 3).

Li, H., I. Chetty, C. Enke, R. Foster, T. Willoughby, P. Kupellian, and T. Solberg (2008). "Dosimetric consequences of intrafraction prostate motion." In: *International journal of radiation oncology, biology, physics* 71.3, pp. 801–812 (cit. on p. 1).

Li, J., M. Lin, M. Buyyounouski, E. Horwitz, and C. Ma (2013). "Reduction of prostate intrafractional motion from shortening the treatment time." In: *Phys. Med. Biol.* 58.14, pp. 4921–4932 (cit. on p. 4).

Li, X., X. Qi, M. Pitterle, K. Kalakota, K. Mueller, B. Erickson, D. Wang, C. Schultz, S. Firat, and J. Wilson (2007). "Interfractional variations in patient setup and anatomic change assessed by daily computed tomography." In: *International journal of radiation oncology, biology, physics* 68.2, pp. 581–591 (cit. on p. 3).

Lim, K., P. Chan, R. Dinniwell, A. Fyles, M. Haider, Y. B. Cho, D. Jaffray, L. Manchul, W. Levin, R. P. Hill, and M. Milosevic (2008). "Cervical cancer regression measured using weekly magnetic resonance imaging during fractionated radiotherapy: radiobiologic modeling and correlation with tumor hypoxia." In: *International journal of radiation oncology, biology, physics* 70.1, pp. 126–133 (cit. on p. 2).

Litzenberg, D., L. Dawson, H. Sandler, M. Sanda, D. McShan, R. K. T. Haken, K. L. Lam, K. K. Brock, and J. M. Balter (2002). "Daily prostate targeting using implanted radiopaque markers". In: *International journal of radiation oncology, biology, physics* 52.3, pp. 699–703 (cit. on p. 3).

Mackie, T., A. Rockwell, J. Kapatoes, K. Ruchala, W. Lu, C. Wu, G. O. L. F. W. Tome, J. Welsh, R. Jeraj, P. Harari, R. Reckwerdt, B. Paliwal, and M. Ritter (2003). "Image guidance for precise conformal radiotherapy". In: *International journal of radiation oncology, biology, physics* 56.1, pp. 89–105 (cit. on p. 1).

Mayyas, E., I. J. Chetty, M. Chetvertkov, N. Wen, T. Neicu, T. Nurushev, L. Ren, M. Lu, H. Stricker, D. Pradhan, B. Movsas, and M. Elshaikh (2013). "Evaluation of multiple image-based modalities for image-guided radiation therapy (IGRT) of prostate carcinoma: a prospective study." In: *Med. Phys.* 40.4, pp. 0417071–0417079 (cit. on p. 4).

Meijer, G., C. Rasch, P. Remeijer, and J. Lebesque (2003). "Three-dimensional analysis of delineation errors, setup errors, and organ motion during radiotherapy of bladder cancer." In: *International journal of radiation oncology, biology, physics* 55.5, pp. 1277–1287 (cit. on p. 3).

Mutanga, T. F., H. de Boer, V. Rajan, M. Dirkx, L. Incrocci, and B. Heijmen (2012). "Day-to-day reproducibility of prostate intrafraction motion assessed by multiple kV and MV imaging of implanted markers during treatment." In: *International journal of radiation oncology, biology, physics* 83.1, pp. 400–407 (cit. on p. 4).

Nam, H., W. Park, S. J. Huh, D. S. Bae, B. G. Kim, J. H. Lee, J. W. Lee, D. H. Lim, Y. Han, H. C. Park, and Y. C. Ahn (2007). "The prognostic significance of tumor

volume regression during radiotherapy and concurrent chemoradiotherapy for cervical cancer using MRI." In: *Gynecologic oncology* 107.2, pp. 320–325 (cit. on p. 2).

Padhani, A. (1999). "Evaluating the effect of rectal distension and rectal movement on prostate gland position using cine MRI". In: *International journal of radiation oncology, biology, physics* 44.3, pp. 525–533 (cit. on p. 1).

Salama, J. K., A. J. Mundt, J. Roeske, and N. Mehta (2006). "Preliminary outcome and toxicity report of extended-field, intensity-modulated radiation therapy for gynecologic malignancies." In: *International journal of radiation oncology, biology, physics* 65.4, pp. 1170–1176 (cit. on p. 1).

Scarbrough, J. T., N. M. Golden, J. Y. Ting, C. D. Fuller, A. K. Wong, P. A. Kupelian, and C. R. Thomas (2006). "Comparison of ultrasound and implanted seed marker prostate localization methods: Implications for image-guided radiotherapy". In: *IJROBP* 65.2, pp. 378–387 (cit. on p. 1).

Tong, X., X. Chen, J. Li, Q. Xu, M. Lin, L. Chen, R. Price, and C. Ma (2015). "Intrafractional prostate motion during external beam radiotherapy monitored by a real-time target localization system". In: *J. OF APPLIED CLINICAL MEDICAL PHYSICS* 16.2, pp. 51–61 (cit. on p. 4).

References from Chapter 2

Middleton, W., A. Kurtz, and B. Hertzberg (2004). *Practical physics in ultrasound*. 3-27. 2nd ed. St Louis, MO: Mosby (cit. on p. 11).

Weyman, A. (1994). *Physical principles of ultrasound*. 3-28. Media, PA: Williams & Wilkins (cit. on p. 10).

References from Chapter 3

Ahmad, R., M. S. Hoogeman, M. Bondar, V. Dhawtal, S. Quint, I. D. Pree, J. W. Mens, and B. J. M. Heijmen (2011). "Increasing treatment accuracy for cervical cancer patients using correlations between bladder-filling change and cervix-uterus displacements: proof of principle." In: *Radiotherapy and oncology* 98.3, pp. 340–346 (cit. on p. 27).

Boda-Heggemann, J., F. M. Köhler, B. Kü, D. Wolff, H. H. Wertz, S. Mai, J. Hesser, F. Lohr, and F. Wenz (2008). "Accuracy of ultrasound-based (BAT) prostate-repositioning: a three-dimensional on-line fiducial-based assessment with cone-beam computed tomography". In: *IJROBP* 70.4, pp. 1247–1255 (cit. on p. 22).

Chan, P., R. Dinniwell, M. Haider, Y. B. Cho, D. Jaffray, G. Lockwood, W. Levin, L. Manchul, A. Fyles, and M. Milosevic (2008). "Inter- and intrafractional tumor and organ movement in patients with cervical cancer undergoing radiotherapy: a cinematic-MRI point-of-interest study". In: *International journal of radiation oncology, biology, physics* 70.5, pp. 1507–1515 (cit. on p. 23).

Cury, F. L. B., G. Shenouda, L. Souhami, M. Duclos, S. L. M. David, F. Verhaegen, R. Cornsbert, and T. Falco (2006). "Ultrasound-based image guided radiotherapy for prostate cancer: comparison of cross-modality and intramodality methods for daily localization during external beam radiotherapy". In: *IJROBP* 66.5, pp. 1562–1567 (cit. on p. 22).

Fuss, M. (2003). "Daily stereotactic ultrasound prostate targeting: Inter-user variability". In: *Technol. CANCER Res. Treat.* 2.2, pp. 161–169 (cit. on p. 25).

Johnston, H., M. Hilts, W. Beckham, and E. Berthelet (2008). "3D ultrasound for prostate localization in radiation therapy: A comparison with implanted fiducial markers". In: *Med. Phys.* 35.6, pp. 2403–2413 (cit. on p. 27).

Jurgenliemk-Schulz, I. M., M. Z. Toet-Bosma, G. A. P. de Kort, H. W. Schreuder, J. M. Roesink, R. J. H. Tersteeg, and U. A. van der Heide (2011). "Internal motion of the vagina after hysterectomy for gynaecological cancer". In: *Radiotherapy and oncology* 98.2, pp. 244–248 (cit. on p. 23).

Lachaine, M. and T. Falco (2013). "Intrafractional prostate motion management with the Clarity Autoscan system". In: *Med. Phys. Int.* 1.1, pp. 72–80 (cit. on p. 28).

Lee, J. E., Y. Han, S. J. Huh, W. Park, M. G. Kang, Y. C. Ahn, and D. H. Lim (2007). "Interfractional variation of uterine position during radical RT: weekly CT evaluation." In: *Gynecologic oncology* 104.1, pp. 145–151 (cit. on p. 27).

McGahan, J. P., J. Ryu, and M. Fogata (2004). "Ultrasound probe pressure as a source of error in prostate localization for external beam radiotherapy". In: *IJTOBP* 60.3, pp. 788–793 (cit. on p. 22).

Molloya, J. A., G. Chan, A. Markovic, S. McNeeley, D. Pfeiffer, B. Salter, and W. A. Tome (2011). "Quality assurance of U.S.-guided external beam radiotherapy for prostate cancer: Report of AAPM Task Group 154". In: *Medical Physics* 38.2, pp. 858–871 (cit. on p. 25).

Pinkawa, M., M. Pursch-Lee, B. Asadpour, B. Gagel, M. Piroth, J. Klotz, S. Nussen, and M. J. Eble (2008). "Image-guided radiotherapy for prostate cancer. Implementation of ultrasound-based prostate localization for the analysis of inter- and intrafraction organ motion". In: *Strahlentherapie und Onkologie* 184.12, pp. 679–685 (cit. on p. 22).

Scarbrough, J. T., N. M. Golden, J. Y. Ting, C. D. Fuller, A. K. Wong, P. A. Kupelian, and C. R. Thomas (2006). "Comparison of ultrasound and implanted seed marker prostate localization methods: Implications for image-guided radiotherapy". In: *IJROBP* 65.2, pp. 378–387 (cit. on p. 22).

Serago, C. F., S. J. Buskirk, T. C. Igel, A. A. Gale, N. E. Serago, and J. D. Earle (2006). "Comparison of daily megavoltage electronic portal imaging or kilovoltage imaging with marker seeds to ultrasound imaging or skin marks for prostate localization and treatment positioning in patients with prostate cancer". In: *IJROBP* 65.5, pp. 1585–1592 (cit. on p. 22).

Serago, C. F., S. J. Chungbin, S. J. Buskirk, G. Ezzell, A. C. Collie, and S. A. Vora (2002). "Initial experience with ultrasound localization for positioning prostate cancer patients for external beam radiotherapy". In: *IJTOBP* 53.5, pp. 1130–1138 (cit. on pp. 22, 24).

Taylor, A. and M. Powell (2008). “An assessment of interfractional uterine and cervical motion: implications for radiotherapy target volume definition in gynaecological cancer”. In: *Radiotherapy and oncology : journal of the European Society for Therapeutic Radiology and Oncology* 88.2, pp. 250–257 (cit. on p. 24).

References from Chapter 4

Abramowitz, M., E. Bossart, R. Flook, X. Wu, R. Brooks, M. Lachaine, F. Lathuiliere, and A. Pollack (2012). “Noninvasive Real-time Prostate Tracking Using a Transperineal Ultrasound Approach”. In: *International journal of radiation oncology, biology, physics* 84.3, pp. 133–134 (cit. on p. 44).

Adamson, J. and Q. Wu (2009). “Inferences about prostate intrafraction motion from pre- and posttreatment volumetric imaging.” In: *International journal of radiation oncology, biology, physics* 75.1, pp. 260–267 (cit. on p. 44).

Artignan, X., M. Smitsmans, J. Lebesque, D. Jaffray, M. van Her, and H. Bartelink (2004). “Online ultrasound image guidance for radiotherapy of prostate cancer: impact of image acquisition on prostate displacement.” In: *International journal of radiation oncology, biology, physics* 59.2, pp. 595–601 (cit. on pp. 37, 40).

Ballhausen, H., M. Li, N. Hegemann, U. Ganswindt, and C. Belka (2015). “Intra-fraction motion of the prostate is a random walk”. In: *Phys. Med. Biol.* 60.2, pp. 549–563 (cit. on pp. 43, 45).

Bittner, N., W. M. Butler, J. L. Reed, B. Murray, B. S. Kurko, K. E. Wallner, and G. S. Merrick (2010). “Electromagnetic tracking of intrafraction prostate displacement in patients externally immobilized in the prone position.” In: *International journal of radiation oncology, biology, physics* 77.2, pp. 490–495 (cit. on p. 43).

Chan, P., R. Dinniwell, M. Haider, Y. B. Cho, D. Jaffray, G. Lockwood, W. Levin, L. Manchul, A. Fyles, and M. Milosevic (2008). “Inter- and intrafractional tumor and organ movement in patients with cervical cancer undergoing radiotherapy: a cinematic-MRI point-of-interest study”. In: *International journal of radiation oncology, biology, physics* 70.5, pp. 1507–1515 (cit. on p. 43).

Choi, Y., D. Kwak, H. S. Lee, W. J. Hur, W. Y. Cho, G. Sung, T. Kim, S. Kim, and S. Yun (2015). “Effect of rectal enema on intrafraction prostate movement during image-guided radiotherapy”. In: *J. Medical Imaging Radiation Oncology* 59.2, pp. 236–242 (cit. on p. 45).

Curtis, W., M. Khan, A. Magnelli, K. Stephans, R. T. P., and Xia (2013). “Relationship of imaging frequency and planning margin to account for intrafraction prostate motion: analysis based on real-time monitoring data.” In: *International journal of radiation oncology, biology, physics* 85.3, pp. 700–706 (cit. on p. 43).

Cury, F. L. B., G. Shenouda, L. Souhami, M. Duclos, S. L. M. David, F. Verhaegen, R. Cornsbert, and T. Falco (2006). “Ultrasound-based image guided radiotherapy for prostate cancer: comparison of cross-modality and intramodality methods for daily

localization during external beam radiotherapy". In: *IJROBP* 66.5, pp. 1562–1567 (cit. on p. 37).

Dawson, L. (2000). "A comparison of ventilatory prostate movement in four treatment positions". In: *International journal of radiation oncology, biology, physics* 48.2, pp. 319–323 (cit. on p. 43).

Deegan, T., R. O. ans T. Holt T, L. Roberts, J. Biggs, A. McCarthy, M. Parfitt, and A. Fielding (2013). "Interobserver variability of radiation therapists aligning to fiducial markers for prostate radiation therapy." In: *J Med Imaging Radiat Oncol.* 57.4, pp. 519–523 (cit. on p. 44).

Dobler, B., S. Mai, C. Ross, D. Wolff, H. Wertz, F. Lohr, and F. Wenz (2006). "Evaluation of possible prostate displacement induced by pressure applied during transabdominal ultrasound image acquisition." In: *Strahlenther. Onkol.* 182.4, pp. 240–246 (cit. on p. 40).

Fargier-Voiron, M., B. Presles, P. Pommier, S. Rit, A. Munoz, and H. Liebgott (2014). "Impact of probe pressur variability on prostate localization for ultrasound-based image-guided radiotherapy." In: *RO* 111, pp. 132–137 (cit. on pp. 37, 40).

Feigenberg, S. J., K. Paskalev, S. McNeeley, E. M. Horwitz, A. Konski, L. Wang, C. Ma, and A. Pollack (2007). "Comparing computed tomography localization with daily ultrasound during image-guided radiation therapy for the treatment of prostate cancer: a prospective evaluation". In: *Journal of applied clinical medical physics* 8.3, pp. 99–110 (cit. on p. 37).

Heuvel, F. V. den, T. Powell, E. Seppi, P. Littrupp, M. Khan, Y. Wang, and J. Forman (2003). "Independent verification of ultrasound based image-guided radiation treatment, using electronic portal imaging and implanted gold markers". In: *Med. Phys.* 30.11, pp. 2878–2879 (cit. on p. 37).

Johnston, H., M. Hilts, W. Beckham, and E. Berthelet (2008). "3D ultrasound for prostate localization in radiation therapy: A comparison with implanted fiducial markers". In: *Med. Phys.* 35.6, pp. 2403–2413 (cit. on pp. 37, 43).

Kotte, A. N. T. J., P. Hofman, J. J. W. Lagendijk, M. van Vulpen, and U. A. van der Heide. (2007). "Intrafraction Motion of the Prostate During External-Beam Radiation Therapy: Analysis of 427 Patients with Implanted Fiducial Markers". In: *International journal of radiation oncology, biology, physics* 69.2, pp. 419–425 (cit. on p. 44).

Kron, T., J. Thomas, C. Fox, A. Thompson, R. Owen, A. Herschtal, A. Haworth, K. Tai, and F. Foroudi (2010). "Intra-fraction prostate displacement in radiotherapy estimated from pre- and post-treatment imaging of patients with implanted fiducial markers." In: *RO* 95.2, pp. 191–197 (cit. on p. 44).

Kupelian, P., K. Langen, T. Willoughby, O. Zeidan, and S. Meeks (2008). "Image-Guided Radiotherapy for Localized Prostate Cancer: Treating a Moving Target". In: *Semin. Radiat. Oncol.* 18.1, pp. 58–66 (cit. on p. 46).

Lachaine, M. and T. Falco (2013). "Intrafractional prostate motion management with the Clarity Autoscan system". In: *Med. Phys. Int.* 1.1, pp. 72–80 (cit. on p. 39).

Langen, K., T. Willoughby, S. Meeks, A. Santhanam, A. Cunningham, L. Levin, and P. Kupelian (2008). "Observations on real-time prostate gland motion using electromagnetic tracking." In: *International journal of radiation oncology, biology, physics* 71.4, pp. 1084–1090 (cit. on p. 40).

Li, H., I. Chetty, C. Enke, R. Foster, T. Willoughby, P. Kupellian, and T. Solberg (2008). "Dosimetric consequences of intrafraction prostate motion." In: *International journal of radiation oncology, biology, physics* 71.3, pp. 801–812 (cit. on p. 45).

McGahan, J. P., J. Ryu, and M. Fogata (2004). "Ultrasound probe pressure as a source of error in prostate localization for external beam radiotherapy". In: *IJTOBP* 60.3, pp. 788–793 (cit. on p. 37).

McNair, H., S. A. Mangar, J. Coffey, B. Shoulders, V. N. Hansen, A. Norman, J. Staffurth, S. A. Sohaib, A. P. Warrington, and D. P. Dearnaley (2006). "A comparison of CT- and ultrasound-based imaging to localize the prostate for external beam radiotherapy". In: *IJROBP* 65.3, pp. 678–687 (cit. on pp. 37, 43).

Meer, S. van der, G. Bloemen-van, J. Hermans, R. Voncken, D. Heuvelmans, C. Gubbels, D. Fontanarosa, P. Visser, L. Lutgens, F. van Gils, and F. Verhaegen (2013). "Critical assessment of intramodality 3D ultrasound imaging for prostate IGRT compared to fiducial markers." In: *Med. Phys.* 40.2013, pp. 0717071–07170711 (cit. on pp. 37, 40).

Ng, J., J. Booth, P. Poulsen, W. Fledelius, E. Worm, and T. E. et al. (2012). "Kilovoltage intrafraction". In: *International journal of radiation oncology, biology, physics* 84.5, pp. 655–661 (cit. on p. 46).

Padhani, A. (1999). "Evaluating the effect of rectal distension and rectal movement on prostate gland position using cine MRI". In: *International journal of radiation oncology, biology, physics* 44.3, pp. 525–533 (cit. on p. 43).

Peng, C., K. Kainz, C. Lawton, and X. A. Li (2008). "A comparison of daily megavoltage CT and ultrasound image guided radiation therapy for prostate cancer". In: *Med. Phys.* 35.12, pp. 5619–5628 (cit. on p. 37).

Pinkawa, M., M. Pursch-Lee, B. Asadpour, B. Gagel, M. Piroth, J. Klotz, S. Nussen, and M. J. Eble (2008). "Image-guided radiotherapy for prostate cancer. Implementation of ultrasound-based prostate localization for the analysis of inter- and intrafraction organ motion". In: *Strahlentherapie und Onkologie* 184.12, pp. 679–685 (cit. on p. 37).

Scarbrough, J. T., N. M. Golden, J. Y. Ting, C. D. Fuller, A. K. Wong, P. A. Kupelian, and C. R. Thomas (2006). "Comparison of ultrasound and implanted seed marker prostate localization methods: Implications for image-guided radiotherapy". In: *IJROBP* 65.2, pp. 378–387 (cit. on pp. 37, 43).

Serago, C. F., S. J. Buskirk, T. C. Igel, A. A. Gale, N. E. Serago, and J. D. Earle (2006). "Comparison of daily megavoltage electronic portal imaging or kilovoltage imaging with marker seeds to ultrasound imaging or skin marks for prostate localization and treatment positioning in patients with prostate cancer". In: *IJROBP* 65.5, pp. 1585–1592 (cit. on pp. 37, 43).

Serago, C. F., S. J. Chungbin, S. J. Buskirk, G. Ezzell, A. C. Collie, and S. A. Vora (2002). "Initial experience with ultrasound localization for positioning prostate cancer patients for external beam radiotherapy". In: *IJTOBP* 53.5, pp. 1130–1138 (cit. on p. 37).

Shah, A. P., P. A. Kupelian, T. R. Willoughby, and S. L. Meeks (2011). "Expanding the use of real-time electromagnetic tracking in radiation oncology". In: *J. of applied clinical medical physics* 12.4, pp. 34–49 (cit. on p. 44).

Shelton, J., P. J. Rossi, H. Chen, Y. Liu, V. A. Master, and A. B. A. B. Jani (2011). "Observations on prostate intrafraction motion and the effect of reduced treatment time using volumetric modulated arc therapy". In: *Pract. Radiat. Oncol.* 1.4, pp. 243–250 (cit. on p. 46).

Smeenk, R., R. Louwe, K. Langen, A. Shah, P. Kupelian, E. van Lin, and J. Kaanders (2012). "An endorectal balloon reduces intrafraction prostate motion during radiotherapy." In: *International journal of radiation oncology, biology, physics* 83.2, pp. 661–669 (cit. on p. 45).

Tong, X., X. Chen, J. Li, Q. Xu, M. Lin, L. Chen, R. Price, and C. Ma (2015). "Intrafractional prostate motion during external beam radiotherapy monitored by a real-time target localization system". In: *J. OF APPLIED CLINICAL MEDICAL PHYSICS* 16.2, pp. 51–61 (cit. on pp. 43, 45).

Vargas, C., A. Saito, W. Hsi, D. Indelicato, A. Falchook, Q. Zengm, K. Oliver, S. Keole, and J. Dempsey (2010). "Cine-magnetic resonance imaging assessment of intrafraction motion for prostate cancer patients supine or prone with and without a rectal balloon." In: *Am. J. Clin. Oncol.* 33.1, pp. 11–6 (cit. on p. 45).

Wilbert, J., K. Baier, C. Hermann, M. Flentjel, and M. Guckenberger (2013). "Accuracy of real-time couch tracking during 3-dimensional conformal radiation therapy, intensity modulated radiation therapy, and volumetric modulated arc therapy for prostate cancer." In: *International journal of radiation oncology, biology, physics* 85.1, pp. 237–242 (cit. on p. 43).

Appendices

APPENDIX A

Information til patienter med livmoderhalskræft, om deltagelse i et videnskabeligt studie (indeholder samtykkeerklæring/fuldmagt)

(In Danish)

Responsible for the project: Medical Physicist, MSc, PhD-candidate, Mariwan Baker.

Registrering af livmoderens placering ved hjælp af ultralydsscanning under udvendig strålebehandling hos patienter med livmoderhalskræft

Onkologisk Afdeling R, Herlev Hospital

A.1 Vil du deltage i et videnskabeligt forsøg, der vedrører fremtidig strålebehandlingaf livmoderhalskræft?

Du er henvist til Onkologisk Afdeling R med henblik på strålebehandling af livmoderhalskræft. I denne deltagerinformation vil vi beskrive, hvad projektet går ud på, og hvad en eventuel deltagelse vil betyde for dig. Det er derfor vigtigt, at du læser informationen grundigt igennem. Du vil også blive informeret mundtligt om projektet af en læge og få mulighed for at stille spørgsmål. Du har ret til betænkningstid før du beslutter dig for, om du vil deltage i forsøget.

Vi vil spørge dig, om du vil deltage i et videnskabeligt projekt. Projektet bliver udført ved at bruge et ultralydssystem, kaldet Clarity. Clarity er udviklet af Elekta, som producerer teknisk medicinsk udstyr. Vi forventer, at i alt 30 patienter deltager i studiet, som foregår i stråleterapien på Herlev Hospital.

A.2 Frivillig deltagelse

Det er frivilligt at deltage, og du kan først deltage kan, efter at vi har modtaget dit skriftlige samtykke. Du kan til enhver tid trække dit samtykke tilbage og udstræde af projektet. Du skal blot give besked til lægen eller en fra personalet i Stråleterapien. Du vælger selv, om du vil angive årsagen til, at du ønsker at stoppe din deltagelse i projektet. Uanset om du siger ja eller nej til at deltage i dette projekt, eller fortryder senere, vil din nuværende behandling ikke blive påvirket. Hvis du beslutter dig for at sige ja til at deltage, skal du underskrive et skriftligt informeret samtykke. Vi beder dig også om at læse det vedlagte materiale Forsøgspersonens rettigheder i et biomedicinsk forskningsprojekt.

A.3 Formål

Clarity-systemet er beregnet til at lokalisere livmoderens placering ved hjælp af ultralyd. Du får ikke direkte gavn af ultralydsscanningerne og modtager heller ikke svar på disse, men din deltagelse i projektet vil, give ny viden om lokalisering af behandlingsområdet og hermed forhåbentlig forbedre strålebehandlingen for andre med samme sygdom.

A.4 Studiets praktiske forløb

For at planlægge din strålebehandling, får du foretaget en CT-scanning. Denne scanning giver vi alle patienter, der skal have strålebehandling. Umiddelbart efter CT-scanningen, vil du blive ultralydsscannet. I praksis betyder det, at en radiograf eller sygeplejerske fører en ultralydsscanner hen over din mave, så din livmoderhals kan ses på en skærm. Det tager ca. 60 minutter i alt. Når du starter dit strålebehandlingsforløb vil du ca 2 gange om uge blive behandlet og ultralydsscannet på apparat ?Odin?. Disse dage vil den samlede behandlingstid være ca. 30 minutter.

A.5 Bivirkninger

Scanningen gør ikke ondt, og der er ingen bivirkninger ved ultralydsscanning.

A.6 Fortrolighed

Al opbevaring af oplysninger vil ske i henhold til gældende regler i persondataloven. Dit navn og CPR-nummer bliver ikke givet videre til nogen. Din anonymitet vil blive sikret således, ingen oplysninger vil kunne føres tilbage til den enkelte deltager ved offentliggørelse af resultaterne. Du kan til hver en tid trække dit samtykke tilbage, hvilket betyder, at der herefter ikke vil blive foretaget yderligere dataindsamling om dig i forbindelse med projektet.

A.7 Information til din egen læge

Din egen læge vil blive orienteret om din deltagelse, hvis du giver din tilladelse.

A.8 Økonomi

Du vil ikke modtage betaling for at deltage i projektet. Studiet er sponsoreret af Elekta. Elektas sponsorat omfatter finansieringen af en Ph.d.-stilling til forskning i forbedring af teknologiens muligheder til fordel for patienterne.

A.9 Kompensation for skader

Du er omfattet af patientforsikringsordningen jf. lov om patientforsikring. Som deltager i kliniske forsøg, er du tillige omfattet af de samme offentlige forsikringsordninger som ved al anden behandling i det danske sundhedsvæsen.

A.10 Adgang til studieresultater

Resultaterne af studiet søges udgivet i et anerkendt engelsksproget tidsskrift samt ved internationale konferencer, hvis de viser sig brugbare. Hvis du er interesseret, kan du efter afslutning af projektperioden og færdiggørelse af dataanalysen, kontakte den ansvarlige -fysiker/Ph.d.-kandidat Mariwan Baker, for yderligere information.
Vi håber, du med denne information har fået tilstrækkeligt indblik i, hvad det vil sige at deltage i projektet, og at du på denne baggrund kan afgøre, om du vil medvirke.

Forsøgsansvarlig for projektet er:
Hospitalsfysiker, PhD-student, Mariwan Baker

Onkologisk Afdeling R, 51AA
Herlev Hospital
e-mail: mariwan.baker@regionh.dk
Lægeansvarlig, Overlæge, Trine Juhler-Nøttrup
Onkologisk Afdeling R, 51AA
Herlev Hospital
Tlf.: 38684856
e-mail: trine.juhler-noettrup@regionh.dk

Informeret samtykke til deltagelse i et biomedicinsk forskningsprojekt.
Registrering af livmoderens placering ved hjælp af ultralyds-scanning under udvendig strålebehandling hos patienter med livmoderhalskræft

A.11 Erklæring fra forsøgspersonen:

Jeg har fået skriftlig og mundtlig information og jeg ved nok om formål, metode, fordele og ulemper til at sige ja til at deltage. Jeg ved, at det er frivilligt at deltage, og at jeg altid kan trække mit samtykke tilbage uden at miste mine nuværende eller fremtidige rettigheder til behandling. Jeg giver samtykke til, at deltage i forskningsprojektet og har fået en kopi af dette samtykkeark samt en kopi af den skriftlige information om projektet til eget brug.
Forsøgspersonens navn:————————————————————-
Dato:———————— Underskrift: ——————- Hvis der kommer nye væsentlige helbredsoplysninger frem om dig i forskningsprojektet vil du blive informeret. Vil du frabede dig information om nye væsentlige helbredsoplysninger, som kommer frem i forskningsprojektet, bedes du markere her: (sæt x)

ønsker du at blive informeret om forskningsprojektets resultat samt eventuelle konsekvenser for dig?:

Ja ————- (sæt x) Nej ————-(sæt x)

APPENDIX B

Information til prostatapatienter,om deltagelse i et videnskabeligt forsøg(indeholder samtykkeerklæring/fuldmagt)

(In Danish)

Responsible for the project: Medical Physicist, MSc, PhD-candidate, Mariwan Baker.

Kontrol af lejring af prostata patienter under udvendig strålebehandling ved hjælp af ultralyd

Onkologisk Afdeling R, Herlev Hospital

B.1 Vil du deltage i et videnskabeligt forsøg, der vedrører fremtidig stråle-behandlingen af af prostata-cancer?

I denne deltagerinformation vil vi beskrive, hvad forsøget går ud på, og hvad deltagelse vil betyde for dig. Det er derfor vigtigt, at du læser informationen grundigt igennem. Du vil også blive informeret mundtligt om forsøget af en læge og få mulighed for at stille spørgsmål. Det vil være en god idé at have en pårørende med, når du bliver informeret, så I er to til at stille spørgsmål og tale om din eventuelle deltagelse. Du har ret til betænkningstid før du beslutter dig for, om du vil deltage i forsøget.
Du er henvist til onkologisk afdeling med henblik på strålebehandling af din prostatacancer. Når du skal have strålebehandling, er det vigtig at skåne så meget af det omgivende normale væv som muligt.

Vi vil spørge dig om du vil deltage i et videnskabeligt forsøg Forsøget bliver udført ved at bruge et nyt ultralyd billede-system, kaldet Clarity (som er udviklet af Elekta) . I praksis betyder det, at en radiograf eller sygeplejerske anbringer en ultralydsscanner på lejet imellem dine ben, og ultralydssscanner mod mellemkødet lige under testiklerne, så din prostata kan ses på en skærm. Det gør ikke ondt, og der er ingen bivirkninger . Det forventes, at i alt 30 patienter deltager i forsøget, som foregår i stråleterapien på Herlev Hospital.

B.2 Frivillig deltagelse

Det er frivilligt at deltage, og du kan først deltage kan, efter at vi har modtaget dit skriftlige samtykke. Du kan til enhver tid trække dit samtykke tilbage og udstræde af projektet. Du skal blot give besked til lægen eller en fra personalet i Stråleterapien. Du vælger selv, om du vil angive årsagen til, at du ønsker at stoppe din deltagelse i projektet. Uanset om du siger ja eller nej til at deltage i dette projekt, eller fortryder senere, vil din nuværende behandling ikke blive påvirket.
Hvis du beslutter dig for at sige ja til at deltage, skal du underskrive et skriftligt informeret samtykke. Vi beder dig også om at læse det vedlagte materiale (Forsøgspersonens rettigheder i et biomedicinsk forskningsprojekt).

B.3 Formål

Formål med forsøget er at vurderer kapaciteten af den nye ultralyd systemet til at evaluere prostata bevægelse i løbet af selve strålebehandlingen.
Clarity-ultralyd-systemet er beregnet til at lokalisere prostatas placering i kroppen og monitorere denne placering under strålebehandlingen.

B.4 Forsøget forløb

Hvordan foregår det?
Ved planlægningen af din strålebehandling, får du foretaget en CT-scanning med henblik på planlægning af behandlingen. Denne skanning er normal procedure hos alle patienter der skal have strålebehandling.
Umiddelbart efter CT scanning, vil du blive ultralyd scannet . I hele behandlingsforløbet (typisk 39 behandlinger) vil der før hver strålebehandling, blive taget digitale-røntgen billeder til kontrol af opstillingen. I løbet af disse behandlinger, vil du blive behandlet på apparat Odin, hvor vi umiddelbart efter afslutningen af selve stråle-behandlingen, vil ultralyds-scanne dig. Selve scanningen tager få minutter og er ikke forbundet med ubehag.

I forbindelse med de strålebehandlinger, hvor du skal ultralydscannes vil behandlingstiden være 10 minutter.

B.5 Nytte ved forsøget

Din deltagelse i forsøget vil forhåbentligt bibringe information som i fremtiden kan hjælpe andre med lignende sygdomme. Resultaterne vil give øget viden om lokalisering af behandlingsområdet under selve behandlingen.

B.6 Bivirkninger, risici, komplikationer og ulemper

Undersøgelsen er ufarlig og udføres af kvalificeret personale. Der er ingen kendte skadelige effekter ved ultralydsskanning. Der er ingen ulemper forbundet med forsøget, udover at nogen patient kan føle lidt ubehag under selve ultralyde- scanningen.
Den øvrige del af planlægningen og behandlingen ændres ikke p.g.a. forsøget.

B.7 Fortrolighed

Al opbevaring af oplysninger vil ske i henhold til gældende regler i persondataloven. Dit navn og CPR-nummer bliver ikke givet videre til nogen. Din anonymitet vil blive sikret således, at ingen oplysninger vil kunne føres tilbage til den enkelte deltager ved offentliggørelse af resultaterne.

Du kan til hver en tid trække dit samtykke tilbage, hvilket betyder, at der herefter ikke vil blive foretaget yderligere dataindsamling i forbindelse med forsøget.

B.8 Information til din egen læge

n egen læge vil blive orienteret om din deltagelse i forsøget, hvis du giver din tilladelse.

B.9 Nye oplysninger

Du vil blive informeret om eventuelle nye fakta eller data, der fremkommer under forsøget, og som kan have indflydelse på, hvorvidt du fortsat ønsker at deltage i forsøget.

B.10 Økonomi

Du vil ikke modtage betaling for at deltage i forsøget. Forsøget er sponsoreret af Elekta (et firma som udvikler medicinsk tekniske udstyr).
Elekta lægger op til at finansiere for en helt PhD-stilling til forskning i teknologiens muligheder for patienterne.

B.11 Kompensation for skader

Du er omfattet af patientforsikringsordningen jf. lov om patientforsikring.
Som deltager i kliniske forsøg, er du tillige omfattet af de samme offentlige forsikringsordninger som ved al anden behandling i det danske sundhedsvæsen.

B.12 Adgang til forsøgsresultater

Forsøgsresultaterne søges publiceret i anerkendt engelsksproget tidsskrift samt ved internationale konferencer, såfremt de viser sig brugbare. Efter afslutning af forsøgsperioden, dvs. afslutning af alle opfølgningsbesøg for alle deltagere og færdiggørelse af dataanalysen, kan deltagerne kontakte den forsøgsansvarlige investigator fysiker/PhD-kandidat Mariwan Baker. Vi håber, du med denne information har fået tilstrækkeligt indblik i, hvad det vil sige at deltage i forsøget, og at du føler dig rustet til at tage beslutningen om din eventuelle deltagelse. Vi beder dig også om at læse det vedlagte materiale ?Forsøgspersonens rettigheder i et biomedicinsk forskningsprojekt?.

B.13 Ansvarlig for projektet

Forsøgsansvarlig for projektet er:
Hospitalsfysiker, PhD-student, Mariwan Baker
Onkologisk Afdeling R, 51AA
Herlev Hospital
e-mail: mariwan.baker@regionh.dk
Lægeansvarlig, Overlæge, Henriette Lindberg
Onkologisk Afdeling R, 51AA
Herlev Hospital
e-mail: henriette.lindberg@regionh.dk

Informeret samtykke til deltagelse i et biomedicinsk forskningsprojekt.
Registrering af livmoderens placering ved hjælp af ultralyds-scanning under udvendig strålebehandling hos patienter med livmoderhalskræft

B.14 Erklæring fra forsøgspersonen:

Jeg har fået skriftlig og mundtlig information og jeg ved nok om formål, metode, fordele og ulemper til at sige ja til at deltage. Jeg ved, at det er frivilligt at deltage, og at jeg altid kan trække mit samtykke tilbage uden at miste mine nuværende eller fremtidige rettigheder til behandling. Jeg giver samtykke til, at deltage i forskningsprojektet og har fået en kopi af dette samtykkeark samt en kopi af den skriftlige information om projektet til eget brug.
Forsøgspersonens navn:————————————————————————-
Dato:———————— Underskrift: ——————- Hvis der kommer nye væsentlige helbredsoplysninger frem om dig i forskningsprojektet vil du blive informeret. Vil du frabede dig information om nye væsentlige helbredsoplysninger, som kommer frem i forskningsprojektet, bedes du markere her: (sæt x)

ønsker du at blive informeret om forskningsprojektets resultat samt eventuelle konsekvenser for dig?:

Ja ————- (sæt x) Nej ————-(sæt x)

APPENDIX C

The project's ethics approval by "De Videnskabsetiske Komiteer"

(In Danish)

Responsible for the project: Medical Physicist, MSc, PhD-candidate, Mariwan Baker.

Region Hovedstaden

Koncern Organisation og Personale

De Videnskabsetiske Komiteer

Region Hovedstaden
Regionsgården
Kongens Vænge 2
3400 Hillerød

Opgang H
Telefon 3866 6395
Direkte 38666320
Mail vek@regionh.dk

Web www.regionh.dk/vek

CVR/SE-nr: 30113713

Protokol nr.: H-4-2013-FSP

Ref.: Lone Gundelach

Dato: 18. marts 2013

Mariwan Baker
Herlev Hospital
Onkologisk Afdeling ®
Herlev Ringvej 75
DK-2730 Herlev

To projekter:

3D-ultralyd ved strålebehandling af cervix kræftpatienter

4D-ultralyd ved strålebehandling af prostata kræftpatienter

Du har ved mail af 11. marts 2013 spurgt, om ovennævnte projekt skal anmeldes til det videnskabsetiske komitesystem.

Jeg har vurderet, at projektet ikke er anmeldelsespligtigt, da der er tale om en sundhedsvidenskabelig intervention af så lille et omfang, at der ikke er tale om et sundhedsvidenskabeligt forskningsprojekt som dette er defineret i komitélovens § 2,[1]. Jeg lægger til grund, at den patienterne alene få nogle ultralydsscanninger udover standardbehandlingen.

Projektet er derfor ikke anmeldelsespligtigt, jf. komitélovens § 1, stk. 4 og kan iværksættes uden tilladelse fra De Videnskabsetiske Komiteer for Region Hovedstaden.

I Danmark har det videnskabsetiske komitesystem til opgave at vurdere sundhedsvidenskabelige forskningsprojekter.

Ved et sundhedsvidenskabeligt forskningsprojekt forstås projekter, der indebærer forsøg på levendefødte menneskelige individer, menneskelige kønsceller, der agtes anvendt til befrugtning, menneskelige befrugtede æg, fosteranlæg og fostre, væv, celler og arvebestanddele fra mennesker, fostre og lign. eller afdøde. Herunder omfattes kliniske forsøg med lægemidler på mennesker og klinisk afprøvning af medicinsk udstyr. .

[1] Lov nr. 593 af 14. juni 2011 om videnskabsetisk behandling af sundhedsvidenskabelige forskningsprojekter som ændret ved L 2012-06-18 nr. 604.

Sundhedsvidenskabelig forskning omhandler primært forskning inden for de lægevidenskabelige fag, den kliniske og den socialmedicinsk-epidemiologiske forskning. Begrebet omfatter, udover forskning af de somatiske sygdomme, tillige de psykiatriske og de klinisk-psykologiske sygdomme og tilstandsformer. Herudover inddrages tilsvarende odontologisk og farmaceutisk forskning under begrebet.

Registerforskningsprojekter, interviewundersøgelser og spørgeskemaundersøgelser skal kun anmeldes, hvis der indgår menneskeligt biologisk materiale i projektet.

Undersøgelser af anonymt biologisk humant materiale skal dog ikke anmeldes til en videnskabsetisk komité, med mindre der er tale om et forskningsprojekt vedrørende befrugtede menneskelige æg samt kønsceller, jf. §§ 25 og 27, stk. 2 i lov om kunstig befrugtning i forbindelse med lægelig behandling, diagnostik og forskning m.v. Det er et krav, at materiale er fuldstændig anonymt (der må ikke være en identifikationskode til data), og at materialet er indsamlet i overensstemmelse med lovgivningen på indsamlingsstedet.

Forsøg på cellelinier eller lignende, der stammer fra et forsøg med indsamling af celler eller væv, som har opnået den nødvendige godkendelse, skal heller ikke anmeldes.

Forsøg, der alene har til formål at fastlægge et kemikaliums toksikologiske grænse i mennesket, er ikke anmeldelsespligtige. Ved et kemikalium forstås i denne forbindelse et stof, der ikke finder terapeutisk anvendelse.

Der ligger således ikke i afvisningen af at bedømme projektet nogen etisk stillingtagen eller negativ vurdering af dets indhold.

Vi gør opmærksom på, at Sundhedsstyrelsen i visse tilfælde skal godkende videregivelse af oplysninger fra patientjournaler. Nærmere oplysning kan findes på Sundhedsstyrelsens hjemmeside.

Behandling af personhenførbare oplysninger er omfattet af persondataloven. Nærmere oplysning herom findes på Datatilsynets hjemmeside.

Klagevejledning:

Komitéens afgørelse kan, jf. komitélovens § 26, stk. 1, indbringes for Den Nationale Videnskabsetiske Komité, senest 30 dage efter afgørelsen er modtaget. Den Nationale Videnskabsetiske Komité kan, af hensyn til sikring af forsøgspersonernes rettigheder, behandle elementer af projektet, som ikke er omfattet af selve klagen.

Klagen skal indbringes elektronisk og ved brug af digital signatur og kryptering, hvis protokollen indeholder fortrolige oplysninger.

Dette kan ske på adressen: dketik@dketik.dk

Klagen skal begrundes og være vedlagt kopi af Den Regionale Videnskabsetiske Komités afgørelse samt de sagsakter, som Den Regionale Videnskabsetiske Komité har truffet afgørelse på grundlag af.

Med venlig hilsen

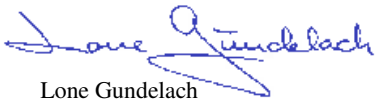

Lone Gundelach
Sekretariatsleder, cand.jur.
Lone.gundelach@regionh.dk

Papers

PAPER A

Inter-operator Variability in Defining Uterine Position Using Three-dimensional Ultrasound Imaging

Authors: Mariwan Baker, Jørgen Arendt Jensen, and Calus F. Behrens.

Published in: Proceedings of the IEEE International Ultrasonics Symposium, pp. 848-851, 2013

Abstract

In radiotherapy the treatment outcome of gynecological (GYN) cancer patients is crucially related to reproducibility of the actual uterine position. The purpose of this study is to evaluate the inter-operator variability in addressing uterine position using a novel 3-D ultrasound (US) system. The study is initiated by US-scanning of a uterine phantom (CIRS 404, Universal Medical, Norwood, USA) by seven experienced US operators. The phantom represents a female pelvic region, containing a uterus, bladder and rectal landmarks readily definable in the acquired US-scans. The organs are subjected to displacement by applied operator-pressure that mimics an actual GYN patient. The transabdominal scanning was performed using a 3D-US system (Clarity Model 310C00, Elekta, Montreal, Canada). It consists of a US acquisition-station, workstation, and a 128- element 1D array curved probe. The iterated US-scans were performed in four subsequent sessions (totally 21 US-scans) in a period of four weeks to investigate the randomness of the inter-operator variability. An additionally US-scan was performed as a reference target volume to the consecutive scans. At first, the phantom was marked with ball bearings for daily laser alignment. In each session the US-scans were acquired by the seven operators. The uterus was outlined in each of the US imagesets using Clarity autosegmentation in the workstation. Further, the shifts in the uterine centre of mass relative to the reference were measured for the three orthogonal directions; left (+)-right (LR), anterior (+)-posterior (AP), and inferior (+)-superior (IS), respectively. The same operator delineated the target volumes.

The average inter-operator deviation ±1SD of the daily US scans was (in mm); LR: day 1 (-0.4±0.9), day 2 (-0.3±0.6), day 3 (- 1.0±1.2), day 4 (1.3±0.5); AP: day 1 (0.0±1.7), day 2 (0.1±0.7), day 3 (-1.0±0.9), day 4 (0.2±1.2); IS: day 1 (-1.5±2.6), day 2 (0.1±1.8), day 3 (0.1±1.1), day 4 (0.5±3.1), respectively. The largest inter-operator discordance was observed to be 4.7 mm in the IS-direction in day 4. Published studies report significantly larger inter-fractional uterine positional displacement, in some cases up to 20 mm, which outweighs the magnitude of current inter-operator variations. Thus, the current US-phantom-study suggests that the inter-operator variability in addressing uterine position is clinically irrelevant.

10.1109/ULTSYM.2013.0218

Inter-operator Variability in Defining Uterine Position Using Three-dimensional Ultrasound Imaging

Mariwan Baker*†‡, Jørgen Arendt Jensen† and Claus F. Behrens*

*Herlev Hospital, Department of Oncology(R) Herlev Ringvej 75, DK-2730 Herlev, Denmark
†Center for Fast Ultrasound Imaging, Dept. of Elec. Eng., Technical University of Denmark, DK-2800 Lyngby, Denmark
‡Center for Nuclear Technologies, Technical University of Denmark, DTU Risø Campus, DK-4000 Roskilde, Denmark.

***Abstract*—In radiotherapy the treatment outcome of gynecological (GYN) cancer patients is crucially related to reproducibility of the actual uterine position. The purpose of this study is to evaluate the inter-operator variability in addressing uterine position using a novel 3-D ultrasound (US) system. The study is initiated by US-scanning of a uterine phantom (CIRS 404, Universal Medical, Norwood, USA) by seven experienced US operators. The phantom represents a female pelvic region, containing a uterus, bladder and rectal landmarks readily definable in the acquired US-scans. The organs are subjected to displacement by applied operator-pressure that mimics an actual GYN patient. The transabdominal scanning was performed using a 3D-US system (Clarity® Model 310C00, Elekta, Montreal, Canada). It consists of a US acquisition-station, workstation, and a 128-element 1D array curved probe. The iterated US-scans were performed in four subsequent sessions (totally 21 US-scans) in a period of four weeks to investigate the randomness of the inter-operator variability. An additionally US-scan was performed as a reference target volume to the consecutive scans. At first, the phantom was marked with ball bearings for daily laser alignment. In each session the US-scans were acquired by the seven operators. The uterus was outlined in each of the US image-sets using Clarity autosegmentation in the workstation. Further, the shifts in the uterine centre of mass relative to the reference were measured for the three orthogonal directions; left (+)-right (LR), anterior (+)-posterior (AP), and inferior (+)-superior (IS), respectively. The same operator delineated the target volumes. The average inter-operator deviation ±1SD of the daily US scans was (in mm); LR: day 1 (-0.4±0.9), day 2 (-0.3±0.6), day 3 (-1.0±1.2), day 4 (1.3±0.5); AP: day 1 (0.0±1.7), day 2 (0.1±0.7), day 3 (-1.0±0.9), day 4 (0.2±1.2); IS: day 1 (-1.5±2.6), day 2 (0.1±1.8), day 3 (0.1±1.1), day 4 (0.5±3.1), respectively. The largest inter-operator discordance was observed to be 4.7 mm in the IS-direction in day 4. Published studies report significantly larger inter-fractional uterine positional displacement, in some cases up to 20 mm, which outweighs the magnitude of current inter-operator variations. Thus, the current US-phantom-study suggests that the inter-operator variability in addressing uterine position is clinically irrelevant.**

I. Introduction

In modern adaptive conformal radiotherapy with tight margins and steep dose gradients, such as intensity-modulated radiotherapy (IMRT), it is essential that the position of the clinical target volume (CTV) is precisely defined prior to each treatment fraction throughout the entire course of treatment. Recent technical innovations have enabled the direct integration of various image verification methods into the linear accelerator (LINAC). This allows patient and tumour positioning to be addressed and corrected. Nowadays, kilovoltage (kV) and megavoltage (MV) planar radiographic imaging, and kV volumetric cone beam CT imaging are standard image verification systems in many radiotherapy centres. Generally, these systems are implemented as Image Guided Radiation Therapy (IGRT) for daily target alignment, which enables correction of position misalignment, thereby improving the precision of radiation treatment [1]. However, the challenge of using these ionizing systems is insufficient soft tissue visualization, for instance of the uterus of GYN cancer patients. In some cases these systems require invasive methods, such as implanted fiducial markers in prostate radiotherapy [2]. Therefore, different non-ionizing 3D ultrasound (3D-US) systems, such as the Elekta 3D Clarity® Soft Tissue Visualization system and the NOMOS B-mode Acquisition and Targeting (BAT) ultrasound system have been developed and introduced into radiotherapy for different cancer sites [3]–[5]. However, these US-systems have been found to be only applicable for cancer sites in soft tissue environments such as in GYN, prostate and postoperative lumpectomy cavity cancer patients. The uterus, where internal position variations are dependent on rectal and bladder filling, is an ideal site for US-scans. Some uncertainty factors such as inter-operator variability due to probe handling are present when using the US-system. Variations in the transducer probe pressure applied have previously been documented during 3D-US scan on prostate patients [6], [7].

The aim of the present study was to quantify the inter-operator variability using the Clarity US-system on a commercial GYN-phantom.

II. Materials and Methods

A phantom was scanned by seven operators in the course of four sessions over a period of four weeks (one session per week), a total of 21 scans (All the operators were not presented for each session). Each radiation therapist (RTT) participated in two weeks of intensive training provided by the manufacturer of Clarity as well as several practice sessions before the start of the study.

A. Phantom

The ultrasound training phantom (CIRS 404, Universal Medical, Norwood, USA) mimics the female pelvic region and

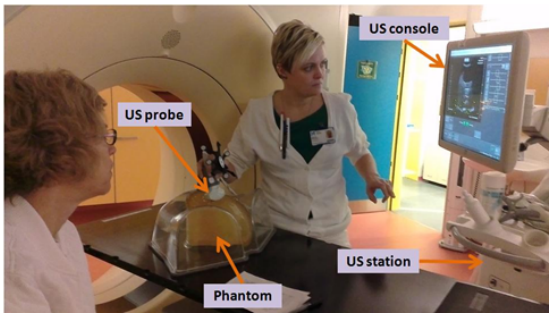

Figure 1. Phantom scanning is performed by means of a convex array probe in the CT-room. Real-time images can be visualized on the US console mounted on the US station.

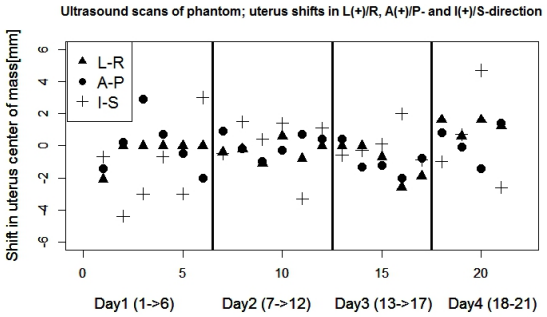

Figure 2. Daily US scans (day 1: 6 operators, day 2: 6 operators, day 3: 5 operators, and day 4: 4 operators). The plot shows uterine COM shifts in the L/R, A/P and I/S directions.

contains a uterus, bladder and rectum representing the standard female pelvic organs (Fig. 1). The organs are subjected to displacement of the exerted probe pressure. The phantom does not contain any skeletal structure such as femur head or pelvic bone. The phantom is constructed of material that is intended for ultrasound scans, thus all organs are easily defined in the acquired US-images. Initially, the phantom was marked with small spherical ball bearings (laser alignment markers), used to aid reproducibility of daily set-up prior to each US-scan session. Use of this technique requires acquisition of a reference US image data-set, and therefore during an initial session the best possible US-scan was selected as position reference to the following four consecutive sessions.

B. Clarity Ultrasound System

The Clarity ultrasound system (Clarity® Model 310C00, Elekta, Montreal, Canada)consists of two US-units: one located in the Computed Tomography (CT) simulation room and one in the treatment room. The two units are connected through a workstation/server. In this study all US-scans were performed in the CT room. Since the objective of the ongoing project at Herlev hospital is to implement the Clarity 3D-US system for both GYN and prostate patients throughout the course of their treatment, the treatment room unit will be utilized for daily IGRT. Each US-unit is equipped with a convex array probe for trans-abdominal 3D US-scanning. Every station consists of a ceiling-mounted infrared (IR) camera that can track the US-probe by monitoring the IR-reflectors/emitters mounted on it. The transducer probe consists of a 128-element 1-D array. To enable superimposition of the acquired 3D-US images to the reference US-image sets, the 3D-US system is calibrated to the same coordinate system as the CT and treatment rooms, respectively. The calibration procedure is accomplished by means of an alignment phantom. Quality assurance checks confirm the system calibration on each day of use. The daily check is passed only when the calibration precision is less than 1 mm.

C. Image Acquisition

The ultrasound image of the phantom (trans-abdominal US-scan) was acquired by all the seven experienced RTTs using the convex array probe. In each phantom scan the US-probe was placed on the first occasion with moderate pressure in the region corresponding to the pubic symphysis and rotated, after which it was swept cranially. Afterwards, the acquired image-sets were reconstructed, and the uterus, bladder and rectum were identified.

D. Organ Delineation and Data Analysis

The uterus, bladder and rectum were delineated in the reconstructed 3D US-image data sets using the Clarity work-station supplied by the manufacturer. In the workstation the delineation can be performed either manually or with aid of auto-segmentation. In this study the assisted segmentation was utilized for all outlined organs. A single operator (MB) conducted a retrospective analysis of the acquired US-image sets and delineated the organs. Descriptive statistics and a single-sample t-test was conducted for the phantom scans. Background variables such as alpha, null and alternative hypothesis, standard deviation (SD) and variance are described using descriptive statistics.

III. Results

A total of 21 US-scans were acquired by the same seven operators over the four sessions.The daily US scans is plotted during the four days and for all presented operators (Fig. 2).

Positional uterine Center of Mass (COM) shifts, in three orthogonal directions and of four days are plotted (Fig. 3). Positive shifts are left, anterior, and inferior. Qualitatively, these plots demonstrate that there are not significant differences in the shifts comparing mean of COM shifts, i.e. mean of the session scans for each day. One can observe that, in each direction (L/R, A/P, and I/S), the results are roughly centred about zero. The mean $\pm$SD of the daily phantom COM-shifts (average inter-operator deviation) was (mm): LR: day 1 (-0.4$\pm$0.9), day 2 (-0.3$\pm$0.6), day 3 (-1.0$\pm$1.2), day 4 (1.3$\pm$0.5); AP: day 1 (0.0$\pm$1.7), day 2 (0.1$\pm$0.7), day 3 (-1.0$\pm$0.9), day 4 (0.2$\pm$1.2); IS: day 1 (-1.5$\pm$2.6), day 2 (0.1$\pm$1.8), day 3 (0.1$\pm$1.1), day 4 (0.5$\pm$3.1), respectively. The largest inter-operator discordance was observed to be 4.7 mm in the IS-direction in day 4. None of the p-values for the three directions is smaller than 0.05. The largest lower/upper range of 95% CI is in I/S-direction in day 4 (-4.54–+5.44) (Fig. 4).

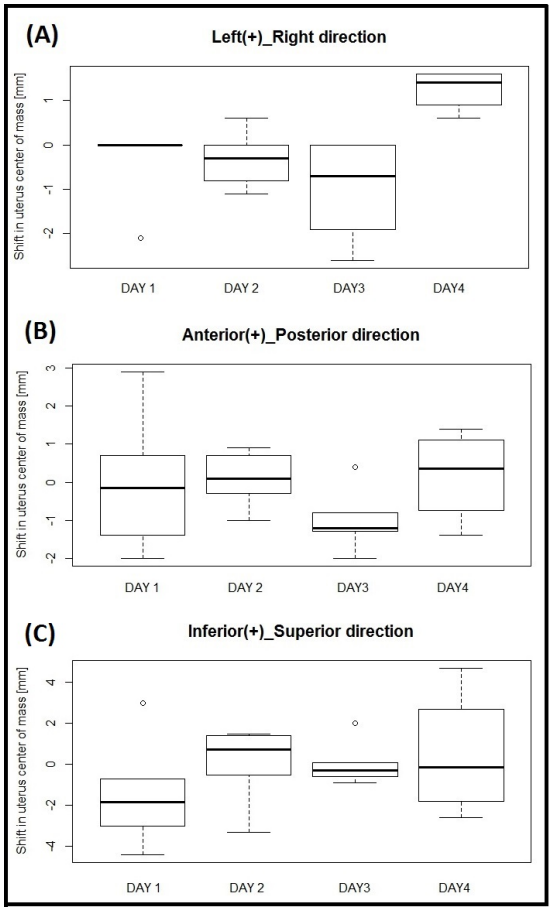

Figure 3. (A), (B) and (C): box-plots of uterine COM-shifts for the phantom on four days in the three cardinal directions; L/R, A/P, and I/S.

IV. Discussion

Inter-fractional positional uncertainty of the uterus, rectum and bladder of GYN patients has been a challenge in radiotherapy, and leads to larger applied set-up margins to account for the target displacement. Recently developed highly conformal (IMRT) treatment enables better dose conformity, thus steeper dose gradients. This means that the delineated CTV and organ at risks (OAR) are more susceptible to the uterine positional displacement. Uterine positional changes have been confirmed in previous reports to be strongly correlated to the daily variations in rectal-bladder filling [8], [9].

Recently, 3D-US is more frequently applied as IGRT-method. It has been used mostly in prostate alignment prior to the treatment fraction. Only few published papers are reporting the application of 3D-US on GYN-patients [10]–[12], but the focus is on quantifying inter-fractional bladder motion and variation in bladder volume rather than uterine positional change. Herlev Hospital is a pioneer in the application of a

		N	SD	Mean	df	t	95%CI (Lower/Upper)	P-value
	Direction of shifts							
Day1	Left-Right	6	0.86	-0.35	5	-1.00	-1.25/0.55	0.36
	Anterior-Posterior	6	1.74	-0.02	5	-0.02	-1.84/1.81	0.98
	Inferior-Superior	6	2.62	-1.47	5	-1.37	-4.22/1.28	0.23
Day2	Left-Right	6	0.60	-0.32	5	-1.29	-0.95/0.31	0.25
	Anterior-Posterior	6	0.71	0.08	5	0.29	-0.67/0.83	0.79
	Inferior-Superior	6	1.83	0.10	5	0.13	-1.82/2.02	0.90
Day3	Left-Right	5	1.17	-1.04	4	-1.99	-2.49/0.41	0.12
	Anterior-Posterior	5	0.88	-0.98	4	-2.48	-2.08/0.12	0.07
	Inferior-Superior	5	1.15	0.06	4	0.12	-1.36/1.48	0.91
Day4	Left-Right	4	0.47	1.25	3	5.29	050/2.00	0.01
	Anterior-Posterior	4	1.22	0.18	3	0.29	-1.76/2.11	0.79
	Inferior-Superior	4	3.14	0.45	3	0.29	-4.54/5.44	0.79

Figure 4. Tabulates values of one sample t.test of obtained uterine shifts using ultrasound scans of a phantom.

novel Clarity 3D-US system with focus on GYN diagnoses. The present study started by applying Clarity on a phantom and it will subsequently be used for GYN patients at Herlev. Different studies on the prostate have concluded that one of the drawbacks of using 3D-US as the IGRT method is probe pressure induced uncertainty of the target and OAR, and the variation in the probe handling by the observers. The challenge experienced by most of our operators during 3D US acquisition was to find an appropriate probe handling technique that captured the entire uterus from the cervical os to the fundus, as the image quality was poor in some cases. Obviously, poor image quality has an adverse influence on uterus delineation, thus leading to uncertainty about COM shifts.

In the present phantom study, we found no statistically significant differences in uterine COM shifts in the term of inter-observer variability (sample t-test with a 95% CI). All the acquired US-scans indicated that uterine COM displacements are in the vicinity of zero, with a daily mean value of less than 2 mm in all three cardinal directions (L/R, A/P and I/S). The recent study paper by Jurgenliemk-Schultz et al., [13], which investigated vaginal positional change and the correlation between vaginal shift and bladder-rectal filling, reported a daily vaginal CTV positional change of up to 2.3 cm in the A/P direction. In another study Chan et al., [14], report that the uterine head (fundus) can vary from day to day by over 24 mm. This large inter-fractional vaginal and uterine positional displacement outweighs the magnitude of our inter-operator variability.

V. Conclusions

Published studies report significantly larger inter-fractional uterine positional displacement, over 20 mm in some directions, which outweighs the magnitude of the current inter-operator variations. Thus, the current US-phantom-study suggests that the inter-operator variability in determining uterine position is clinically irrelevant.

ACKNOWLEDGEMENT

Sincere thanks to our hard-working colleagues who helped to conduct this study; Gullander L. (RTT), Pedersen S. K (RTT),

Zarp T (RTT), Jacobsson S (RTT), Pazhang S (radiographer), and Lynnerup V. K (radiographer).

CONFLICT OF INTEREST

The current study is a part of three years PhD research project at Herlev that is supported by Elekta, Inc.

REFERENCES

[1] T. R. Mackie, J. Kapatoes, K. Ruchala, W. Lu, C. Wu, G. Olivera, L. Forrest, W. Tome, J. Welsh, R. Jeraj, P. Harari, P. Reckwerdt, B. Paliwal, and M. Ritter, "Image guidance for precise conformal radiotherapy," *International journal of radiation oncology, biology, physics*, vol. 56, no. 1, pp. 89–105, May 2003. [Online]. Available: http://linkinghub.elsevier.com/retrieve/pii/S0360301603000907

[2] D. Litzenberg, L. a. Dawson, H. Sandler, M. G. Sanda, D. L. McShan, R. K. Ten Haken, K. L. Lam, K. K. Brock, and J. M. Balter, "Daily prostate targeting using implanted radiopaque markers," *International journal of radiation oncology, biology, physics*, vol. 52, no. 3, pp. 699–703, March 2002. [Online]. Available: http://www.ncbi.nlm.nih.gov/pubmed/11849792

[3] J. Boda-Heggemann, F. M. Köhler, B. Küpper, D. Wolff, H. Wertz, S. Mai, J. Hesser, F. Lohr, and F. Wenz, "Accuracy of ultrasound-based (BAT) prostate-repositioning: a three-dimensional on-line fiducial-based assessment with cone-beam computed tomography," *IJROBP*, vol. 70, no. 4, pp. 1247–1255, March 2008.

[4] M. Pinkawa, M. Pursch-Lee, B. Asadpour, B. Gagel, M. D. Piroth, J. Klotz, S. Nussen, and M. J. Eble, "Image-guided radiotherapy for prostate cancer. Implementation of ultrasound-based prostate localization for the analysis of inter- and intrafraction organ motion." *Strahlentherapie und Onkologie*, vol. 184, no. 12, pp. 679–685, December 2008.

[5] F. L. B. Cury, G. Shenouda, L. Souhami, M. Duclos, S. L. Faria, M. David, F. Verhaegen, R. Corns, and T. Falco, "Ultrasound-based image guided radiotherapy for prostate cancer: comparison of cross-modality and intramodality methods for daily localization during external beam radiotherapy." *IJROBP*, vol. 66, no. 5, pp. 1562–1567, December 2006.

[6] J. P. McGahan, J. Ryu, and M. Fogata, "Ultrasound probe pressure as a source of error in prostate localization for external beam radiotherapy." *IJTOBP*, vol. 60, no. 3, pp. 788–793, November 2004. [Online]. Available: http://www.ncbi.nlm.nih.gov/pubmed/15465195

[7] C. F. Serago, S. J. Chungbin, S. J. Buskirk, G. a. Ezzell, a. C. Collie, and S. a. Vora, "Initial experience with ultrasound localization for positioning prostate cancer patients for external beam radiotherapy." *IJTOBP*, vol. 53, no. 5, pp. 1130–1138, August 2002. [Online]. Available: http://www.ncbi.nlm.nih.gov/pubmed/12128112

[8] A. Taylor and M. E. B. Powell, "An assessment of interfractional uterine and cervical motion: implications for radiotherapy target volume definition in gynaecological cancer." *Radiotherapy and oncology : journal of the European Society for Therapeutic Radiology and Oncology*, vol. 88, no. 2, pp. 250–257, August 2008. [Online]. Available: http://www.ncbi.nlm.nih.gov/pubmed/18538873

[9] R. Ahmad, M. S. Hoogeman, M. Bondar, V. Dhawtal, S. Quint, I. De Pree, J. W. Mens, and B. J. M. Heijmen, "Increasing treatment accuracy for cervical cancer patients using correlations between bladder-filling change and cervix-uterus displacements: proof of principle." *Radiotherapy and oncology*, vol. 98, no. 3, pp. 340–346, March 2011. [Online]. Available: http://www.ncbi.nlm.nih.gov/pubmed/21295877

[10] R. Ahmad, M. S. Hoogeman, S. Quint, J. W. Mens, I. de Pree, and B. J. M. Heijmen, "Inter-fraction bladder filling variations and time trends for cervical cancer patients assessed with a portable 3-dimensional ultrasound bladder scanner." *Radiotherapy and oncology*, vol. 89, no. 2, pp. 172–179, November 2008. [Online]. Available: http://www.ncbi.nlm.nih.gov/pubmed/18703248

[11] A. Jhingran, M. Salehpour, M. Sam, L. Levy, and P. Eifel, "Vaginal motion and bladder and rectal volumes during pelvic intensity modulated radiation therapy after hysterectomy," *International journal of radiation oncology, biology, physics*, vol. 82, no. 1, pp. 256–262, January 2012.

[12] D. Yee, M. Parliament, S. Rathee, S. Ghosh, L. Ko, and B. Murray, "Cone beam CT imaging analysis of interfractional variations in bladder volume and position during radiotherapy for bladder cancer," *International journal of radiation oncology, biology, physics*, vol. 76, no. 4, pp. 1045–1053, March 2010. [Online]. Available: http://www.ncbi.nlm.nih.gov/pubmed/19540057

[13] I. M. Jurgenliemk-Schulz, M. Z. Toet-Bosma, G. a. P. de Kort, H. W. R. Schreuder, J. M. Roesink, R. J. H. a. Tersteeg, and U. a. van der Heide, "Internal motion of the vagina after hysterectomy for gynaecological cancer." *Radiotherapy and oncology*, vol. 98, no. 2, pp. 244–248, February 2011. [Online]. Available: http://www.ncbi.nlm.nih.gov/pubmed/21159394

[14] P. Chan, R. Dinniwell, M. a. Haider, Y.-B. Cho, D. Jaffray, G. Lockwood, W. Levin, L. Manchul, A. Fyles, and M. Milosevic, "Inter- and intrafractional tumor and organ movement in patients with cervical cancer undergoing radiotherapy: a cinematic-mri point-of-interest study," *International journal of radiation oncology, biology, physics*, vol. 70, no. 5, pp. 1507–1515, April 2008. [Online]. Available: http://www.ncbi.nlm.nih.gov/pubmed/18164850

PAPER B

Determining inter-fractional motion of the uterus using 3D ultrasound imaging during radiotherapy for cervical cancer

Authors: Mariwan Baker, Jørgen Arendt Jensen, and Calus F. Behrens.

Published in: Proceedings of the SPIE, the Medical Imaging 2014: Ultrasonic Imaging and Tomography, Vol. 9040 90400Y-1, 2014

Abstract

Uterine positional changes can reduce the accuracy of radiotherapy for cervical cancer patients. The purpose of this study was to; 1) Quantify the inter-fractional uterine displacement using a novel 3D ultrasound (US) imaging system, and 2) Compare the result with the bone match shift determined by Cone- Beam CT (CBCT) imaging. Five cervical cancer patients were enrolled in the study. Three of them underwent weekly CBCT imaging prior to treatment and bone match shift was applied. After treatment delivery they underwent a weekly US scan. The transabdominal scans were conducted using a Clarity US system (Clarity Model 310C00). Uterine positional shifts based on soft-tissue match using US was performed and compared to bone match shifts for the three directions. Mean value ($\pm$1 SD) of the US shifts were (mm); anterior-posterior (A/P): (3.8$\pm$5.5), superior-inferior (S/I) (-3.5$\pm$5.2), and left-right (L/R): (0.4$\pm$4.9). The variations were larger than the CBCT shifts. The largest inter-fractional displacement was from -2 mm to +14 mm in the AP-direction for patient 3. Thus, CBCT bone matching underestimates the uterine positional displacement due to neglecting internal uterine positional change to the bone structures. Since the US images were significantly better than the CBCT images in terms of soft-tissue visualization, the US system can provide an optional image-guided radiation therapy (IGRT) system. US imaging might be a better IGRT system than CBCT, despite difficulty in capturing the entire uterus. Uterine shifts based on US imaging contains relative uterus-bone displacement, which is not taken into consideration using CBCT bone match.

Determining inter-fractional motion of the uterus using 3D ultrasound imaging during radiotherapy for cervical cancer

Mariwan Baker[1,2,3], Jørgen Arendt Jensen[2], and Claus F. Behrens[1]

1 Department of Oncology, Radiotherapy Research Unit, Herlev Hospital, University of Copenhagen, Herlev, Denmark
2 Center for Fast Ultrasound Imaging, Dept. of Elec. Eng., Technical University of Denmark, DK-2800 Lyngby, Denmark
3 Center for Nuclear Technologies, Technical University of Denmark, DTU Risø Campus, Roskilde, Denmark

E-mail: mariwan.baker@regionh.dk

ABSTRACT

Uterine positional changes can reduce the accuracy of radiotherapy for cervical cancer patients. The purpose of this study was to; 1) Quantify the inter-fractional uterine displacement using a novel 3D ultrasound (US) imaging system, and 2) Compare the result with the bone match shift determined by Cone-Beam CT (CBCT) imaging.Five cervical cancer patients were enrolled in the study. Three of them underwent weekly CBCT imaging prior to treatment and bone match shift was applied. After treatment delivery they underwent a weekly US scan. The transabdominal scans were conducted using a Clarity US system (Clarity® Model 310C00). Uterine positional shifts based on soft-tissue match using US was performed and compared to bone match shifts for the three directions. Mean value (±1 SD) of the US shifts were (mm); anterior-posterior (A/P): (3.8±5.5), superior-inferior (S/I) (-3.5±5.2), and left-right (L/R): (0.4±4.9). The variations were larger than the CBCT shifts. The largest inter-fractional displacement was from -2 mm to +14 mm in the AP-direction for patient 3. Thus, CBCT bone matching underestimates the uterine positional displacement due to neglecting internal uterine positional change to the bone structures. Since the US images were significantly better than the CBCT images in terms of soft-tissue visualization, the US system can provide an optional image-guided radiation therapy (IGRT) system. US imaging might be a better IGRT system than CBCT, despite difficulty in capturing the entire uterus. Uterine shifts based on US imaging contains relative uterus-bone displacement, which is not taken into consideration using CBCT bone match.

1 INTRODUCTION

Local recurrence of cervical cancer remains a challenge worldwide despite using advanced treatment techniques [1]. In addition to surgery and chemotherapy, radiotherapy is an effective treatment modality. However, radiation complications, such as gastrointestinal toxicity, are experienced by patients undergoing radiation treatment [2]. Modern conformal radiotherapy with tight margins and steep dose gradients, such as intensity-modulated radiotherapy (IMRT) and volumetric conformal arc therapy, allows a reduction of undesired radiation doses to healthy organs but requires more precise daily tumour alignment prior to each fraction throughout the entire course of the treatment.

Today's Image Guided Radiation Therapy (IGRT) methods, such as the electronic portal image device (EPID) and the kV volumetric cone beam CT (CBCT), are widely utilized for daily patient alignment and enable online correction of positional tumor misalignments, thereby improving the precision of the delivery of

Medical Imaging 2014: Ultrasonic Imaging and Tomography, edited by Johan G. Bosch, Marvin M. Doyley, Proc. of SPIE Vol. 9040, 90400Y · © 2014 SPIE
CCC code: 1605-7422/14/$18 · doi: 10.1117/12.2043173

the prescribed radiation dose to the delineated target [3]. However, the weakness of using these ionizing system are insufficient soft tissue visualization, for instance in visualizing the uterus of gynecological (GYN) cancer patients or identifying the prostate gland and surrounding soft tissue organs at risk (OARs) in prostate cancer patients. As a result, bone matching is frequently applied as a daily tumor alignment method in cervical cancer treatment. For cervical cancer patients, large margins are applied around delineated gross tumor volume (GTV), to ensure target radiation dose coverage. The large margin is due to the complexity of the pelvis with its tumor and normal organ motion as well as deformation dynamics, which adversely impacts on the irradiated healthy tissues [4]. Additionally, tumor volume regression is reported to be substantial, with up to 80% reduction by the end of the treatment period [5-7]. Different imaging methodologies such as implanted fiducial markers as a reference point [8-10] are employed in patients with cervical cancer to determine uterus and/or target motion. Use of the tumor surrogate method limits analysis of uterine shifts, because implanted fiducial markers can fall out, migrate, or be displaced due to tumor shrinkage and organ deformation. On the other hand, MRI imaging provides an outstanding visualization of the uterus and cervix, enabling discrimination from other organs [4, 9, 11]. The application of MRI as IGRT for daily tumor alignment requires MRI/LINAC accessibility, which is costly and rarely used clinically [12-13]. Therefore, various cheaper non-ionized 3D US systems have been developed, such as the 3D Clarity® Soft Tissue Visualization system (Clarity® Model 310C00, Elekta, Montreal, Canada) and the NOMOS B-mode Acquisition and Targeting (BAT) ultrasound system [14-16]. However, these US systems can only be used for cancer sites in a soft tissue environment such as GYN, prostate and postoperative lumpectomy cavity in breast cancer patients. The prostate and uterus, where internal position variations are partly dependent on rectal-bladder filling, are ideal sites for US-scans. Furthermore, different uncertainty factors such as probe handling, image quality, and inter-operator variability are involved in the use of a US system. Inter-operator variations in US transducer probe pressure have been documented earlier for prostate patients [17-18]. In the present study, the main purpose was to quantify the magnitude of the inter-fractional uterine displacement, based on soft tissue match, using a novel 3D US imaging system. A specific purpose was to compare the US results with the bone match shifts determined by means of CBCT imaging.

2 MATERIALS AND METHODS

Five cervical cancer patients, mean age 60 years (51/68), were enrolled in this study. All underwent radiotherapy at Herlev hospital. One patient was excluded due to incontinence, while a second was excluded after acquisition of US images in the CT simulation room. The patient in question had a nephrostomy with an implanted catheter, which resulted in very poor image quality.Each of the patients underwent daily EPID and weekly CBCT setup verification imaging. Since the uterus cannot be visualized using either EPID or CBCT, all the shifts are based on bone match. Immediately after treatment the patients underwent a weekly US scan performed by two experienced operators. Seven RTTs participated in an extensive two week training program provided by the commercial vendor as well as several practice sessions prior to the start of the study.

2.1 Clarity ultrasound system

The Clarity ultrasound system consists of two US-units: one located in the CT simulation room and the second in the treatment room. The two units are connected through a workstation/server. The treatment room unit is utilized as intra-modality IGRT. Each US unit is equipped with a convex-probe for trans-abdominal 3D US scanning. A ceiling-mounted infrared (IR) camera tracks the US-probe by monitoring the IR-reflectors mounted on each probe (Fig. 1. A). To enable superimposition of the 3D US images of the treatment room onto the reference US image sets of the CT room, the US system is calibrated to the same coordinate system as the CT and treatment rooms. The calibration procedure is accomplished by means of a dedicated alignment phantom provided by the vendor. Quality assurance checks confirm the calibration on each day of use.

2.2 CT-US simulation and treatment planning

All the patients underwent a CT scan. Two radiographers with experience of the Clarity system were responsible for each patient. The patient alignment was performed by means of the room lasers. A US image was acquired immediately after the CT scan (Fig. 1.A-B). For each scan the US probe was placed in the pubic symphysis region and then rotated/swept followed by a probe slide in the cranial direction. This US image acquisition method is known as the sweep/slide technique and enables capture of the entire uterus. The sweep technique alone is a proper scan on prostate cancer patients, as the prostate is smaller and the entire target can be captured by a transabdominal sweep scan. Firm pressure, which might lead to uterus displacement, was avoided when performing the scan, as the focus was on obtaining clear images to facilitate identification of the complex pelvic structure. Since the CT images were to be superimposed onto US images, the same patient setup is necessary for CT and US scans. All the cervical cancer patients underwent MRI scans after CT image acquisition. The GTVand OARs were delineated on CT-MR fusion image datasets by the gynecological oncologist. The CT datasets were transferred to the planning system for 3D treatment planning.

2.3 Organ delineation

Initially the delineated target and normal structures were exported from the treatment planning system to the Clarity workstation. Moreover, the previously delineated bladder and rectum, based on standard MRI, were copied to the CT-US fusion to assist the US based target delineation. Subsequently, the CT-US image fusion was performed and the uterus delineated in the reconstructed 3D US-image data sets. Finally, the delineated uterus, including the cervix, uterine body and fundus, was approved as the Planning Reference Volume (PRV) for subsequent weekly US scans in the treatment room. In this study the assisted segmentation in the Clarity workstation was utilized for uterus delineation. Export/import from the treatment planning system to the Clarity workstation, CT/US fusion and uterus delineation were performed by one of two radiographers or one physicist. In addition, a single operator (MB) conducted a retrospective analysis of the acquired US image sets and delineated the organs.

2.4 Treatment room

The patient was prepared for daily treatment by aligning her to the lasers by means of marks on the skin, i.e. to reproduce the patient setup position in the CT-simulation room. In this study and prior to the treatment, the weekly CBCT images were acquired, and clinical alignment was performed based on bone matching. The weekly US scans were performed immediately after acquiring CBCT and treatment delivery. Further, the soft tissue match performed by superimposing the segmented uterus in the 3D US image acquired at the treatment unit onto the reference PRV from the CT-simulation, thus potential uterus shifts, uterine center of mass (COM) shifts, of the target were recorded. Finally, the correlated differences in shifts from the US and CBCT matches were compared.

2.5 Statistical analysis

A paired t-test was applied to compare US with CBCT shifts to check probability differences between the paired values of the two samples. This was determined by screening the variation of values within each sample and producing a single digit t-value. Despite the different type of image matching in this test, soft tissue versus bone matches, the t-test is applicable, since the aim was to investigate inter-fractional displacements using two different imaging modalities. Furthermore, the p-values were calculated for a 95% confidence interval (CI). Due to the low number of patients the t-test assumption of normal distribution must be treated with caution.

3 RESULTS

Positional uterine center of mass (COM) shifts detected by ultrasound imaging and shifts based on bone alignment using CBCT images in three orthogonal directions are presented in Fig. 2. Positive shifts are anterior, inferior and right. The figure shows 14 scans of each CBCT and US for the three patients, patient 1 five scans, patient 2 four scans, and patient 3 five scans. The plot reveals larger displacement shifts for US than CBCT,

especially in the case of patient 2. This can be explained by the fact that US soft tissue matching takes uterus to bone shifts into account compared to only bone matching using CBCT. In this study a great effort was made to perform soft tissue matching based on acquired CBCT, but it was not possible due to poor image quality and thus discrimination of the soft tissue organs was almost impossible. As a result all the performed CBCT matches are based on bone match. The difference between US and CBCT can be clearly observed by examining the box-plots of the shifts for each patient (Fig. 3 A, B, C). These differences are obvious for patients 1 and 2 in the AP- and SI-directions, while for patients 2 and 3 the larger deviations can be seen in the LR-direction. In the plot for the three patients based on a total of 14 scans, the larger deviation was visible in US scans in all three directions (Fig. 3 D). The overall mean (± 1SD) of the weekly uterine COM-shifts (US) and bone match shifts (CBCT) was (mm); US/CBCT: AP (3.8±5.5)/(2.8±2.0), SI (-3.0±5.2)/(2.8±2.0), LR (-2.7±1.7)/(-1.0±3.3), respectively (Table.1). The results demonstrate that inter-fractional displacements are greater with US than CBCT. The largest inter-fractional displacement using US was from -2 mm to +14 mm in the AP-direction for patient 3, while with CBCT the largest shift was from -5 mm to +5 mm in the LR-direction also for patient 3.

The t-values and mean of differences were individually calculated for each patient, while the overall values for all three directions were estimated by means of the paired t-test (Table. 2). No significant differences between US and CBCT shifts ($p > 0.05$) were found in any direction, which might be explained by the low number of scans. The largest lower/upper range of 95% CI was in the LR-direction in patient 3 (-6.7 to +10.8).

4 DISCUSSION

Inter-fractional positional uncertainty of the uterus, rectum and bladder in GYN patients has been a challenge in radiotherapy, leading to the application of larger set-up margins to account for target displacement. Modern conformal treatment (IMRT and volumetric modulated arc therapies) enables better dose conformity, and thus steeper dose gradients. The delineated target and OARs are more susceptible to daily uterine positional displacements and rectal-bladder filling variations. These variations should be taken into account prior to each treatment throughout the course of treatment. The challenge involved in using CBCT and EPID, the most common IGRT imaging modalities today, is the difficulty identifying the soft tissue organs in the pelvis, due to the inability of these systems to visualize soft tissue, making it difficult to compensate for daily internal shifts. In most radiotherapy centers the daily target alignment of cervical cancer patients is based on bone matching, which is also standard in our department. However, bone matching does not take the relative uterine positional displacement into account.

Recently, 3D US has been more frequently applied as an IGRT method and mainly used for prostate alignment prior to the treatment fraction [19-20]. The advantage of ultrasound imaging is believed to be the capacity of this method to visualize soft tissue in the pelvis, especially on the bladder-uterus and bladder-prostate intersections. Very few published papers have reported the application of 3D US in GYN patients [21]. The published data in this study mostly quantifies inter-fractional bladder motion and variations in bladder volume rather than uterine positional changes. For instance, in a US study of 24 patients, Ahmed et al. (2008) concluded that the bladder volume decreased dramatically by a mean of 71% compared to the planning CT scan. This phenomenon was also observed in our study. Fig. 5 illustrates the reduction in bladder volume from the start of the treatment until week 5, the final week of treatment, despite the fact that the patients adhered to a standard bladder-rectum filling protocol. A moderately full bladder provides better propagation of US-waves and hence a clearer US image by sharpening the interface between bladder and uterus. Bladder volume reduction presents a challenge as it affects the daily uterine and bladder position as well as making the use of ultrasound as a daily IGRT modality more difficult. Tumor regression during radiotherapy is also a challenge. In a study based on weekly CT image acquisition, Lee's group [9] found an average tumor volume reduction greater than 27% in the third week compared to the initial CT planning image set.

A number of US studies on the prostate conclude that one of the drawbacks of using 3D US such as the IGRT method is probe pressure induced uncertainty on the target and OARs. In one study, Chan et al.'s 2008 [4] MRI-based study divided the uterus into three sections; cervical os, uterine canal, and uterine fundus. They reported that the fundus can vary from day to day by over 24 mm. Our result from patient 3 revealed an inter-fractional

displacement of the uterine center of mass by 16 mm in the AP-direction, which supports the result of Chan et al. The recent study by Jurgenliemk-Schultz et al. [22], which investigated vaginal positional change and the correlation between vaginal shift and bladder-rectal filling, reported a daily vaginal CTV positional change of up to 23 mm in the AP-direction. In the present study we observed that the inter-fractional variation was larger with US than CBCT. This can be explained by the fact that CBCT is based on bone matching, which does not take the effect of the relative uterine displacement on the bone structure into account. Initially, the goal of acquiring 3D CBCT in this study was to perform soft tissue matches. However, the poor image quality was an obstacle to distinguishing the target from the organs. White et al. conducted a study [23] of inter-observer variations in delineation of the prostate, based on five CBCT scans performed by five genitourinary oncologists. They found that the standard deviation for volume determination of the prostate was 8.93 cm^3 with large variability (3.98-19.00 cm^3), but the average standard deviation for center of mass displacement was small, measuring 0.7, 1.8, and 2.8 mm in the LR, AP, and SI-directions. Despite disagreement about how best to delineate the prostate gland, the small inter-observer variability in COM displacement suggests the potential of CBCT as soft tissue image guidance, thus replacing the tumor surrogate method of implanted fiducial markers. However, it should be noted that the study was conducted on a small number of scans and the matches were performed by expert observers, which is not a clinical reality today. Since the pelvis of GYN patients is more complex due to multiple structures moving relative to each other as well as deformation and tumor regression during radiation therapy, replicating the study on GYN patients is almost impossible.

In the present study some of the operators experienced difficulty applying the sweep/slide technique for capturing the entire uterus. First of all, the bladder must be identified, which is always easier in the sagittal plane and then the probe rotated by 90 degrees to the transversal plane, in which the scan was performed. An auto-scan probe would be a better solution, since after identifying the uterus in sagittal plane through a single click, the US scan and reconstruction of the uterine region could be conducted. Another challenge was the decrease in bladder filling during the treatment period, which adversely affected the image quality. This made it more difficult to identify the uterine-bladder interface and thus inducing errors in determining the uterine position and consequently variations in the inter-fractional displacements.

5 CONCLUSION

US imaging might be a better IGRT system than CBCT, despite difficulty in capturing the entire uterus. Uterine shifts based on US imaging contains relative uterus-bone displacement, which is not taken into consideration using CBCT bone match. A trial study based on more patients is required to validate statistical differences between CBCT and US.

6 CONFLICT OF INTEREST

The present study is a part of a three year PhD research project at Herlev Hospital, which is fully funded by Elekta, Inc.

Acknowledgement

Warm thanks to my hard-working colleagues, who helped me to accomplish this study; Gullander L. (RTT), Pedersen S. K (RTT), Zarp T (RTT), Jacobsson S (RTT), Pazhang S (radiographer), and Lynnerup V. K (radiographer).

References

[1] P. J. Eifel, a Jhingran, J. Brown, C. Levenback, and H. Thames, “Time course and outcome of central recurrence after radiation therapy for carcinoma of the cervix.,” *Int. J. Gynecol. Cancer*, vol. 16, no. 3, pp. 1106–11, 2006.

[2] J. K. Salama, A. J. Mundt, J. Roeske, and N. Mehta, “Preliminary outcome and toxicity report of extended-field, intensity-modulated radiation therapy for gynecologic malignancies.,” *Int. J. Radiat. Oncol. Biol. Phys.*, vol. 65, no. 4, pp. 1170–6, Jul. 2006.

[3] T. R. Mackie, J. Kapatoes, K. Ruchala, W. Lu, C. Wu, G. Olivera, L. Forrest, W. Tome, J. Welsh, R. Jeraj, P. Harari, P. Reckwerdt, B. Paliwal, M. Ritter, H. Keller, J. Fowler, and M. Mehta, “Image guidance for precise conformal radiotherapy,” *Int. J. Radiat. Oncol.*, vol. 56, no. 1, pp. 89–105, May 2003.

[4] P. Chan, R. Dinniwell, M. a Haider, Y.-B. Cho, D. Jaffray, G. Lockwood, W. Levin, L. Manchul, A. Fyles, and M. Milosevic, “Inter- and intrafractional tumor and organ movement in patients with cervical cancer undergoing radiotherapy: a cinematic-MRI point-of-interest study.,” *Int. J. Radiat. Oncol. Biol. Phys.*, vol. 70, no. 5, pp. 1507–15, Apr. 2008.

[5] K. Lim, P. Chan, R. Dinniwell, A. Fyles, M. Haider, Y.-B. Cho, D. Jaffray, L. Manchul, W. Levin, R. P. Hill, and M. Milosevic, “Cervical cancer regression measured using weekly magnetic resonance imaging during fractionated radiotherapy: radiobiologic modeling and correlation with tumor hypoxia.,” *Int. J. Radiat. Oncol. Biol. Phys.*, vol. 70, no. 1, pp. 126–33, Jan. 2008.

[6] B. M. Beadle, A. Jhingran, M. Salehpour, M. Sam, R. B. Iyer, and P. J. Eifel, “Cervix regression and motion during the course of external beam chemoradiation for cervical cancer.,” *Int. J. Radiat. Oncol. Biol. Phys.*, vol. 73, no. 1, pp. 235–41, Jan. 2009.

[7] H. Nam, W. Park, S. J. Huh, D. S. Bae, B. G. Kim, J. H. Lee, J. W. Lee, D. H. Lim, Y. Han, H. C. Park, and Y. C. Ahn, “The prognostic significance of tumor volume regression during radiotherapy and concurrent chemoradiotherapy for cervical cancer using MRI.,” *Gynecol. Oncol.*, vol. 107, no. 2, pp. 320–5, Nov. 2007.

[8] R. O. S. J. P. K. Aatee, M. A. J. J. O. Lofsen, M. A. B. J. V Erstraate, S. A. Q. Uint, and B. E. N. J. M. H. Eijmen, “DETECTION OF ORGAN MOVEMENT IN CERVIX CANCER PATIENTS USING A FLUOROSCOPIC ELECTRONIC PORTAL IMAGING DEVICE AND RADIOPAQUE MARKERS,” vol. 54, no. 2, pp. 576–583, 2002.

[9] J. E. Lee, Y. Han, S. J. Huh, W. Park, M. G. Kang, Y. C. Ahn, and D. H. Lim, “Interfractional variation of uterine position during radical RT: weekly CT evaluation.,” *Gynecol. Oncol.*, vol. 104, no. 1, pp. 145–51, Jan. 2007.

[10] X. A. Li, X. S. Qi, M. Pitterle, K. Kalakota, K. Mueller, B. a Erickson, D. Wang, C. J. Schultz, S. Y. Firat, and J. F. Wilson, “Interfractional variations in patient setup and anatomic change assessed by daily computed tomography.,” *Int. J. Radiat. Oncol. Biol. Phys.*, vol. 68, no. 2, pp. 581–91, Jun. 2007.

[11] L. van de Bunt, I. M. Jürgenliemk-Schulz, G. a P. de Kort, J. M. Roesink, R. J. H. a Tersteeg, and U. a van der Heide, “Motion and deformation of the target volumes during IMRT for cervical cancer: what margins do we need?,” *Radiother. Oncol.*, vol. 88, no. 2, pp. 233–40, Aug. 2008.

[12] J. J. W. Lagendijk, B. W. Raaymakers, A. J. E. Raaijmakers, J. Overweg, K. J. Brown, E. M. Kerkhof, R. W. van der Put, B. Hårdemark, M. van Vulpen, and U. a van der Heide, “MRI/linac integration.,” *Radiother. Oncol.*, vol. 86, no. 1, pp. 25–9, Jan. 2008.

[13] E. M. Kerkhof, B. W. Raaymakers, U. a van der Heide, L. van de Bunt, I. M. Jürgenliemk-Schulz, and J. J. W. Lagendijk, “Online MRI guidance for healthy tissue sparing in patients with cervical cancer: an IMRT planning study.,” *Radiother. Oncol.*, vol. 88, no. 2, pp. 241–9, Aug. 2008.

[14] S. J. Feigenberg, K. Paskalev, S. McNeeley, E. M. Horwitz, A. Konski, L. Wang, C. Ma, and A. Pollack, "Comparing computed tomography localization with daily ultrasound during image-guided radiation therapy for the treatment of prostate cancer: a prospective evaluation.," *J. Appl. Clin. Med. Phys.*, vol. 8, no. 3, p. 2268, Jan. 2007.

[15] J. Boda-Heggemann, F. M. Köhler, B. Küpper, D. Wolff, H. Wertz, S. Mai, J. Hesser, F. Lohr, and F. Wenz, "Accuracy of ultrasound-based (BAT) prostate-repositioning: a three-dimensional on-line fiducial-based assessment with cone-beam computed tomography.," *Int. J. Radiat. Oncol. Biol. Phys.*, vol. 70, no. 4, pp. 1247–55, Mar. 2008.

[16] F. L. B. Cury, G. Shenouda, L. Souhami, M. Duclos, S. L. Faria, M. David, F. Verhaegen, R. Corns, and T. Falco, "Ultrasound-based image guided radiotherapy for prostate cancer: comparison of cross-modality and intramodality methods for daily localization during external beam radiotherapy.," *Int. J. Radiat. Oncol. Biol. Phys.*, vol. 66, no. 5, pp. 1562–7, Dec. 2006.

[17] J. P. McGahan, J. Ryu, and M. Fogata, "Ultrasound probe pressure as a source of error in prostate localization for external beam radiotherapy.," *Int. J. Radiat. Oncol. Biol. Phys.*, vol. 60, no. 3, pp. 788–93, Nov. 2004.

[18] C. F. Serago, S. J. Chungbin, S. J. Buskirk, G. a Ezzell, a C. Collie, and S. a Vora, "Initial experience with ultrasound localization for positioning prostate cancer patients for external beam radiotherapy.," *Int. J. Radiat. Oncol. Biol. Phys.*, vol. 53, no. 5, pp. 1130–8, Aug. 2002.

[19] T. J. Scarbrough, N. M. Golden, J. Y. Ting, C. D. Fuller, A. Wong, P. a Kupelian, and C. R. Thomas, "Comparison of ultrasound and implanted seed marker prostate localization methods: Implications for image-guided radiotherapy.," *Int. J. Radiat. Oncol. Biol. Phys.*, vol. 65, no. 2, pp. 378–87, Jun. 2006.

[20] C. F. Serago, S. J. Buskirk, T. C. Igel, A. a Gale, N. E. Serago, and J. D. Earle, "Comparison of daily megavoltage electronic portal imaging or kilovoltage imaging with marker seeds to ultrasound imaging or skin marks for prostate localization and treatment positioning in patients with prostate cancer.," *Int. J. Radiat. Oncol. Biol. Phys.*, vol. 65, no. 5, pp. 1585–92, Aug. 2006.

[21] R. Ahmad, M. S. Hoogeman, S. Quint, J. W. Mens, I. De Pree, and B. J. M. Heijmen, "Inter-fraction bladder filling variations and time trends for cervical cancer patients assessed with a portable 3-dimensional ultrasound bladder scanner q," *Radiother. Oncol.*, vol. 89, no. 2, pp. 172–179, 2008.

[22] I. M. Jürgenliemk-Schulz, M. Z. Toet-Bosma, G. a P. de Kort, H. W. R. Schreuder, J. M. Roesink, R. J. H. a Tersteeg, and U. a van der Heide, "Internal motion of the vagina after hysterectomy for gynaecological cancer.," *Radiother. Oncol.*, vol. 98, no. 2, pp. 244–8, Feb. 2011.

[23] E. a White, K. K. Brock, D. a Jaffray, and C. N. Catton, "Inter-observer variability of prostate delineation on cone beam computerised tomography images.," *Clin. Oncol. (R. Coll. Radiol).*, vol. 21, no. 1, pp. 32–8, Feb. 2009.

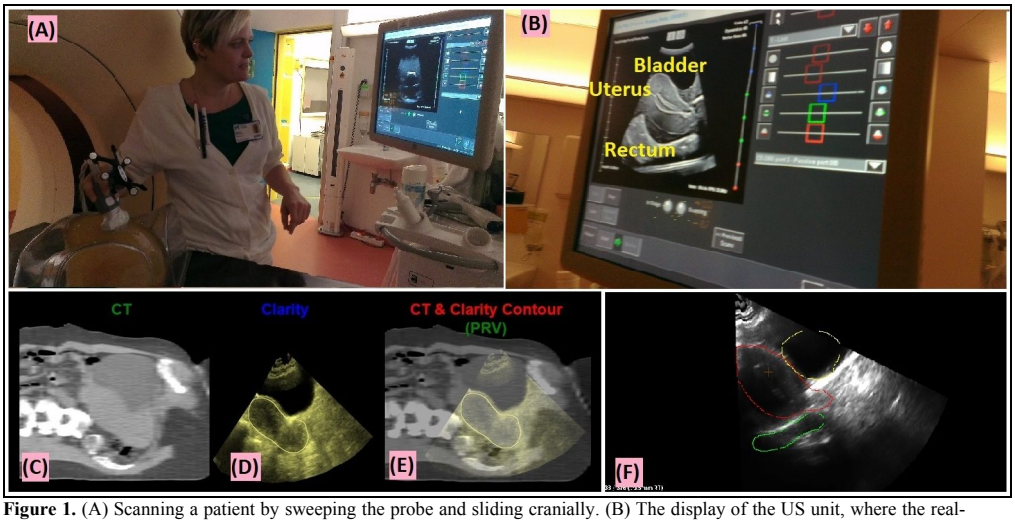

Figure 1. (A) Scanning a patient by sweeping the probe and sliding cranially. (B) The display of the US unit, where the real-time images can be observed. (C), (D), and (E) The fusion of acquired US images with the CT images sets to obtain a planning reference volume (PRV). (F) The US image, acquired in the treatment room is compared with the PRV to detect the uterine shift.

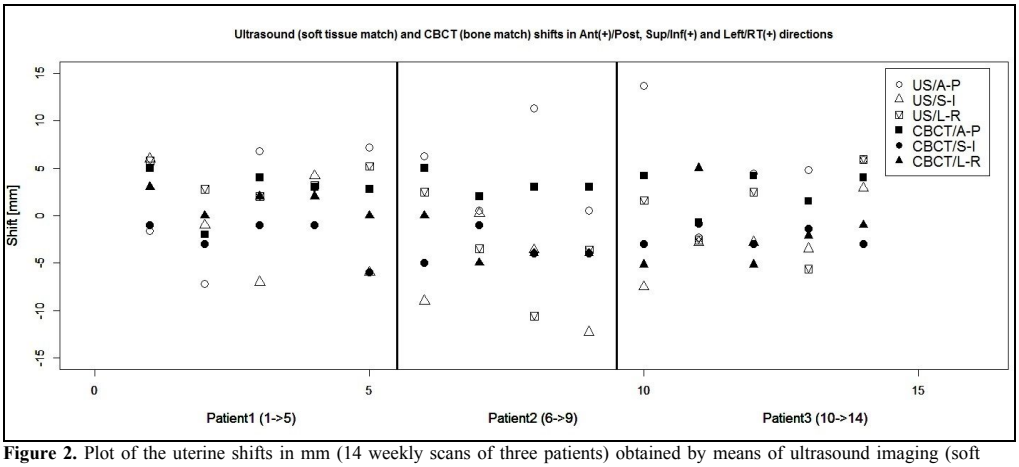

Figure 2. Plot of the uterine shifts in mm (14 weekly scans of three patients) obtained by means of ultrasound imaging (soft tissue matches) and corresponding shifts using CBCT imaging (bone match) for the three cardinal directions; anterior-posterior (AP), superior-inferior (SI), and left-right (LR).

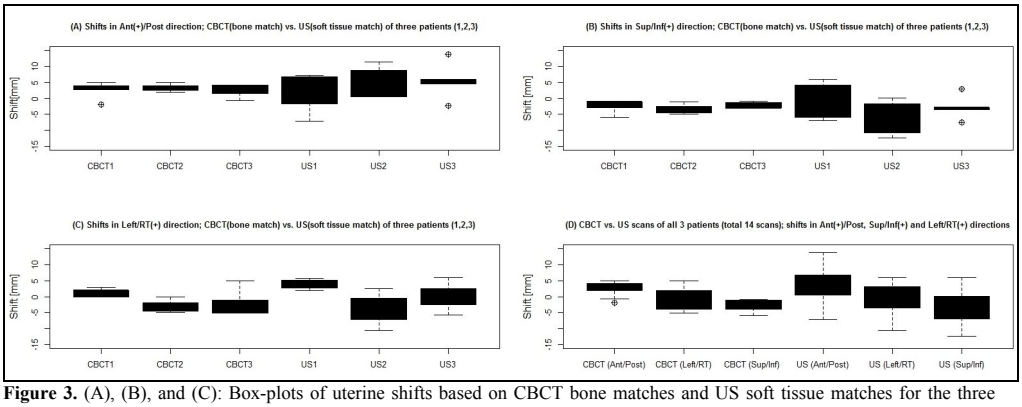

Figure 3. (A), (B), and (C): Box-plots of uterine shifts based on CBCT bone matches and US soft tissue matches for the three patients in the three cardinal directions; LR, AP, and SI. (D): The overall shifts for the patients in all directions.

Table. 1 The overall mean (3 patients, 14 scans), median, and standard deviations of the uterine inter-fractional shifts for ultrasound and CBCT matches in all three directions.

	Ultrasound			CBCT		
	Anterior/ Posterior	**Superior/ Inferior**	**Left/ Right**	**Anterior/ Posterior**	**Superior/ Inferior**	**Left/ Right**
Median	**4.6**	**-3.2**	**2.2**	**3.0**	**-3.0**	**-0.5**
Mean (±1SD)	**3.8 (±5.5)**	**-3.0 (±5.2)**	**0.4 (±4.9)**	**2.8 (±2.0)**	**-2.7 (±1.7)**	**-1.0 (±3.3)**

Table2. Values of paired t-test of obtained matching shifts using weekly ultrasound and CBCT scans of cervical cancer patients. The p-values are calculated for a 95% confidence interval (CI).

		N	Mean Of diff.	df	t	95% CI (lower/upper)	P-value
	Direction						
Patient 1	**Anterior-Posterior**	5	-0.92	4	-0.43	-6.93/5.09	0.692
	Superior-Inferior	5	1.64	4	0.72	-4.65/7.93	0.509
	Left-Right	5	2.4	4	2.74	-0.03/4.83	0.052
Patient 2	**Anterior-Posterior**	4	1.40	3	0.57	-6.35/9.15	0.606
	Superior-Inferior	4	-2.68	3	-1.22	-9.66/4.31	0.310
	Left-Right	4	-0.55	3	-2.67	-7.11/6.01	0.807
Patient 3	**Anterior-Posterior**	5	2.67	4	1.41	-2.57/7.92	0.230
	Superior-Inferior	5	-0.49	4	-0.28	-5.39/4.40	0.793
	Left-Right	5	2.05	4	0.65	-6.74/10.85	0.552
Three patients	**Anterior-Posterior**	14	1.03	13	0.84	-1.60/3.65	0.414
	Superior-Inferior	14	-0.36	13	-0.29	-2.96/2.25	0.773
	Left-Right	14	1.43	13	1.14	-1.29/4.16	0.276

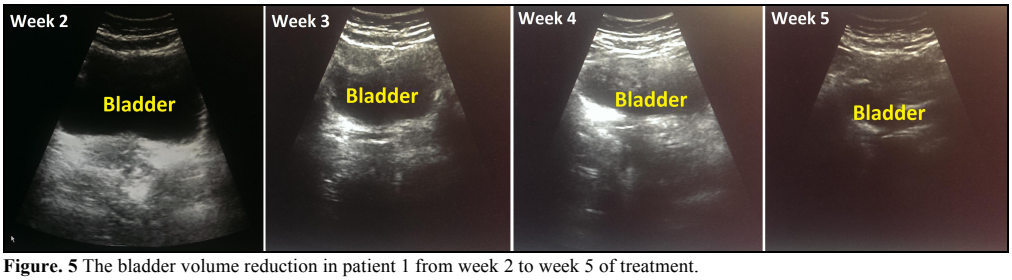

Figure. 5 The bladder volume reduction in patient 1 from week 2 to week 5 of treatment.

PAPER C

Impact of ultrasound probe pressure on uterine positional displacement in gynecologic cancer patients

Authors: Mariwan Baker, Trine Juhler-Nøttrup, and Calus F. Behrens.

Published in: Future Medicine Women's Health, pp. 583-590, 2014

Abstract

Aim: The aim of this study was to quantify the uterine positional displacement induced by ultrasound probe pressure on a phantom and address the daily uterine motion in a healthy volunteer.
Materials & methods: The phantom mimics the female pelvic region. The incorporated organs were subjected to displacement. A total of 42 phantom scans and 16 volunteer scans were acquired. The uterine shifts were measured in three directions.
Results & discussion: The difference of uterine positional displacements, using pressure versus without pressure on the phantom, was not statistically significant. The daily uterine positional variations of the volunteer were larger than the probe pressure induced displacements.
Conclusion: The larger daily uterine shifts of the volunteer outweighed the submillimeter impact of the probe pressure in all directions.

Research Article

For reprint orders, please contact: reprints@futuremedicine.com

Women's Health

Impact of ultrasound probe pressure on uterine positional displacement in gynecologic cancer patients

Aim: The aim of this study was to quantify the uterine positional displacement induced by ultrasound probe pressure on a phantom and address the daily uterine motion in a healthy volunteer. **Materials & methods:** The phantom mimics the female pelvic region. The incorporated organs were subjected to displacement. A total of 42 phantom scans and 16 volunteer scans were acquired. The uterine shifts were measured in three directions. **Results & discussion:** The difference of uterine positional displacements, using pressure versus without pressure on the phantom, was not statistically significant. The daily uterine positional variations of the volunteer were larger than the probe pressure induced displacements. **Conclusion:** The larger daily uterine shifts of the volunteer outweighed the submillimeter impact of the probe pressure in all directions.

Keywords: phantom • positional displacement • probe pressure • ultrasound • uterus

Mariwan Baker*[1,2], Trine Juhler-Nøttrup[1] & Claus F Behrens[1]

[1]Department of Oncology(R), Radiotherapy Research Unit, Herlev Hospital, Herlev Ringvej 75, Herlev, Denmark

[2]Center for Nuclear Technologies, Technical University of Denmark, DTU Risø Campus, Roskilde, Denmark

*Author for correspondence: mariwan.baker@regionh.dk

In modern conformal radiotherapy with tight margins and steep dose gradients, such as intensity-modulated radiotherapy, it is essential that the position of the clinical target volume is precisely defined prior to each treatment fraction throughout the entire course of treatment.

Technical innovations have enabled the direct integration of various image verification methods into the treatment unit. In many cases this allows for patient and tumor monitoring and position correction. Nowadays, kV and MV planar radiographic imaging and volumetric cone beam computed tomography (CT) imaging are standard image verification systems in many radiotherapy centers. Generally, these systems are implemented as image-guided radiotherapy (IGRT) for daily target alignment, and thereby improving the precision of the radiotherapy treatment. However, one of the challenges of using these ionizing systems is insufficient soft tissue visualization (e.g., of the uterus of gynecologic [GYN] cancer patients or identification of the prostate gland and surrounding organs at risk [OAR] in prostate cancer patients). In some cases these systems require invasive methods, such as implanted fiducial markers in prostate radiotherapy. Therefore, different nonionizing 3D-ultrasound (US) systems, such as the Elekta 3D Clarity® Soft Tissue Visualization system (Elekta, Montreal, Canada) and the NOMOS B-mode Acquisition and Targeting ultrasound system (NOMOS Corporation, PA, USA) have been developed and introduced into radiotherapy [1–5]. The prostate and uterus, for which internal position variations are dependent on rectal and bladder filling, are ideal sites for US scans. However, different uncertainty factors in terms of probe handling, image quality and interoperator variability are present when using the US systems. Variations in the transducer probe pressure applied have previously been documented during 3D US on prostate patients [6,7].

The aim of the present study was to quantify the magnitude of probe pressure induced uncertainty using the Clarity US system on a commercial GYN phantom. An additional aim was to compare the pressure induced uncertainty with the overall interfractional variations by utilizing the US system on a healthy volunteer.

Future Medicine part of fsg

Materials & methods

A phantom was scanned by seven operators in four sessions on different days. Each operator performed two scans per session, one without pressure (WOP) or light probe pressure and one with maximum pressure (WP). All the US experienced operators were not presented in all sessions, thus, only a total of 42 scans were acquired. A healthy volunteer was scanned by the available Clarity operators in three sessions, leading to a total of 16 scans, over a period of 3 weeks (one session per week). Each operator participated in 2 weeks of intensive training provided by the manufacturer of Clarity, as well as several practice sessions before the start of the study.

Phantom

The US training phantom (Model CIRS 404) mimics the female pelvic region and contains a uterus, bladder and rectum representing the standard female pelvic organs (Figure 1A & B). The organs are subjected to displacement due to the exerted probe pressure. The phantom does not contain any skeletal structure, such as femur head or pelvic bone. The phantom is intended for US scans, thus all organs are easily defined in the acquired US images (Figure 1C). Initially, the phantom was marked with small spherical ball bearings (laser alignment markers), used to aid reproducibility of daily setup prior to each US scan session. During an initial session the best possible US scan was selected as position reference to the following four sessions.

Volunteer

The volunteer, a healthy young woman, was instructed to have an empty rectum and full bladder prior to each session. A moderately full bladder ensures better propagation of the US waves and hence a clearer US image by enhancing the image and sharpening the interface between bladder and uterus/cervix/vaginal canal. The fixation was in supine position by means of a Vac Fix fixation system to ensure position reproducibility between sessions. The volunteer was instructed to remain still throughout each session. Consistent positioning of the volunteer was enabled by the alignment of natural skin markers to the isocenter lasers of the CT room. A US transabdominal scan of the pelvic region was performed repeatedly by each operator until adequate image quality

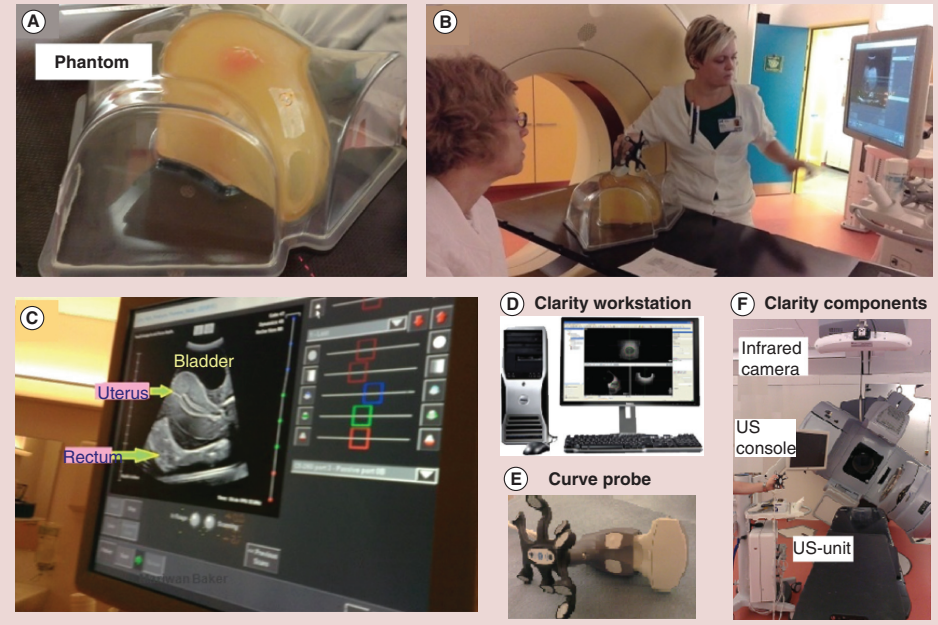

Figure 1. Clarity ultrasound system. (A) Phantom. **(B)** Phantom US scanning by means of a curve probe in the computed tomography room. **(C)** Clarity US console, in which the phantom organs (bladder, uterus and rectum) are easily recognizable. **(D)** The Clarity workstation, in which the fusion and organ delineation are performed. **(E)** 2D curve probe. **(F)** The Clarity unit and ceiling-mounted infrared camera in the treatment room.
US: Ultrasound.

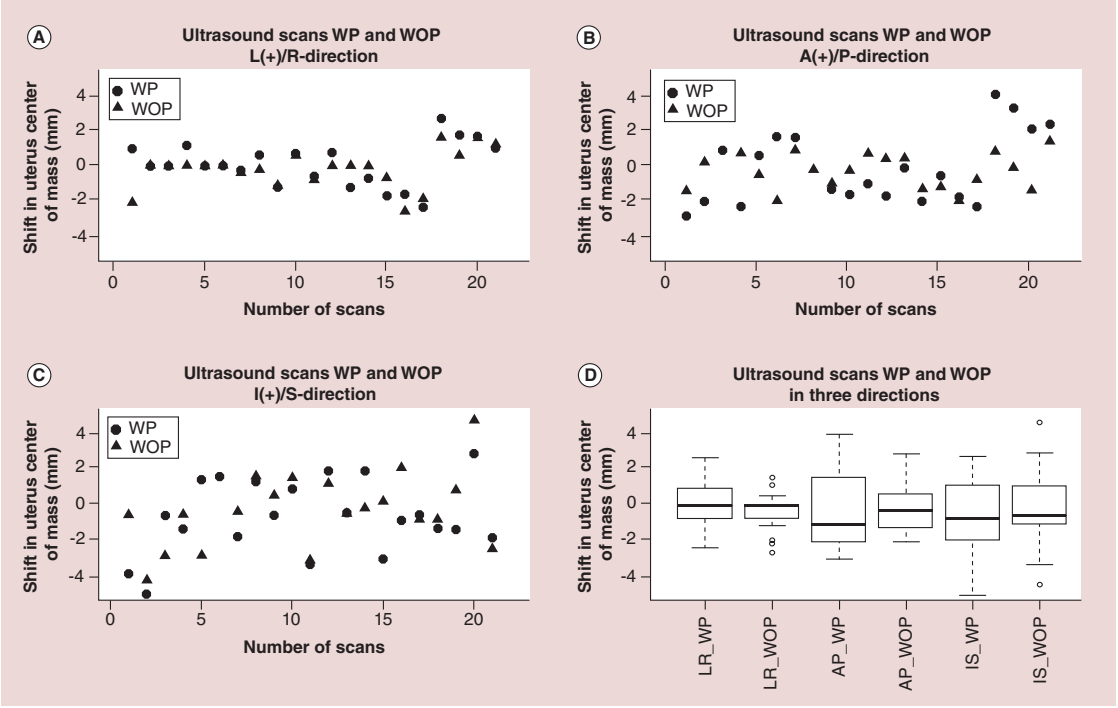

Figure 2. Plots of the COM shifts based of ultrasound scans of the phantom uterus. WP & WOP in **(A)** L/R, **(B)** A/P and **(C)** I/S directions. **(D)** Boxplot for WP and WOP for all three cardinal directions (L/R, A/P, I/S).
A: Anterior; I: Inferior; L: Left; P: Posterior; R: Right; S: Superior; WOP: Without pressure; WP: With pressure.

was achieved. During the first session the best scan, in which the organs were clearly definable, was selected as a reference for the following three sessions.

Clarity US system

The Clarity Soft Tissue Visualization system (Clarity Model 310C00) consists of two US units: one located in the CT simulation room and one in the treatment room. The two units are connected through a workstation/server. In this study all US scans were performed in the CT room. Since the objective of the ongoing project at Herlev Hospital is to implement the Clarity 3D US system for both GYN and prostate patients throughout the course of their treatment, the treatment room unit will be utilized only for daily IGRT.

Each US unit is equipped with a curve probe for transabdominal 3D US scanning. Each station consists of a ceiling-mounted infrared camera that can track the US probe by monitoring the infrared reflectors/emitters mounted on it (Figure 1E & F).

To enable superimposition of the acquired 3D US images and the reference US image, the 3D US system is calibrated to the same room coordinate system as the CT and treatment room, respectively. The calibration procedure is accomplished by means of an alignment phantom. Quality assurance checks confirm the system calibration on each day of use.

Image acquisition

The US image of the phantom (transabdominal US scan) was acquired by the seven experienced operators using the curve probe (Figure 1B). In each phantom scan the US probe was placed on the first occasion with minimal pressure and on the second with firm pressure in the region corresponding to the pubic symphysis and rotated, after which it was swept cranially. No firm pressure was applied on the volunteer, as the focus was on obtaining clear images, where the complex pelvic structure could be identified.

Organ delineation & data analysis

The uterus, bladder and rectum were delineated in the reconstructed 3D US image datasets using the Clarity workstation supplied by the manufacturer. In the workstation the delineation can be performed either manually or with aid of autosegmentation. In this study the assisted segmentation was utilized for all outlined organs. A single operator (MB) conducted a retrospective analysis

Table 1. Paired *t*-test values of the mean uterine shifts using ultrasound scans of the phantom with pressure & without pressure.

Directions	Number of scans	Standard deviation (mm)	Difference between the means (mm)	95% CI (lower/upper)	p-value
Left–right	21	0.93	-0.29	-1.03/0.45	0.43
Anterior–posterior	21	2.13	0.10	-0.99/1.18	0.86
Inferior–superior	21	1.87	0.50	-0.85/1.85	0.45

of the acquired US image sets and delineated the organs for both the phantom and the volunteer.

Descriptive statistics and the paired sample *t*-test were employed to evaluate the statistical significance of the mean differences between probe pressure and no probe pressure. The p-value was calculated for a 95% CI, (i.e., the significance at $\alpha = 0.05$).

Results

Positional shifts of the phantom uterus center of mass (COM) in the three orthogonal directions WP (depicted as circles) and WOP (triangles) are presented (Figure 2A–C). Positive shifts are left, anterior and inferior. Qualitatively, these plots demonstrate that there are no significant differences when comparing the shifts between WP and WOP.

The overall mean (±1 SD) of the phantom COM shifts are (mm); WP/WOP: LR (0.1 ± 1.2)/(-0.2 ± 1.1), AP (-0.3 ± 2.1)/(-0.2 ± 1.2) and IS (-0.8 ± 2.1)/(-0.3 ± 2.2). The largest recorded shift is observed in the I/S-direction; +5 mm (WOP) and -5 mm (WP). The mean of the COM shifts in all three directions (L/R, A/P, I/S) for WP and WOP are centered around zero (Figure 2D). The spread in the recorded shifts, (i.e., the standard deviations) for WP is larger than WOP in all directions. This is caused by larger interoperator variations while applying strong probe pressure. For each of the three directions a paired two sample *t*-test was utilized to test whether there are any statistical significant differences in the means of the shifts between WP and WOP. No statistical significant differences in any direction are observed (i.e., none of the p-values are below 0.05). The largest lower/upper 95% CI range was found in the I/S-direction (-0.85/-1.85) (Table 1).

For the volunteer the recorded mean COM shift on day 3 in L/R direction is approximately 10 mm relative to the reference, while on days 1 and 2 the lateral shift is less than 2 mm (Figure 3). Furthermore, in the A/P direction the mean shifts are less than 2 mm on days 1 and 2, but more than 5 mm on day 3. The largest interfractional displacement is observed in the I/S direction, with a mean value of -7.7 mm, +7.6 mm and -6.9 mm on days 1, 2 and 3, respectively (Table 2). This clinically critical shift is visible in Figure 4. One can clearly see that the bladder is fuller on day 2 than on day 1, causing correlated uterine positional displacement. It is worth mentioning that on day 2 only four US scans (four operators) took place compared with six on days 1 and 3.

Discussion

Interfractional positional uncertainty of the uterus, rectum and bladder in GYN patients is a challenge in radiotherapy as it leads to the application of large planning target volume (PTV) margins. Previous reports have confirmed that uterine positional changes are strongly correlated with daily variation in bladder–rectum filling [8–10]. Thus, there is a need to incorporate IGRT methods into radiotherapy to identify and correct possible uterine and OAR positional changes. At present the 3D US IGRT method has mainly been used for prostate alignment prior to treatment [11–17]. Only a few published papers have reported the application of 3D US in GYN patients [18–20], and with the focus on quantifying interfractional bladder motion and variation in bladder volume rather than uterine positional change. For instance, in a US study of 24 cervical cancer patients, Ahmad *et al.* concluded that the mean bladder volume decreased dramatically by 71% compared with the treatment planning CT scan [18]. Herlev Hospital is a pioneer in the application of the Clarity 3D US system with a focus on GYN diagnoses. The present study started by applying Clarity on a phantom and a healthy volunteer and it will subsequently be tested for GYN patients at Herlev Hospital.

Different studies on the prostate have concluded that one of the drawbacks of using 3D US as the IGRT method is probe pressure-induced uncertainty of the target and OAR locations. However, to our knowledge, no specific probe pressure study on GYN patients has been published. In the present phantom study, we found no statistically significant differences in uterine COM shifts using pressure versus no pressure. All the acquired US scans indicated that uterine COM displacements were in the vicinity of zero, with a daily mean value of less than 1 mm in all three cardinal directions (L/R, A/P and I/S). Since the shifts of the bladder–uterus interface is interesting to study – as a portion of the bladder receives an undesirable high

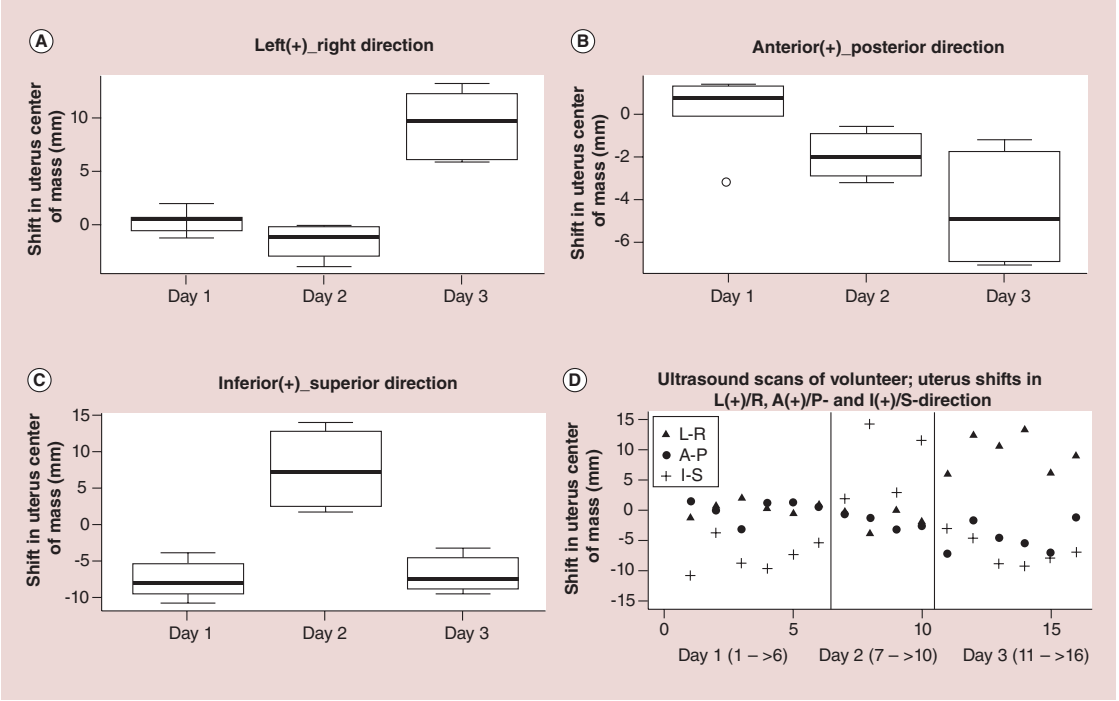

Figure 3. Omnidirectional shifts of uterine center of mass of a volunteer. (A–C) Boxplots of uterine COM shifts for the volunteer on 3 days in the three cardinal directions; L/R, A/P and I/S. **(D)** Plot of uterine COM shifts; the daily ultrasound scans (day 1: six scans, day 2: four scans and day 3: six scans) in the L/R, A/P and I/S directions.
A: Anterior; I: Inferior; L: Left; P: Posterior; R: Right; S: Superior;

radiation dose owing to its proximity to the uterus – further studies focusing on the bladder–uterus interface are necessary. In an MRI study by Chan *et al.*, the uterus was divided into three sections; cervical os, uterine canal and uterine fundus [21]. GYN patients underwent a pelvic MRI scan before treatment followed by weekly scans. The interfractional displacement was largest at the fundus, moderate along the canal and smallest at the cervical os. A similar study using 3D US is recommended to verify these findings.

Our volunteer study revealed a clinically critical large interfractional displacement in all three directions. The largest uterine positional displacement was 15 mm in the I/S direction between days 1 and 2. Although our volunteer US scans are limited to three sessions, the result agrees well with a recent study by Jurgenliemk-Schultz *et al.*, which investigated vaginal positional change and the correlation between vaginal shift and bladder–rectal filling [22]. These authors reported a vaginal clinical target volume positional change of up to 2.3 cm in the A/P direction. However, in contrast to previous studies, they did not find any correlation between vaginal positional displacement and bladder–rectal filling, except an extremely weak one in the case of A/P position shift and rectal filling.

The challenge experienced by most of our operators during 3D US acquisition was to find an appropriate probe handling technique that captured the entire uterus from the cervical os to the fundus, as the image quality was poor in some cases. Obviously, poor image quality has an adverse influence on uterine delineation, thus leading to uncertainty in COM shifts. This challenge is illustrated in the boxplots (Figure 3) and by the SD (Table 2) of the uterine COM shifts on day 2, which was more than 6 mm in the I/S direction. The plot in Figure 3D illustrates the large dispersion of COM shifts on day 2 in the I/S direction. Our experience of suboptimal image quality is confirmed by the study of Johnston *et al.*, who compared assisted segmentation (employed in the present study) and manual segmentation of prostate patients using the Clarity 3D US system [23]. During quality classification of the acquired US images, they found that up to 33% were of bad quality, which hinders accurate outlining of the target.

Finally, it should be noted that the phantom used is not necessary representative of a real GYN patient,

Table 2. Mean values with standard deviations of the uterine shifts in the volunteer scanned by seven operators.

	Directions	Number of operators/scans	Mean (mm)	Standard deviation (mm)
Day 1	Left–right	6	0.27	1.09
	Anterior–posterior	6	0.18	1.71
	Inferior–superior	6	-7.65	2.64
Day 2	Left–right	4	-1.58	1.74
	Anterior–posterior	4	-1.95	1.21
	Inferior–superior	4	7.55	6.12
Day 3	Left–right	6	9.48	3.08
	Anterior–posterior	6	-4.47	2.53
	Inferior–superior	6	-6.85	2.47

therefore a clinical study is needed to validate the results of this study. The daily bladder and rectal volume variations can strongly affect the position of the uterus, which cannot be simulated by our phantom. Furthermore, statistical evaluation of the interfractional uterine positional changes based on a single volunteer must be considered with caution, and a clinical study is needed to validate the present result.

Conclusion

The large daily uterine positional displacement of the volunteer outweighs the submillimeter impact of probe pressure in all directions. The difference in phantom uterine COM shifts using probe pressure versus no probe pressure is not statistically significant. Based on a single volunteer case, a large uncertainty in using 3D US on GYN patients is the poor quality of the acquired image due to the challenge of handling the probe. A clinical study is required to validate phantom probe pressure-induced uncertainty. The large interfractional variations based on a single volunteer warrant further investigation.

Future perspective

In radiotherapy, it is vital that the daily target alignment is correctly applied prior to each treatment. Today's widely used X-ray IGRT techniques are poor in terms of visualizing soft tissue in the female pelvic region and for this reason bone match instead of soft tissue match is employed. However, it has been previously demonstrated that uterine mobility relative to the bone structure can be several centimeters in all directions. In the present study we have shown daily uterine positional displacements of several centimeters using the novel Clarity US system. US is nonionizing, fast, inexpensive and good for visualizing soft tissue organs. Despite challenges in probe handling to obtain optimal images, the US is a good choice as a future IGRT system for cervical cancer patients.

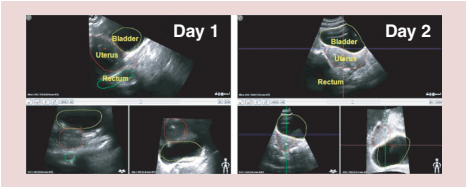

Figure 4. Outlined organs (bladder, uterus and rectum), sagittal, transversal and frontal cross-sections, in the Clarity workstation. The uterine positional shift is obvious from days 1 to 2.

Acknowledgements

Sincere thanks to our hardworking colleagues who helped to conduct this study; L Gullander (radiation therapist), SK Pedersen (radiation therapist), T Zarp (radiation therapist), S Jacobsson (radiation therapist), S Pazhang (radiographer) and VK Lynnerup (radiographer).

Financial & competing interests disclosure

The current study is a part of a 3 year PhD research project at Herlev Hospital that is funded by Elekta, Inc. The authors have no other relevant affiliations or financial involvement with any organization or entity with a financial interest in or financial conflict with the subject matter or materials discussed in the manuscript apart from those disclosed.

No writing assistance was utilized in the production of this manuscript.

Ethical conduct of research

The authors state that they have obtained appropriate institutional review board approval or have followed the principles outlined in the Declaration of Helsinki for all human or animal experimental investigations. In addition, for investigations involving human subjects, informed consent has been obtained from the participants involved.

Executive summary

Background

- In radiotherapy it is important that the target is correctly aligned to the planned images on a daily basis.
- This study quantifies the impact of ultrasound probe pressure on uterine displacement in a phantom and compares positional uncertainty with the daily uterine motion of a young healthy volunteer.
- The phantom mimics the female pelvic region and incorporates organs that are at risk of probe pressure displacement.

Aim

- To quantify the uterine positional uncertainty induced by ultrasound probe pressure on a phantom and determine the day-to-day uterine displacement of a young healthy volunteer.

Materials & methods

- A uterine phantom and a volunteer underwent ultrasound scans conducted by seven operators. The phantom mimics the female pelvic region and is easily defined in ultrasound scans. A total of 42 phantom scans, 21 with light probe pressure (without pressure) and 21 using strong probe pressure (with pressure) and 16 volunteer scans were performed. Shifts in the uterine center of mass relative to the reference volumes were measured in three directions; left–right (LR), anterior–posterior (AP) and inferior–superior (IS).

Results & discussion

- For the phantom the difference between with pressure and without pressure was not statistically significant ($p > 0.43$ for each cardinal direction). The mean (±1 SD) of the daily center of mass displacements of the uterine position in the volunteer, as recorded by the seven observers, were (mm); LR: day 1 (0.3 ± 1.1), day 2 (-1.6 ± 1.7), day 3 (9.5 ± 3.1), AP: day 1 (0.2 ± 1.7), day 2 (-2 ± 1.2), day 3 (-4.5 ± 2.5) and IS: day 1 (-7.7 ± 2.6), day 2 (7.6 ± 6.1), day 3 (-6.5 ± 2.5), respectively.
- The study reveals no significant shifts in any direction using light or strong probe pressure.

Conclusion

- The larger daily uterine positional displacement in all directions in the volunteer outweighs the submillimeter displacement due to the probe pressure. A clinical study is required to validate the phantom probe pressure-induced uncertainty. The large interfractional variations based on a single volunteer warrant further investigation.

References

Papers of special interest have been highlighted as:
• of interest; •• of considerable interest

1 Peng C, Kainz K, Lawton C, Li XA. A comparison of daily megavoltage CT and ultrasound image guided radiation therapy for prostate cancer. *Med. Phys.* 35(12), 5619–5628 (2008).

2 Boda-Heggemann J, Köhler FM, Küpper B *et al.* Accuracy of ultrasound-based (BAT) prostate-repositioning: a three-dimensional on-line fiducial-based assessment with cone-beam computed tomography. *Int. J. Radiat. Oncol. Biol. Phys.* 70(4), 1247–1255 (2008).

3 Feigenberg SJ, Paskalev K, McNeeley S *et al.* Comparing computed tomography localization with daily ultrasound during image-guided radiation therapy for the treatment of prostate cancer: a prospective evaluation. *J. Appl. Clin. Med. Phys.* 8(3), 299–110 (2007).

4 Pinkawa M, Pursch-Lee M, Asadpour B *et al.* Image-guided radiotherapy for prostate cancer. Implementation of ultrasound-based prostate localization for the analysis of inter- and intrafraction organ motion. *Strahlenther. Onkol.* 184(12), 679–685 (2008).

5 Cury FLB, Shenouda G, Souhami L *et al.* Ultrasound-based image guided radiotherapy for prostate cancer: comparison of cross-modality and intramodality methods for daily localization during external beam radiotherapy. *Int. J. Radiat. Oncol. Biol. Phys.* 66(5), 1562–1567 (2006).

6 McGahan JP, Ryu J, Fogata M. Ultrasound probe pressure as a source of error in prostate localization for external beam radiotherapy. *Int. J. Radiat. Oncol. Biol. Phys.* 60(3), 788–793 (2004).

•• **The aim of the phantom study is to explore the ultrasound probe pressure by comparing acquired ultrasound images to the reference computed tomography (CT) images. The phantom mimics a male pelvis with water-filled rectum and bladder and a clay sphere representing the prostate. The structures are subject to displacement while exerting probe pressure. McGahan *et al.* observed target displacement due to strong probe pressure. They concluded that care must be taken to avoid any large target displacement when applying the ultrasound probe.**

7 Serago CF, Chungbin SJ, Buskirk SJ, Ezzell G, Collie C, Vora S. Initial experience with ultrasound localization for positioning prostate cancer patients for external beam radiotherapy. *Int. J. Radiat. Oncol. Biol. Phys.* 53(5), 1130–1138 (2002).

8 Taylor A, Powell MEB. An assessment of interfractional uterine and cervical motion: implications for radiotherapy target volume definition in gynaecological cancer. *Radiother. Oncol.* 88(2), 250–257 (2008).

•• **Based on MRI scans of 33 gynecological cancer patients, the uterine positional variations are addressed in three orthogonal directions. Correlation of rectal volume variation with cervical position is observed, while bladder filling led to more uterine body displacements.**

9 Ahmad R, Hoogeman MS, Bondar M *et al.* Increasing treatment accuracy for cervical cancer patients using correlations between bladder-filling change and cervix–uterus displacements: proof of principle. *Radiother. Oncol.* 98(3), 340–346 (2011).

• **This prospective study based on 13 cervical cancer patients compared the target/uterine displacement pre- and post-treatment CT scans. The tip of the uterus was found to be displaced by several centimeters. Large uterine positional errors were determined, which adversely affect the accuracy of radiation treatment delivery.**

10 Hun SJ, Park W, Han Y. Interfractional variation of uterine position during radical RT: weekly CT evaluation. *Gynecol. Oncol.* 104(1), 145–151 (2007).

• **A total of 66 patients underwent two MRI scans, one before radiation treatment and one during the treatment, which revealed large uterine positional displacement, especially in the case of larger tumors. Hun *et al.* conclude that for younger patients (<60 years), extra care must be taken during the delivery of intensity-modulated radiation treatment.**

11 Buchali A, Koswig S, Dinges S *et al.* Impact of the filling status of the bladder and rectum on their integral dose distribution and the movement of the uterus in the treatment planning of gynecological cancer. *Radiother. Oncol.* 52(1), 29–34 (1999).

12 McNair H, Mangar S, Coffey J *et al.* A comparison of CT- and ultrasound-based imaging to localize the prostate for external beam radiotherapy. *Int. J. Radiat. Oncol. Biol. Phys.* 65(3), 678–687 (2006).

13 Scarbrough TJ, Golden NM, Ting JY *et al.* Comparison of ultrasound and implanted seed marker prostate localization methods: implications for image-guided radiotherapy. *Int. J. Radiat. Oncol. Biol. Phys.* 65(2), 378–387 (2006).

14 Serago CF, Buskirk SJ, Igel TC, Gale A, Serago NE, Earle JD. Comparison of daily megavoltage electronic portal imaging or kilovoltage imaging with marker seeds to ultrasound imaging or skin marks for prostate localization and treatment positioning in patients with prostate cancer. *Int. J. Radiat. Oncol. Biol. Phys.* 65(5), 1585–1592 (2006).

15 Langen K, Pouliot J, Anezinos C *et al.* Evaluation of ultrasound-based prostate localization for image-guided radiotherapy. *Int. J. Radiat. Oncol. Biol. Phys.* 57(3), 635–644 (2003).

16 Orton NP, Jaradat H, Tomeé W. Clinical assessment of three-dimensional ultrasound prostate localization for external beam radiotherapy. *Med. Phys.* 33(12), 4710–4717 (2006).

17 Gayou O, Miften M. Comparison of mega-voltage cone-beam computed tomography prostate localization with online ultrasound and fiducial markers methods. *Med. Phys.* 35(2), 531–538 (2008).

18 Ahmad R, Hoogeman MS, Quint S, Mens JW, De Pree I, Heijmen BJM. Inter-fraction bladder filling variations and time trends for cervical cancer patients assessed with a portable 3-dimensional ultrasound bladder scanner. *Radiother. Oncol.* 89(2), 172–179 (2008).

19 Jhingran A, Salehpour M, Sam M, Levy L, Eifel PJ. Vaginal motion and bladder and rectal volumes during pelvic intensity-modulated radiation therapy after hysterectomy. *Int. J. Radiat. Oncol. Biol. Phys.* 82(1), 256–262 (2012).

• **Jhingran *et al.* performed a clinical study of 24 cervical cancer patients to investigate rectal and bladder volume variations throughout the course of the radiation treatment. The patients underwent a CT scan before treatment and twice weekly during the course of treatment. Despite a bladder-filling protocol, large bladder variations were unavoidable.**

20 Yee D, Parliament M, Rathee S, Ghosh S, Ko L, Murray B. Cone beam CT imaging analysis of interfractional variations in bladder volume and position during radiotherapy for bladder cancer. *Int. J. Radiat. Oncol. Biol. Phys.* 76(4), 1045–1053 (2010).

• **In this clinical study the daily positional bladder variations of ten bladder cancer patients undergoing radiation treatment were determined in all three orthogonal coordinates using daily cone beam CT imaging. Yee *et al.* observed significant positional bladder variations, which could adversely influence the outcome of radiation treatment.**

21 Chan P, Dinniwell R, Haider M *et al.* Inter- and intrafractionaltumor and organ movement in patients with cervical cancer undergoing radiotherapy: a cinematic-MRI point-of-interest study. *Int. J. Radiat. Oncol. Biol. Phys.* 70(5), 1507–1515 (2008).

•• **Chan *et al.* investigated the inter- (day to day) and intrafractional (time corresponding to the treatment delivery) uterine positional displacements of 20 cervical cancer patients using weekly MRI scans. The uterus was divided into three regions; uterine head, uterine body and uterine opening. The largest displacement was observed in the uterine head, which requires a minimum margin of 4 cm to ensure inclusion of the target in the treatment field. This large margin is not applied in any radiotherapy centers, therefore rescanning of cervical cancer patients during the course of treatment is essential to ensure that they derive maximum benefit from the treatment.**

22 Jürgenliemk-Schulz IM, Toet-Bosma MZ, De Kort G *et al.* Internal motion of the vagina after hysterectomy for gynaecological cancer. *Radiother. Oncol.* 98(2), 244–248 (2011).

23 Johnston H, Hilts M, Beckham W, Berthelet E. 3D ultrasound for prostate localization in radiation therapy: a comparison with implanted fiducial markers. *Med. Phys.* 35(6), 2403–2413 (2008).

•• **Compares prostate shifts in ultrasound scans with those of fiducial markers implanted into the prostate. Ultrasound-based shifts are larger than fiducial marker shifts in all three directions; therefore transabdominal ultrasound is not an optimal alternative to the widely applied fiducial markers image-guided radiotherapy.**

PAPER D

Prostate displacement during transabdominal ultrasound image-guided radiotherapy assessed by real-time four-dimensional transperineal monitoring

Authors: Mariwan Baker, and Calus F. Behrens.

Published in: Acta Oncologica, 2015

Abstract

Background: Transabdominal ultrasound (TAUS) imaging is currently available for localizing the prostate in daily image-guided radiotherapy (IGRT). The aim of this study was to determine the induced prostate displacement during such TAUS imaging. The prostate displacement was monitored using a novel transperineal four-dimensional (4D) US (TPUS) system.
Material and methods: Ten prostate cancer patients, with a mean age of 68 years (58/76), were US scanned in the computed tomography (CT) room utilizing the Clarity 4D TPUS monitoring system. The patients were asked to comply with a moderate bladder fi lling protocol. After US-CT fusion, the prostate volume was delineated and used as a reference for weekly US imaging in the treatment room. Immediately after treatment delivery the TPUS monitoring system was set up. During real-time monitoring of the prostate, a conventional 2D probe was applied to simulate a TAUS scan. The time dependent prostate displacements induced by the 2D probe pressure were recorded for the three orthogonal directions. In total 42 monitoring curves with applied 2D probe were recorded.
Results: Data analysis of 42 US scans resulted in pressure induced prostate displacements with mean values ($\pm$ 1 SD) (mm); inferior (+)-superior (I/S): (-0.1 $\pm$ 0.8); left (+)-right (L/R): (0.2 $\pm$ 0.7); and anterior (+)-posterior (A/P): (-0.1 $\pm$ 1.0).

The majority of the displacements were within 1-2 mm. Only two scans (5%) (A/P direction) and 16% of Euclidean distances were larger than 2.0 mm. The largest displacement was 2.6 mm in the anterior direction.
Conclusion: The novel 4D TPUS system was capable of tracking and recording the prostate positional displacements. The study demonstrated that the prostate induced displacements due to applied TAUS IGRT are small, and in most cases clinically irrelevant to prostate radiotherapy.

Acta Oncologica, 2015; Early Online: 1–7

Taylor & Francis
Taylor & Francis Group

ORIGINAL ARTICLE

Prostate displacement during transabdominal ultrasound image-guided radiotherapy assessed by real-time four-dimensional transperineal monitoring

MARIWAN BAKER[1,2] & CLAUS F. BEHRENS[1]

[1]*Department of Oncology, Radiotherapy Research Unit, Herlev Hospital, University of Copenhagen, Herlev, Denmark and* [2]*Center for Nuclear Technologies, Technical University of Denmark, DTU Risø Campus, Roskilde, Denmark*

ABSTRACT

Background. Transabdominal ultrasound (TAUS) imaging is currently available for localizing the prostate in daily image-guided radiotherapy (IGRT). The aim of this study was to determine the induced prostate displacement during such TAUS imaging. The prostate displacement was monitored using a novel transperineal four-dimensional (4D) US (TPUS) system.

Material and methods. Ten prostate cancer patients, with a mean age of 68 years (58/76), were US scanned in the computed tomography (CT) room utilizing the Clarity 4D TPUS monitoring system. The patients were asked to comply with a moderate bladder filling protocol. After US-CT fusion, the prostate volume was delineated and used as a reference for weekly US imaging in the treatment room. Immediately after treatment delivery the TPUS monitoring system was set up. During real-time monitoring of the prostate, a conventional 2D probe was applied to simulate a TAUS scan. The time dependent prostate displacements induced by the 2D probe pressure were recorded for the three orthogonal directions. In total 42 monitoring curves with applied 2D probe were recorded.

Results. Data analysis of 42 US scans resulted in pressure induced prostate displacements with mean values ($\pm$ 1 SD) (mm); inferior (+)-superior (I/S): (-0.1 ± 0.8); left (+)-right (L/R): (0.2 ± 0.7); and anterior (+)-posterior (A/P): (-0.1 ± 1.0). The majority of the displacements were within 1–2 mm. Only two scans (5%) (A/P direction) and 16% of Euclidean distances were larger than 2.0 mm. The largest displacement was 2.6 mm in the anterior direction.

Conclusion. The novel 4D TPUS system was capable of tracking and recording the prostate positional displacements. The study demonstrated that the prostate induced displacements due to applied TAUS IGRT are small, and in most cases clinically irrelevant to prostate radiotherapy.

In external beam radiotherapy for the prostate cancer, it is imperative to minimize damage to surrounding healthy tissues while delivering a high dose to the prostate. As the position of the prostate can vary substantially between treatment fractions and possibly even during treatment delivery [1–3], methods for precise localization on the prostate are warranted. Different kilovoltage (kV) and megavoltage (MV) image-guided radiotherapy (IGRT) methods have been developed. However, the kV and MV imaging modalities have poor soft tissue visualization, therefore, in many clinics, implanted fiducial markers (FM) in the prostate utilized as a surrogate for the prostate localization [4]. However, implanting FMs are an invasive method and not available in all clinics.

Ultrasound (US), a non-ionizing and non-invasive imaging modality, has been introduced as an alternative inexpensive IGRT method. Clinically, two models of US-IGRT systems, intermodal US (BAT system) and intramodal US (Clarity system) have been introduced [5]. In intermodal US, the US images from the treatment room are matched to computed tomography (CT)-reference images, whilst in intramodal US the US images are matched to the US-reference images from the simulation room. Both systems are based on transabdominal US (TAUS) imaging, using a two-dimensional (2D) US probe. Several studies have been conducted comparing the US-based IGRT to the FM-based IGRT [6–10].

Correspondence: M. Baker, Department of Oncology, Radiotherapy Research Unit, Herlev Hospital, University of Copenhagen, Herlev, Denmark. E-mail: mariwan.baker@regionh.dk

(Received 16 May 2015; accepted 8 June 2015)
ISSN 0284-186X print/ISSN 1651-226X online
DOI: 10.3109/0284186X.2015.1061208

One of the disadvantages of TAUS imaging is the inter-operator variability. For example, variations in exerted probe pressure have been reported to have an impact on prostate position in various studies. One study was designed to investigate pressure induced displacement of the prostate by US scanning of a phantom mimicking a male pelvic area [11]. The disadvantage of such tissue-equivalent phantoms is that the static anatomical structures cannot represent the uniqueness of a patient's organs, in which daily variations in bladder, rectal filling, and shape occur. In another approach, volunteers were TAUS scanned using a fixed 2D probe on a robotic arm [12]. The probe was first placed above the pubis symphysis, and moved vertically towards the prostate step by step, acquiring images at each stage. One limitation of this test is that the TAUS scan of the prostate requires a sweep technique, as opposed to only a vertical probe movement. Moreover, a recently published work, based on TAUS scan of volunteers and prostate patients, demonstrated that applied probe pressure may cause up to 8 mm of prostate displacement while applying "strong pressure" [13]. However, it was impossible in the study to observe any prostate displacements while applying "soft pressure" defined as the minimum pressure required for acquiring sufficient image quality. Thus, a study to simulate the daily in-room TAUS IGRT while recording the induced prostate displacement is required, and this was the motive for our study.

Currently, a system based on an automatic mechanically sweeping US probe, the Clarity transperineal US (TPUS) autoscan (Elekta, Stockholm, Sweden), is being introduced into radiotherapy. The system offers 4D real-time tracking of the prostate.

The aim of this study was to determine prostate displacement, due to applied TAUS probe pressure, by continuously 4D monitoring the prostate utilizing the TPUS autoscan.

Material and methods

Patients

Ten prostate cancer patients, with a mean age of 68 years (the age range of 58–76), were scanned weekly by two of six experienced radiation therapists (RTTs), using the TPUS autoscan. The study was approved by the ethical committee according to "World medical association declaration of Helsinki". Every patient was verbally informed of the objective of the study, and signed a printed statement of informed consent before participation. Furthermore, the patients were instructed to follow a moderate bladder filling protocol, which involved not urinating after leaving their home on their way to their daily radiation treatment. In this study, the US monitoring images were used for research purposes only and not applied clinically. One patient was excluded after 1 fraction owing to his unwillingness to participate anymore. A total of 48 US scans were acquired, from which six US scans were excluded due to inferior image quality.

Clarity ultrasound (US) system

The Clarity US system consists of two mobile US units: one located in the CT simulation room and the second in the treatment room. The two units are connected through a workstation. The workstation was used for prostate delineation, as well as for retrieving the prostate monitoring curves.

The US unit has a console screen, where anatomical structures can be observed and image quality optimized, using different brightness and contrast settings. The unit also has a conventional convex 2D probe and the novel autoscan probe for TAUS and TPUS scanning, respectively (Supplementary Figure 1C, D, available online at http://www.informahealthcare.com/doi/abs/10.3109/0284186X.2015.1061208). Details of the Clarity characteristics, 3D image reconstructions, and system calibration are described in another paper [14]. In short, a ceiling-mounted infrared (IR) camera can track the US probes by monitoring the IR-reflectors attached to them. This is essential for determining the geographical position of the reconstructed anatomical structures.

CT-simulation, autoscan imaging and CT-US fusion

After the CT scan acquisition, the patient was prepared for the US scan using vendor provided knee cushions resting over the autoscan base (a kit to which the autoscan probe was attached) (Supplementary Figure 1A available online at http://www.informahealthcare.com/doi/abs/10.3109/0284186X.2015.1061208). The patient was instructed to remain still during image acquisition. Afterwards, the CT-US image fusion was performed and the prostate gland delineated. Finally, the delineated prostate was approved as a reference volume for subsequent weekly US scans in the treatment room.

Image acquisition and prostate monitoring in the treatment room

The patient was prepared for daily treatment using FM-IGRT. Immediately after the treatment, the patient was repositioned in preparation for autoscan monitoring. The TAUS scan was simulated, using a 2D probe, while the prostate was continuously monitored using the TPUS autoscan (Supplementary

Figure 1E available online at http://www.informahealthcare.com/doi/abs/10.3109/0284186X.2015.1061208). The autoscan, unique in its positioning in relation to the patient's perineal region, and hence outside of the irradiated area, is designed to address the intra-fractional prostate motion during radiation delivery, which was not the aim of this study. During the simulation, no US images were acquired with the 2D probe, i.e. the probe was used as a dummy. However, the trained RTTs were instructed to reproduce the sweeping technique and associated applications of pressure required to acquire adequate US image quality. Furthermore, the RTTs were asked to avoid observing the impact of the pressure on the console screen. The prostate displacements due to the exerted probe pressure were recorded for retrospective analysis. Supplementary Figure 1E shows an example of prostate displacements in inferior-superior (I/S), left-right (L/R), and anterior-posterior (A/P) directions during the 2D probe simulation.

Data collection and statistical analysis

The recorded curves, showing the real-time prostate center of mass (COM) position in all three directions, were retrieved from the Clarity server by one observer (MB). For each curve the displacement as function of time (t) was analyzed relative to a chosen reference position at time t_0, a start time shortly before the 2D probe was applied. The overall mean [$\pm$ 1 standard deviation (SD)], maximum, and minimum of the prostate displacements (relative to the prostate position at t_0) were derived for the three directions. Furthermore, the maximum Euclidean distance [Max(D(t))] was computed as the length of the vector between the position of the COM of the prostate at t, the time where the prostate displacement is largest, and t_0. The statistical program R was used to analyze the data.

Results

All patients encompassed in this study were cooperative, and none of them expressed any discomfort during the autoscan setup, or from the applied probe pressure. Data analysis of 42 US scans resulted in pressure induced prostate displacements with mean values ($\pm$ 1 SD) of -0.1 mm ($\pm$ 0.8 mm), 0.2 mm ($\pm$ 0.7 mm), and -0.1 mm ($\pm$ 1.0 mm) in I(+)/S, L(+)/R, and A(+)/P directions, respectively. In addition, the mean of maximum Euclidean distance [(D(t))>] was computed to be 1.3 mm ($\pm$ 0.7 mm) (Table I). Furthermore, the largest displacement was calculated to be 2.6 mm in the anterior direction and 2.9 mm for D(t). Moreover, the majority of the displacements were found to be within 1–2 mm, and only two scans (5%) (A/P direction) and 16% of Max(D(t)) were larger than 2.0 mm.

Table I. Mean, standard deviations (SD), max of prostate displacement, and displacements larger than 0.5, 1.0, 2.0 mm in all three directions, including Euclidean distance Max(D(t)).

	Directions			
	I(+)/S[a]	L(+)/R	A(+)/P	Max(D(t))[b]
Mean $\pm$ SD (mm)	-0.1 ± 0.8	0.2 ± 0.7	-0.1 ± 1.0	1.3 ± 0.7
Max (mm)	1.2/−1.8	1.6/−1.1	2.6/−2.2	2.9
Displacement >0.5 mm	49%	47%	58%	81%
Displacement >1.0 mm	16%	14%	33%	60%
Displacement >2.0 mm	0%	0%	5%	16%

[a]A/P, anterior-posterior; I/S, inferior-superior; L/R, left-right; [b]Max(D(t)) maximum Euclidean distance.

The simulation time employing the TAUS probe was from approximately 15 to 20 seconds (Supplementary Figure 2A–C, available online at http://www.informahealthcare.com/doi/abs/10.3109/0284186X.2015.1061208). The largest dispersal was observed to be in the A/P direction. It was also observed that, after releasing the 2D probe, the prostate could be permanently displaced. Moreover, the mean displacement was shown to be within $\pm$ 0.2 mm in all three directions (Figure 1). Additionally, the mean lateral displacement was about 0.2 mm to the left.

Individual boxplots of all nine patients demonstrated some variations in prostate displacements between them and even for individual patients (Figure 2A–C). The first patient (pt1) showed the largest day-to-day variations in A/P direction, which can, first of all, be attributed to daily changes in the patient and, second, to the inter-operator pressure variability. Additionally, the boxplot of the overall displacements revealed that the first and the third quartiles were within $\pm$ 1.0 mm in all three directions (Figure 2D). Finally, the last boxplot in the figure indicates that the median of the Euclidean distance is about 1.3 mm.

Discussion

Transabdominal US-IGRT in prostate radiotherapy poses some challenges concerning variations in applied probe pressure, and US image interpretation. This can lead to inter-operator variability, in particular among users with little or no US experience. The American Association of Physicists in Medicine (AAPM) emphasizes that US training is essential and can be divided into "initial vendor-provided training and continuous clinical training" [15]. Experienced US users were reported to be more consistent in

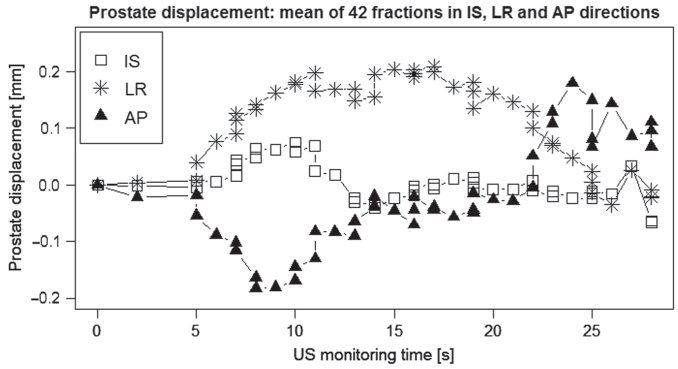

Figure 1. Prostate displacement; Monitoring graphs show the prostate displacement due to applied probe pressure (mean of 42 scans) in I/S, L/R, and A/P directions.

image acquisition and better at identifying anatomical structures, with less inter-operator variability [16].

This study was designed to determine the influence of TAUS probe pressure on prostate location by utilizing continuous tracking of the prostate employing the novel 4D TPUS autoscan. The accuracy of the prostate monitoring algorithm was validated by Lachaine et al. [17]. They utilized a robotic stage regulator on a US phantom with certain motion patterns. They discovered the mean and standard deviation of the differences between the measured and the regulator to be -0.0 ± 0.2 mm, 0.2 ± 0.4 mm, and -0.2 ± 0.2 mm in the I/S, L/R, and A/P directions, respectively. Another comparison study between the TPUS autoscan system and the Calypso system (Varian Medical Systems, Palo Alto, CA, USA) was performed by Abramowitz et al. [18]. The Calypso system utilizes transponders implanted into the prostate for positional tracking. Abramowitz et al. designed a motorized phantom combined with a prostate-equivalent structure. They found good agreement between the two systems in tracking the embedded prostate-like sphere.

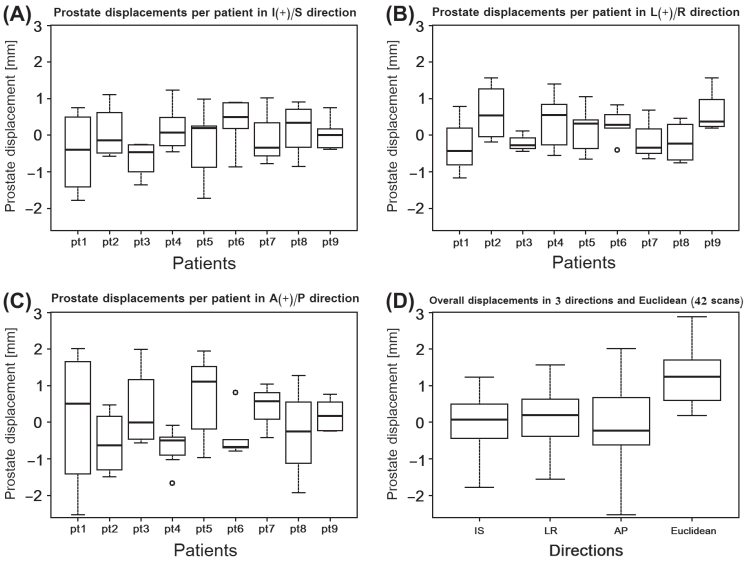

Figure 2. Boxplots of the prostate displacements; (A–C) Boxplots of the prostate displacements for nine patients in I/S, L/R, and A/P directions (D) Boxplot of overall prostate displacements in I/S, L/R, and A/P directions, including Euclidean distance. The horizontal band indicates the median, the lower and the upper edges of the box explain the first (25th) and third (75th) quartiles. The lower and the upper extremes of the whiskers, display the minimum and maximum values in absence of single data point outliers.

In a study by Fargier-Voiron et al. [13], the impact of probe pressure on prostate displacement was investigated in 16 volunteers and eight patients. They applied soft, moderate and strong TAUS probe pressure to displace the prostate. The induced displacement was then quantified by comparing the position of the prostate under moderate and strong pressure with the prostate position under soft pressure. Thus only the difference between prostate position under soft pressure and the prostate position under moderate or strong pressure could be assessed. They reported the mean and standard deviations of the Euclidean prostate displacements of 2.5 ± 1.2 mm and 3.3 ± 1.6 mm for moderate and strong pressure (relative to soft pressure), which are greatly larger than our Euclidean displacement of 1.3 ± 0.7 mm. Furthermore, Fargier-Voiron et al. measured the maximum prostate displacement to 7.5 mm, using strong pressure, in the inferior direction, compared to our maximal displacement of only 2.6 mm in the anterior direction. However, in our study the measured prostate displacement is between no probe pressure (rest position) and soft probe pressure, which reflects the clinical routine practice of TAUS-IGRT. Another limitation of Fargier-Voiron et al. study was that they only had one TAUS scan per volunteer/patient. In our study we observed large day-to-day variations in pressure displacements for individual patients. In another study, Van der Meer et al. [14] used TAUS probe pressure applied at four levels; no, low, intermediate, and high. As in the study by Fargier-Voiron et al., prostate displacement was measured relative to the US scan applying the least amount of pressure (level of "no pressure"). Applying a low pressure, defined by them as 1 cm skin displacement, sufficient to achieve good image quality, yielded a mean prostate displacement of 0.0 mm, -0.5 mm, and -0.7 mm in I(+)/S, L(+)/R, and A(+)/P directions, respectively. This is comparable to our corresponding sub-millimeter results of −0.1 mm, 0.2, and -0.1 mm. However, Van der Meer et al. reported the average Euclidean distance for the prostate displacement, for low pressure, to be about 3.0 mm, which is larger than our outcome of 1.3 mm. Artignan et al. [12] performed a similar TAUS scan study of volunteers, in which the probe was affixed to a rigid arm, enabling it to move towards the prostate in graded steps. As in the studies by Van der Meer et al. and Fargier-Voiron et al., the reference image was the US scan with the least amount of pressure. Artignan et al. defined a skin displacement of 1.2 cm, of the same magnitude as Van der Meer et al., as sufficient for obtaining adequate US image quality. This pressure resulted in a mean Euclidean vector displacement of 3.1 mm. According to Artignan et al., the displacement is not limited to one direction as was also the case in our study, hence displacements opposite to the direction of the probe pressure were observed.

The result of mean lateral displacement of 0.2 mm (Figure 1) might be explained by the fact that the probe simulation was applied from the right hand side of the patient (Supplementary Figure 1B available online at http://www.informahealthcare.com/doi/abs/10.3109/0284186X.2015.1061208), resulting in the probe being slightly tilted to the right, and hence inducing partial lateral pressure to the left rather than a strictly vertical pressure. Furthermore, the maximal displacement was showed to be 1.2 mm, 1.6 mm, and 2.6 mm in I/S, L/R, and A/P directions, which conforms to a study by Dobler et al. [19] that resulted in corresponding measures of 3.0 mm, 0.8 mm, and 2.8 mm. Dobler et al. investigated displacement of eight iodine seeds, inserted into the prostate during Brachy therapy. The seeds' positions were tracked by using real-time x-ray simulation while applying TAUS probe imaging using minimum probe pressure. They calculated the absolute displacement of the seeds to be larger than 2.0 mm in 7% of cases for all three directions which was consistent with our obtained results of 0%, 0%, and 5% in I/S, L/R, and A/P directions. In another study, Serago et al. [20] initiated a probe simulated study (no US scans were performed but a Styrofoam dummy was used) using two consecutive CT scans of 16 prostate patients; one without probe simulation and one with probe simulation. They discovered that in nine of the patients there was no measurable prostate movement, and the remaining seven patients had "discernible" displacements. In the patients with prostate displacement, they calculated the average displacement to be 3.1 mm.

Surprisingly, the prostate displacements from our study were less than all previous reported displacements in all directions, except for the results obtained by Dobler et al. The reason might be that Dobler et al. were using a similar method as in our approach, i.e. observing the pressure displacements in real-time and, importantly, not using a US scan with minimal pressure as reference. Most of the other studies were implementing either US/US (Clarity system) or US/CT (BAT system) image matching in order to measure the prostate COM displacements. Van der Meer et al. [14] studied the US/US matching procedure to determine intra-, and inter-operator matching variability through investigating 817 matches of a total of 376 US-scans. They discovered the intra-operator/inter-operator variability (1 SD) to be 0.8 mm/1.8 mm (I/S), 0.7 mm/1.3 mm (L/R), and 1.0 mm/1.4 mm (A/P), respectively. In another study, Langen et al. [21]

investigated US/CT matching and found inter-operator variability, among eight observers, to be larger than 2.0 mm (difference between any two matches) in about 50% of the matches in all three directions. The variability in US/US-, and US/CT-matching might adversely affect the accuracy of the measured prostate displacements, and consequently generate larger values.

As with all such studies, there are limitations that offer opportunities for further research. For example, the monitoring algorithm was validated as fairly precise in all cardinal directions, but the sub-millimeter uncertainty, admittedly, corresponded to approximately 10% of the magnitude of the prostate displacements measured in this study. Another limitation was that the TAUS simulations may not reflect a real routine clinical practice, in which anatomical structures can be visualized. We were unable to simultaneously acquire TAUS images while TPUS monitoring, using the same US unit, since another Clarity system was required to do so. In our approach, the operators followed specific instructions to simulate a TAUS scan with the amount of pressure that they would normally use. However, it was not possible to validate that the operators in fact used enough probe pressure. Moreover, although a gentle transperineal attach of the autoscan was carried out with caution, a counter-effect of the probe's head might influence the position of the prostate, and hence changing the magnitude and likewise the direction of the prostate displacements during TAUS simulation. In brief, further similar research, by enrollment of a larger patient population and acquiring larger number of real TAUS scans per patient, are recommended to validate and to strengthen this study.

In conclusion, the novel 4D autoscan US system was able to track and record positional displacements of the prostate. In this study we demonstrated that the displacements of the prostate induced by the applied TAUS IGRT were small, and in most cases clinically irrelevant to prostate radiotherapy.

Acknowledgments

We would like to thank all our colleagues who helped to conduct this study; Gullander L. (RTT), Pedersen S. K (RTT), Zarp T (RTT), Jacobsson S (RTT), Pazhang S (radiographer) and Lynnerup V. K (radiographer). This study is a part of PhD research project, supported by Elekta Inc.

Declaration of interest: The authors report no conflicts of interest. The authors alone are responsible for the content and writing of the paper.

References

[1] Huang E, Dong L, Chandra A, Kuban DA, Rosen II, Evans A, et al. Intrafraction prostate motion during IMRT for prostate cancer. Int J Radiat Oncol Biol Phys 2002;53: 261–8.

[2] Ghilezan MJ, Jaffray DA, Siewerdsen JH, Van Herk M, Shetty A, Sharpe MB, et al. Prostate gland motion assessed with cine-magnetic resonance imaging (cine-MRI). Int J Radiat Oncol Biol Phys 2005;62:406–17.

[3] Langen KM, Jones DTL. Organ motion and its management. Int J Radiat Oncol Biol Phys 2001;50:265–78.

[4] Van der Heide UA, Kotte ANTJ, Dehnad H, Hofman P, Lagenijk JJW, van Vulpen M. Analysis of fiducial marker-based position verification in the external beam radiotherapy of patients with prostate cancer. Radiother Oncol 2007;82: 38–45.

[5] Cury FLB, Shenouda G, Souhami L, Duclos M, Faria SL, David M, et al. Ultrasound-based image guided radiotherapy for prostate cancer: Comparison of cross-modality and intramodality methods for daily localization during external beam radiotherapy. Int J Radiat Oncol Biol Phys 2006;66:1562–7.

[6] Johnston H, Hilts M, Beckham W, Berthelet E. 3D ultrasound for prostate localization in radiation therapy: A comparison with implanted fiducial markers. Med Phys 2008;35:2403–13.

[7] Van den Heuvel F, Powell T, Seppi E, Littrupp P, Khan M, Wang Y, et al. Independent verification of ultrasound based image-guided radiation treatment, using electronic portal imaging and implanted gold markers. Med Phys 2003;30:2878–87.

[8] McNair HA, Mangar SA, Coffey J, Shoulders B, Hansen VN, Norman A, et al. A comparison of CT- and ultrasound-based imaging to localize the prostate for external beam radiotherapy. Int J Radiat Oncol Biol Phys 2006;65:678–87.

[9] Scarbrough TJ, Golden NM, Ting JY, Fuller CD, Wong A, Kupelian PA, et al. Comparison of ultrasound and implanted seed marker prostate localization methods: Implications for image-guided radiotherapy. Int J Radiat Oncol Biol Phys 2006;65:378–87.

[10] Serago CF, Buskirk SJ, Igel TC, Gale AA, Serago NE, Earle JD. Comparison of daily megavoltage electronic portal imaging or kilovoltage imaging with marker seeds to ultrasound imaging or skin marks for prostate localization and treatment positioning in patients with prostate cancer. Int J Radiat Oncol Biol Phys 2006;65:1585–92.

[11] McGahan JP, Ryu J, Fogata M. Ultrasound probe pressure as a source of error in prostate localization for external beam radiotherapy. Int J Radiat Oncol Biol Phys 2004;60: 788–93.

[12] Artignan X, Smitsmans MHP, Lebesque JV, Jaffray DA, van Her M, Bartelink H. Online ultrasound image guidance for radiotherapy of prostate cancer: Impact of image acquisition on prostate displacement. Int J Radiat Oncol Biol Phys 2004;59:595–601.

[13] Fargier-Voiron M, Presles B, Pommier P, Rit S, Munoz A, Liebgott H, et al. Impact of probe pressure variability on prostate localization for ultrasound-based image-guided radiotherapy. Radiother Oncol 2014;111:132–7.

[14] Van der Meer S, Bloemen-van Gurp E, Hermans J, Voncken R, Heuvelmans D, Gubbels C, et al. Critical assessment of intramodality 3D ultrasound imaging for prostate IGRT compared to fiducial markers. Med Phys 2013;40:071707/1–11.

[15] Molloy JA, Chan G, Markovic A, McNeeley S, Pfeiffer D, Salter B, et al. Quality assurance of U.S.-guided external beam radiotherapy for prostate cancer: Report of AAPM Task Group 154. Med Phys 2011;38:857–71.

[16] Fuss M. Daily stereotactic ultrasound prostate targeting: Inter-user variability. Technol CANCER Res Treat 2003;2:161–9.
[17] Lachaine M, Falco T. Intrafractional prostate motion management with the Clarity Autoscan system. Med Phys Int 2013;1:72–80.
[18] Abramowitz MC, Bossart E, Flook R, Wu X, Brooks R, Lachaine M, et al. Noninvasive real-time prostate tracking using a transperineal ultrasound approach. Int J Radiat Oncol 2012;84:S133.
[19] Dobler B, Mai S, Ross C, Wolff D, Wertz H, Lohr F, et al. Evaluation of possible prostate displacement induced by pressure applied during transabdominal ultrasound image acquisition. Strahlenther Onkol 2006;182:240–6.
[20] Serago CF, Chungbin SJ, Buskirk SJ, Ezzell GA, Collie AC, Vora SA. Initial experience with ultrasound localization for positioning prostate cancer patients for external beam radiotherapy. Int J Radiat Oncol Biol Phys 2002;53:1130–8.
[21] Langen K., Pouliot J, Anezinos C, Aubin M, Gottschalk A, Hsu I-C, et al. Evaluation of ultrasound-based prostate localization for image-guided radiotherapy. Int J Radiat Oncol 2003;57:635–44.

Supplementary material available online

Supplementary Figure 1 and 2 available online at http://www.informahealthcare.com/doi/abs/10.3109/0284186X.2015.1061208

PAPER E

Evaluation of uterine ultrasound imaging in cervical radiotherapy; a comparison of autoscan and conventional probe

Authors: Mariwan Baker, David T. Cooper, and Calus F. Behrens.

Submitted to: Radiation Oncology, August 2015

Abstract

Background: In cervical radiotherapy, it is essential that the uterine position is correctly determined prior to the treatment delivery. The aim of this study was to evaluate a novel autoscan ultrasound (A-US) probe by comparing it to a conventional US (C-US) probe.
Methods: Nine healthy volunteers were US scanned by seven operators, using the Clarity system (Clarity, Elekta, Stockholm, Sweden). In total 72 scans; 36 from the C-US (manual sweeping) and 36 from the A-US probe (automatic sweeping), were acquired. Two observers delineated the uterine structure. One observer re-delineated the same structure for evaluating intraoperator variability. Data of uterine volume, uterine centre of mass (COM), and maximum uterine lengths, in three orthogonal directions, were analyzed.
Results: In 53% of the C-US probe scans the whole uterus was captured, compared with 89% using the A-US probe. F-test on 36 scans demonstrated statistically significant differences in interobserver COM SD when comparing the C-US with the A-US probe for the I/S ($p < 0.006$), L/R ($p < 0.012$) and A/P-directions ($p < 0.001$). The median of the inter-observer COM distance (Euclidean distance for 36 scans) was reduced from 8.5 mm (C-US) to 6.0 mm (A-US). An F-test on 36 scans showed strong significant differences ($p < 0.000006$) in SD of the Euclidean interobserver distance when comparing the C-US with the A-US scans. The average dice coefficient when comparing the two observers was 0.67 (C-US) and 0.75 (A-US). The predictive interval demonstrated better inter-observer delineation concordance using the A-US

probe.
Conclusions: The A-US probe imaging might be a better choice of image-guided radiotherapy system for correcting for daily uterine positional changes in cervical radiotherapy.
Keywords: Ultrasound, uterus, target, radiotherapy, 3D probe, delineation variability, inter-observer, intra-observer.

Evaluation of uterine ultrasound imaging in cervical radiotherapy; a comparison of autoscan and conventional probe

Mariwan Baker[1,2,3] M.Sc., David T. Cooper[4] B.Sc. and Claus F. Behrens[1] Ph.D.

1 Department of Oncology, Radiotherapy Research Unit, Herlev Hospital, University of Copenhagen, Herlev, Denmark
2 Center for Fast Ultrasound Imaging, Dept. of Elec. Eng., Technical University of Denmark, DK-2800 Lyngby, Denmark
3 Center for Nuclear Technologies, Technical University of Denmark, DTU Risø Campus, Roskilde, Denmark
4 Elekta Ltd., Montréal, Québec, Canada

Mariwan Baker
Herlev Hospital, University of Copenhagen, Herlev
Department of Oncology (R)
Division of Radiotherapy (51AA)
Herlev Ringvej 75
DK-2730 Herlev
Denmark
Phone: +46-76 190 9108
e-mail: mariwan.baker@regionh.dk

David Cooper: david.cooper@elekta.com
Claus F. Behrens: claus.behrens@regionh.dk

ABSTRACT

Background: In cervical radiotherapy, it is essential that the uterine position is correctly determined prior to the treatment delivery. The aim of this study was to evaluate a novel autoscan ultrasound (A-US) probe by comparing it to a conventional US (C-US) probe.

Methods: Nine healthy volunteers were US scanned by seven operators, using the Clarity® system (Clarity®, Elekta, Stockholm, Sweden). In total 72 scans; 36 from the C-US (manual sweeping) and 36 from the A-US probe (automatic sweeping), were acquired. Two observers delineated the uterine structure. One observer re-delineated the same structure for evaluating intra-operator variability. Data of uterine volume, uterine centre of mass (COM), and maximum uterine lengths, in three orthogonal directions, were analyzed.

Results: In 53% of the C-US probe scans the whole uterus was captured, compared with 89% using the A-US probe. F-test on 36 scans demonstrated statistically significant differences in inter-observer COM SD when comparing the C-US with the A-US probe for the I/S ($p < 0.006$), L/R ($p < 0.012$) and A/P-directions ($p < 0.001$). The median of the inter-observer COM distance (Euclidean distance for 36 scans) was reduced from 8.5 mm (C-US) to 6.0 mm (A-US). An F-test on 36 scans showed strong significant differences ($p < 0.000006$) in SD of the Euclidean inter-observer distance when comparing the C-US with the A-US scans. The average dice coefficient when comparing the two observers was 0.67 (C-US) and 0.75 (A-US). The predictive interval demonstrated better inter-observer delineation concordance using the A-US probe.

Conclusions: The A-US probe imaging might be a better choice of image-guided radiotherapy system for correcting for daily uterine positional changes in cervical radiotherapy.

Keywords: Ultrasound, uterus, target, radiotherapy, 3D probe, delineation variability, inter-observer, intra-observer.

Background

In cervical radiotherapy organ motion, tumour regression and setup variations may occur, and therefore daily pre-treatment verification imaging is desirable (1,2). Recently, various 3D US systems have been introduced as alternative inexpensive image guided radiotherapy (IGRT), such as the Clarity® system (Clarity® Model 310C00, Elekta, Stockholm, Sweden) (3–5).

In cervical IGRT there are some challenges in using US imaging system such as inter-operator variability while performing transabdominal scans (6). Another drawback is that daily US probe pressure variations might cause organ and target displacement (7). There is limited literature on cervix US scan, but many papers on prostate US scanning. Some studies have claimed that prostate displacement might occur due to probe pressure (8–10), while others have speculated that the impact on uterus displacement is less significant (11).

The conventional US (C-US) probe is a frequently used US IGRT system. For example, the Clarity C-US probe, a transabdominal imaging tool, can acquire US images of the prostate in the transversal plane, using a manual sweep technique. US scanning of the uterus require a sweep-slide technique, which was shown to be cumbersome and might lead to undesired inter-operator variability (12). Moreover, operators experience a visual challenge in identifying the uterus in the transversal plane, though normally it is easily recognizable in the sagittal plane. In this study, a novel Clarity autoscan US (A-US) probe was utilized to acquire images in the sagittal plane. The semiautomatic A-US probe inherits a mechanically motorized head, enabling automatic transabdominal sweep scans after manual positioning of the probe above the pubis symphysis. The A-US probe is a modification of a autoscan probe (13) that was initially designed for transperineal prostate scanning and real-time tracking of the prostate, to address intrafractional prostate motion. The hypothesis of the present study was that the novel A-US probe may be a better IGRT alternative than the conventional C-US probe in cervical radiotherapy.

Methods

Volunteers

Nine healthy volunteers, with a mean age of 44 years (27/57), were scanned by six radiation therapy technologists (RTTs) and one physicist, using C-US and A-US probes. The study was approved by the national ethical committee, and voluntary informed consent was obtained for each participant according to the *World Medical Association Declaration of Helsinki (1975/2000)*. The volunteers were placed in a supine position and instructed to remain still throughout the subsequent scans. To ensure better image quality, the volunteers were requested to comply with a moderate bladder-filling protocol.

Clarity ultrasound system

The Clarity consists of two mobile units (one in the computer tomography (CT) room and the second in the treatment room), which are connected through a workstation/server. The workstation was used for target delineation, measuring uterine length as well as retrieving the volume (calculated by Clarity), distance and inter-observer uterine volume overlap. Details of US 3D image reconstructions and precision of the system are explained thoroughly in a previous study (6). In short, a ceiling-mounted infrared (IR) camera, capable of tracking the US probes by monitoring the IR-reflectors affixed to them, is central for determining the geographical position of the reconstructed anatomical structures (Suppl. figure 1).

C-US and A-US probes

The C-US probe consists of a transducer array of 128 elements, using central frequency of 3.4 MHz. The probe is provided with IR reflectors fixed in a way that can be detected by the ceiling mounted IR-camera (Suppl. figure 1 (A, D, F)). The camera cannot detect the reflectors if the probe, for instance, turned 90 degrees, thus, this restricting image acquisition to the transversal plane only. Initially, the probe is tilted backwards to localize the vaginal region, followed by sweeping to the vertical position. Approximately half of the uterine volume can be captured by the sweep, thus a cranial slide technique is required to cover the rest of the uterus.

The A-US probe comprises the similar type of transducer, but with a central frequency of 5 MHz. Initially and prior to acquiring the scan, the desired uterine structure is identified in the sagittal plane. The semiautomatic transabdominal scan is achieved by localizing the central slice of the uterus and then allowing the motorized head to automatically sweep over the uterine volume.

Image acquisition and organ delineation

The C-US probe images were superimposed onto the A-US probe images. Two observers (MB and DTC), a physicist and a US specialist, independently delineated the uterine structure in the 72 acquired scans; 36 from the C-US and 36 from the A-US probe. The outlined uterine structures served to determine inter-observer contouring variability. After approximately two weeks, the observer MB recontoured the uterus to investigate intra-observer variability. The uterus delineation procedure was always carried out as follows: The uterus was first delineated in three slices in the transversal plane; one slice in the cranial, and one slice in the caudal uterine peripheral endings, and a third in the centre of the uterus. Secondly, the uterus was outlined in the central sagittal slice. Finally, based on manually drawn contours the system's segmentation algorithm was used to segment the whole uterus. The same window and level settings of the segmentation algorithm were used for both observers. The algorithm is based on a discrete dynamic contouring (DDC) algorithm. Basically, it starts with an initial contour and moves the points in a graded sequence to balance external forces (that push points towards gradients in the image) and internal forces (that maintain smoothness) (14,15). The delineated uterine structures were classified into two groups: one with all scans and the other with the best scans (scans where both C-US and A-US images showed the whole uterus).

Data collection and statistical analysis

The inter-observer differences in uterine COM position between observer one (OBS 1) and observer two (OBS 2) were calculated in the Inferior-Superior (I/S), Left-Right (L/R) and Anterior-Posterior (A/P) directions, respectively. Furthermore, the overall mean (± 1 standard deviation (SD)) of the differences was calculated to compare the C-US and A-US probe scans. Moreover, the maximum uterine length (largest length of the delineated uterus) was measured in the three directions. Finally, the Euclidean space distance (3D vector) of COM between OBS 1 and OBS 2 was calculated for both the C-US and the A-US probe scans.

In addition, an F-test was applied to compare the variance in inter-observer COM differences for the C-US and the A-US probes in all three cardinal directions. The null hypothesis was that there was no significant difference in variance. The p-values were calculated for a 95% confidence interval (CI). Statistical predictive inference was applied to illustrate the prediction interval for OBS 1 and OBS 2 in determining the uterine volume, when comparing the C-US and A-US probes. Similarly, the predictive inference was applied on the maximum uterine length. Finally, the Dice coefficient or Sørensen-Dice index (DI) was utilized to check the overlap of uterine volume outlined by OBS 1 (V1) and OBS 2 (V2) (equation 1). For the data and statistical analysis the statistical program R (version 2.15.3) was used.

$$DI = \frac{2|V1 \cap V2|}{|V1| + |V2|} \quad (1)$$

Results and discussion

Figure 1(A, B) illustrates that the A-US probe can yield images with slightly better spatial resolution than the C-US probe. Additionally, Figure 1 (C, D) exemplifies a uterus scan, where the image is incomplete using the C-US probe, due to difficulty identifying the uterus in the transversal plane while manually scanning the pelvic region. As a result, the whole uterus was captured in only 19 (53%) scans using the C-US probe, whereas the corresponding figure for the A-US probe was 32 (89%).

Table 1 summarizes the calculated overall mean of inter-observer COM differences using the C-US and A-US probes in all three orthogonal directions. Similarly, the computed mean of intra-observer COM differences are tabulated. When comparing the A-US with the C-US probe, the reduction in SD was statistically significant (F-test) in all three directions, the only exception being intra-observer delineations in the A/P-direction. Additionally, the largest inter-observer difference was 23 mm in the A/P-direction using the C-US probe, whereas the largest value was 9 mm in the I/S-direction when using the A-US probe. Finally, the largest SD was found to be 6.6 mm for inter-observer COM differences in the A/P-direction using the C-US probe.

Application of the F-test on all 36 scans demonstrated statistically significant different SD for inter-observer COM when comparing the C-US with the A-US probe for the I/S ($p < 0.006$), L/R ($p < 0.012$) and A/P-directions ($p < 0.001$) (Table 2.). In contrast, the corresponding F-test on the best 19 scans indicated no significant differences, except for a weak difference in the A/P-direction ($p < 0.04$).

Euclidean COM distances for inter and intra-observer scans were calculated (Figure 2). For inter-observer and all scans (A), the median of the distances was reduced from 8.5 mm (C-US) to 6.0 mm (A-US), whereas for the best scans (B) the reduction was only from 5.3 mm (C-US) to 4.9 (A-US). However, the intra-observer graphs (C, D) illustrate that for all and for the best scans, the median of distance is around 5.0 mm, irrespective of whether the C-US or A-US probe was employed. Moreover, an F-test revealed that for all scans and inter-observer COM distance, there were strong significant differences in SD when comparing the C-US with the A-US probe scans ($p < 0.0001$). However, the difference was not significant for intra-observer distances.

The mean uterine volume was calculated as 117 ± 59 cm^3 and 125 ± 64 cm^3 for the C-US and the A-US probe scans, respectively. The dice coefficient index (mean inter-observer) was calculated as 0.67 and 0.75 for the C-US and A-US probe scans, respectively. Furthermore, when applying regression analysis

for the uterine volume of OBS 1 as a function of the uterine volume of OBS 2, the predicted interval (dashed lines) remained almost unchanged when comparing all C-US and A-US scans (Figure 3 A, B). However, for the best scans, the interval was obviously smaller for the A-US than for the C-US scans (Figure 3 C, D). Moreover, when analysing the uterine volume for intra-observer, the predicted interval was significantly reduced for the A-US compared with the C-US scans, for all and for the best scans (Figure 3 E-H).

Finally, the predictive interval was applied on maximum uterine length for all 36 scans (Figure 4). The A-US scans revealed smaller/narrower predictive interval compared with the C-US scans, especially in the I/S and A/P directions.

Transabdominal US imaging has been used as prostate inter-fraction IGRT but, to our knowledge, there are very few studies employing such imaging in external cervical radiotherapy. A clinical trial for a cervical brachytherapy study comprising 192 patients, based on transabdominal US scan, was recently published (16). The study compared US imaging with magnetic resonance imaging (MRI) modality and demonstrated that the US scan can replace MRI as an alternative image guided modality. Another brachytherapy study (17), also applying US transabdominal scan versus MRI imaging and including 20 patients, verified a strong correlation between the modalities in uterine, cervical and central disease delineations. In a previous US study of the Clarity C-US probe on cervical cancer patients, the pros and cons of the C-US probe system were addressed (12). Inter-operator uncertainties due to difficulty in performing sweep-slide imaging in addition to variation in probe pressure limit the use of the C-US probe as a cervical IGRT system. Thus, the overall quality of the acquired US image is a result of a combination of different factors stemming, particularly the operator's performance. The American Association of Physicists in Medicine (AAPM) stresses that clinical US training of the operators is of utmost prominence (18).

The A-US transducer used in this study inherits identical characteristics as the real-time monitoring autoscan (13), initially designed for transperineal prostate tracking, but modified to perform transabdominal imaging. Since the system was not provided with a robotic arm, and our software was not adapted for real-time monitoring, the probe was incapable of real-time tracking of the uterus, thus unable to determine intrafractional motion, which otherwise would be an interesting field to investigate. Even though there is no study regarding applying transperineal scan for the GYN-patients, it is doubtful if this technique is clinically possible due to complexity of the female anatomical structures and the large uterine volume.

All the operators in the current study reported that it was easier to handle the A-US probe, particularly when identifying the uterus and bladder in the sagittal plane. Furthermore, image acquisition was performed more quickly and less probe pressure was exerted during A-US probe scanning. Moreover the image detail of the A-US probe scan was slightly better than that of the C-US probe (Figure 1), the reason being the higher transducer frequency used in the former. The higher frequency provides better spatial (axial and lateral) resolution. Additionally, the study revealed that the A-US is superior to the C-US probe for capturing the whole uterine volume (Suppl. figure 1 C, D).

The SD of the COM differences demonstrated that the A-US probe scans resulted in less inter- and intra-observer variability. The A-US probe yielded also a lower median COM difference in all three directions. However, for the best scans the F-test indicated no statistically significant differences due to better inter-observer delineation concordance for scans with the whole uterus imaged, irrespective of the type of probe. These findings warranted further investigation of the uterine COM point by examining the Euclidean space distance between the C-US and A-US uterine COM. The inter-observer boxplot of Euclidean distances revealed a median distance reduction of 2.5 mm with the A-US probe. However, when the whole uterine volume was imaged (best scans), the benefit provided by the A-US probe is minimal (Figure 2 B).

As one uterine COM point did not reveal substantial data on the outlined large uterine volume, the maximum uterine length in all three directions was examined. The predictive interval indicated better inter-observer concordance when applying the A-US compared to the C-US probe. However, the benefit

was limited in the L/R-direction, which can be attributed to the poor lateral image resolution in both the C-US and the A-US probe scans. This agrees well with a previous study based on patients with an intact uterus (19). Nevertheless, due to better spatial resolution of the A-US probe images in the sagittal plane, especially in the vicinity of the fundus, bladder-uterus and the posterior part of the uterus, the observers were more consistent than when using the C-US probe images.

The large SD of the uterine volume confirms significant inter-observer contouring variability. This could result from the fact that in the "all scans" group, a number of scans do not contain an image of the whole uterus and therefore the observers estimated the missing part, leading to larger variations. Another reason might be the challenge in contouring the uterine structure in the vaginal region, where larger inter-observer deviations were anticipated. These results suggest the need for target delineation guidelines to improve contouring consistency and thus higher inter-observer spatial concordance. To emphasize this necessity, the predictive interval indicated that the same observer most likely followed a similar delineation procedure leading to less intra-observer variability compared with the discordance in inter-observer delineation.

The dice coefficient index verified good concordance using the A-US probe (CI = 0.75) but only modest concordance with the C-US probe (CI = 0.67). The highest inter-observer discordance stems from inaccurate uterine segmentation in the missing part of the imaged uterus using the C-US probe. The present result is comparable to a MRI/CT based cervix, uterus, vagina and parametria delineation study (20) performed by 19 experienced observers, where the kappa-value, a statistic tool to measure inter-observer overlap agreement, for uterine delineation was 0.57.

Despite promising results of using the A-US probe for IGRT, the present study suffering from statistical limitations. Firstly, this volunteer study should be replicated on cervical cancer patients, including larger number of participants and a greater number of acquired scans. The cervical tumour can, for instance, be large and deform the actual shape of the uterus, possibly leading to greater inter-observer delineation variability. Secondly, the mean age of patients is normally higher than that of our volunteers (44 years). In the present study, we experienced that the uterine structure was easier to identify visually in the younger volunteers. Thirdly, target contouring should preferably be performed by several specialized radiologists and/or oncologists. Lastly, a quantitative image analysis of the C-US and A-US probe images is recommended for future study.

Conclusions

The A-US probe imaging might be a better modality than the C-US probe imaging in terms of better spatial resolution, facilitating the capture of the whole uterus, and less applied probe pressure. In our results, the A-US probe lead to less inter-operator variability and consequently less contouring variations. In conclusion, the A-US probe compared to C-US probe US imaging might be better IGRT system for correcting for daily uterine positional changes in cervical radiotherapy.

Competing interests: The author(s) declare that they have no competing interests

Authors' contributions: MB carried out the uterine delineations, participated in designing the study, performed statistical analysis, carried out the sequence alignment and drafted the manuscript. DTC carried out target delineations. CFB participated in the design of the study, revising the manuscript. All authors read and approved the final manuscript.

Acknowledgements

We would like to thank all our colleagues who helped us to conduct this study; Gullander L. (RTT), Pedersen S. K (RTT), Zarp T (RTT), Jacobsson S (RTT), Pazhang S (radiographer**)** and Lynnerup V. K (radiographer). We would also like to acknowledge Elekta's support for this study.

References

1. Beadle BM, Jhingran A, Salehpour M, et al. Cervix regression and motion during the course of external beam chemoradiation for cervical cancer. Int J Radiat Oncol Biol Phys [Internet]. 2009; 73(1):235–41.

2. Chan P, Dinniwell R, Haider M a, et al. Inter- and intrafractional tumor and organ movement in patients with cervical cancer undergoing radiotherapy: a cinematic-MRI point-of-interest study. Int J Radiat Oncol Biol Phys. 2008; 70(5):1507–15.

3. Baker M, Jensen JA, Behrens CF. Inter-operator variability in defining uterine position using three-dimensional ultrasound imaging. 2013 IEEE International Ultrasonics Symposium (IUS). 2013;848–51.

4. Cury FLB, Shenouda G, Souhami L, et al. Ultrasound-based image guided radiotherapy for prostate cancer: comparison of cross-modality and intramodality methods for daily localization during external beam radiotherapy. Int J Radiat Oncol Biol Phys. 2006;66(5):1562–67.

5. Pinkawa M, Pursch-Lee M, Asadpour B, et al. Image-guided radiotherapy for prostate cancer. Implementation of ultrasound-based prostate localization for the analysis of inter- and intrafraction organ motion. Strahlenther Onkol. 2008;184(12):679–85.

6. Van der Meer S, Bloemen-van Gurp E, Hermans J, et al. Critical assessment of intramodality 3D ultrasound imaging for prostate IGRT compared to fiducial markers. Med Phys. 2013;40:071707–1 – 071707–11.

7. Artignan X, Smitsmans MHP, Lebesque J V, et al. Online ultrasound image guidance for radiotherapy of prostate cancer: impact of image acquisition on prostate displacement. Int J Radiat Oncol Biol Phys. 2004;59(2):595–601.

8. McGahan JP, Ryu J, Fogata M. Ultrasound probe pressure as a source of error in prostate localization for external beam radiotherapy. Int J Radiat Oncol Biol Phys. 2004;60(3):788–93.

9. Serago CF, Chungbin SJ, Buskirk SJ, et al. Initial experience with ultrasound localization for positioning prostate cancer patients for external beam radiotherapy. Int J Radiat Oncol Biol Phys. 2002;53(5):1130–38.

10. Fargier-Voiron M, Presles B, Pommier P, et al. Impact of probe pressure variability on prostate localization for ultrasound-based image-guided radiotherapy. Radiother Oncol. 2014;111(1):132–7.

11. Baker M, Juhler-Nøttrup T, Behrens CF. Impact of ultrasound probe pressure on uterine positional displacement in gynecologic cancer patients. Womens Health. 2014;10(6):583–590.

12. Baker M. Determining inter-fractional motion of the uterus using 3D ultrasound imaging during radiotherapy for cervical cancer. Spie Medical Imaging: Ultrasonic Imaging and Tomograph. 2014;Spie 9040.

13. Lachaine M, Falco T. Intrafractional prostate motion management with the Clarity Autoscan system. Med Phys Int. 2013;1(1):72–80.

14. Ding M, Chiu B, Gyacskov I, et al. Fast prostate segmentation in 3D TRUS images based on continuity constraint using an autoregressive model. Med Phys. 2007;34(11):4109.

15. Ding M, Chen C, Wang Y, et al. Prostate segmentation in 3D US images using the cardinal-spline-based discrete dynamic contour. Proceedings of Spie - the International Society for Optical Engineering. 2003;69–76.

16. Van Dyk S, Kondalsamy-Chennakesavan S, Schneider M, et al. Comparison of measurements of the uterus and cervix obtained by magnetic resonance and transabdominal ultrasound imaging to identify the brachytherapy target in patients with cervix cancer. Int J Radiat Oncol Biol Phys. 2014;88(4):860–5.

17. Mahantshetty U, Khanna N, Swamidas J, et al. Trans-abdominal ultrasound (US) and magnetic resonance imaging (MRI) correlation for conformal intracavitary brachytherapy in carcinoma of the uterine cervix. Radiother Oncol. 2012;102(1):130–4.

18. Molloy JA, Chan G, Markovic A, et al. Quality assurance of U.S.-guided external beam radiotherapy for prostate cancer: Report of AAPM Task Group 154. Med Phys. 2011;38(2):857-71.

19. Collen C, Engels B, Duchateau M, et al. Volumetric imaging by megavoltage computed tomography for assessment of internal organ motion during radiotherapy for cervical cancer. Int J Radiat Oncol Biol Phys. 2010;77(5):1590–5.

20. Fyles AW, Lim K, Small W, et al. Variability in Delineation of Clinical Target Volumes for Cervix Cancer Intensity-modulated Pelvic Radiotherapy. Int J Radiat Oncol. 2009; (Suppl.),75(3):83–4.

TABLE 1. Mean inter and intra-observer differences in uterine COM for the three directions, using C-US and A-US probes.

Directions	Inter-observer[a] Mean [mm] ± 1SD		Intra-observer Mean [mm] ± 1SD	
	C-US probe	A-US probe	C-US probe	A-US probe
I(+)/S[b]	3.2 ± 6.3	1.8 ± 3.9	-0.9 ± 6.1	-1.3 ± 3.2
L(+)/R	0.9 ± 5.5	0.0 ± 3.6	0.2 ± 5.8	-2.1 ± 3.8
A(+)/P	-0.4 ± 6.6	0.4 ± 3.6	-0.7 ± 3.5	0.8 ± 3.5

[a]Inter-observer: the differences between two observers; Intra-observer: the differences between two delineations by the same observer.
[b]I/S: Inferior-Superior; L/R: Left-Right; A/P: Anterior-Posterior.

TABLE 2. F-test of the SD for inter-observer uterine COM differences as well as inter and intra-observer Euclidean COM distances in all the three orthogonal directions. The test is done for all scans and the best scans.

Directions	All scans (n = 36)			Best scans[a] (n = 19)		
	Ratio of variances	95% CI[b] Upper/Lower	*p*	Ratio of variances	95% CI Upper/Lower	*p*
I(+)/S	2.61	(1.33 to 5.33)	0.006	1.16	(0.45 to 3.01)	0.7571
L(+)/R	2.38	(1.21 to 4.67)	0.012	1.84	(0.71 to 4.77)	0.2067
A(+)/P	3.29	(1.68 to 6.45)	0.001	2.83	(1.09 to 7.35)	0.0331
Euclidean (inter-observer)	4.90	(2.50 to 9.61)	0.000006			
Euclidean (intra-observer)	1.83	(0.93 to 3.59)	0.077			

[a]Best scans: The US scans where the whole uterus is captured both with the A-US and the C-US probe.
[b]CI: Confidence Interval.

Figure 1

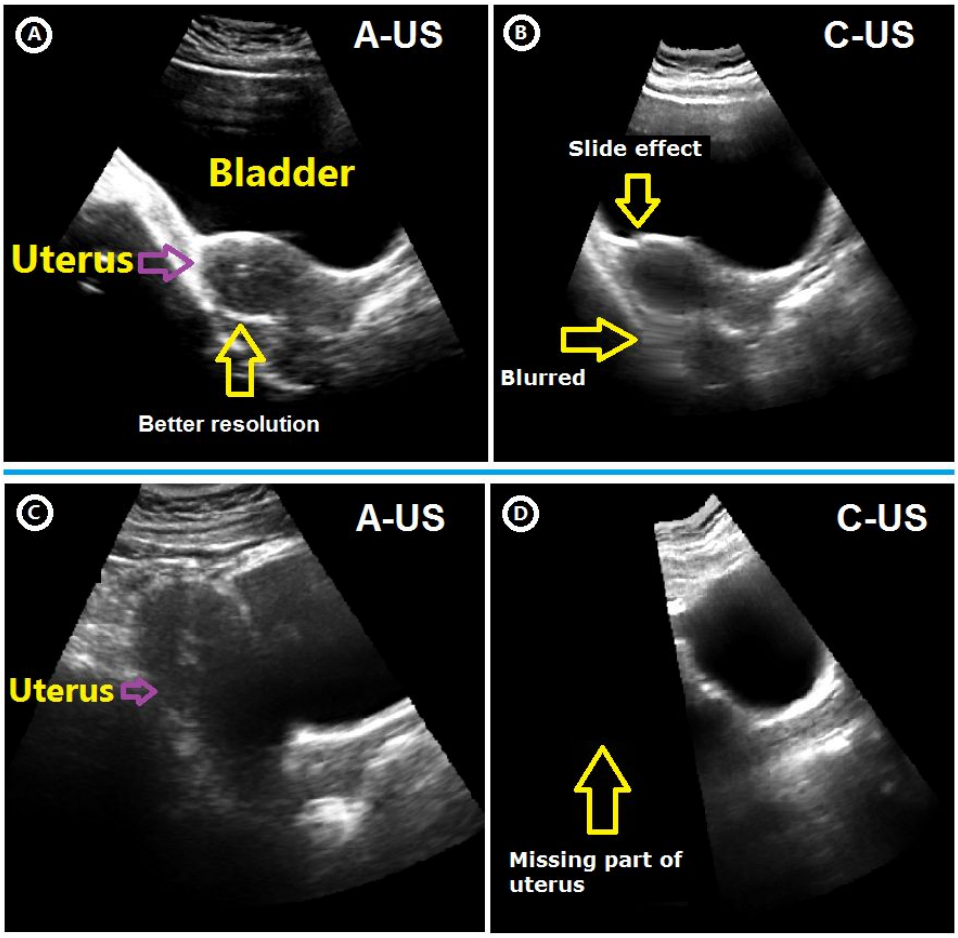

Figure 1. Ultrasound (US) images using C-US and A-US probes. (A) Volunteer 1 ultrasound image of bladder and uterus using the A-US probe. **(B)** The same volunteer but using C-US probe, where image distortion and lower image quality can be observed. **(C)** Volunteer 2 using the A-US probe, where the whole uterus is captured. **(D)** The same volunteer but using the C-US probe, where only half of the uterus is imaged.

Figure 2

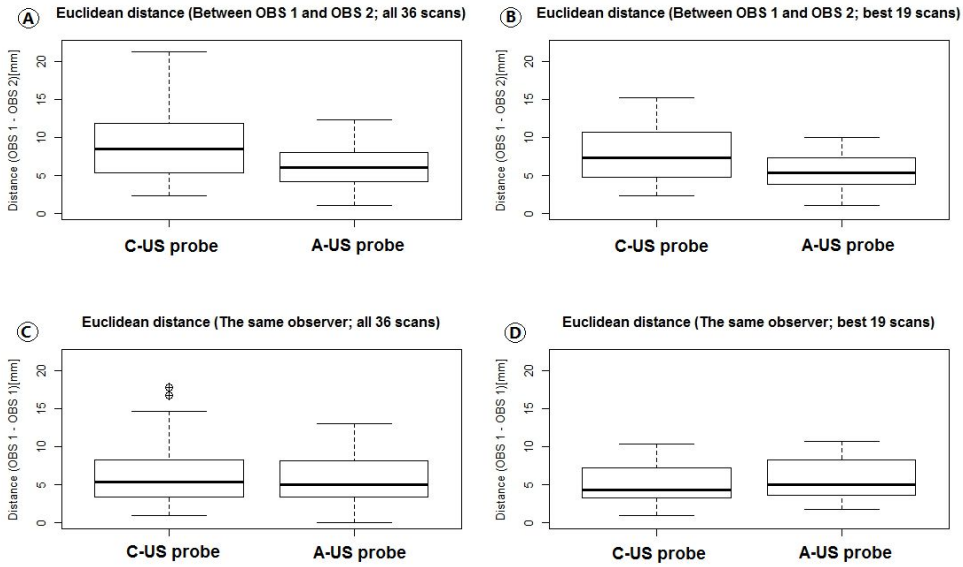

Figure 2. Median (horizontal line), 25th and 75th percentiles (box), and range (whiskers) of Euclidean distances between uterine Centre of Mass (COM) delineated by OBS 1 and OBS 2, and the same observer twice (OBS 1). (A, B) Distance differences (OBS 1 minus OBS 2) for the C-US and A-US probes using all 36 scans and best 19 scans, respectively. (C, D) Distance differences (two delineations by the same observer (OBS 1)) for the C-US and A-US probes using all 36 scans and best 19 scans, respectively.

Figure 3

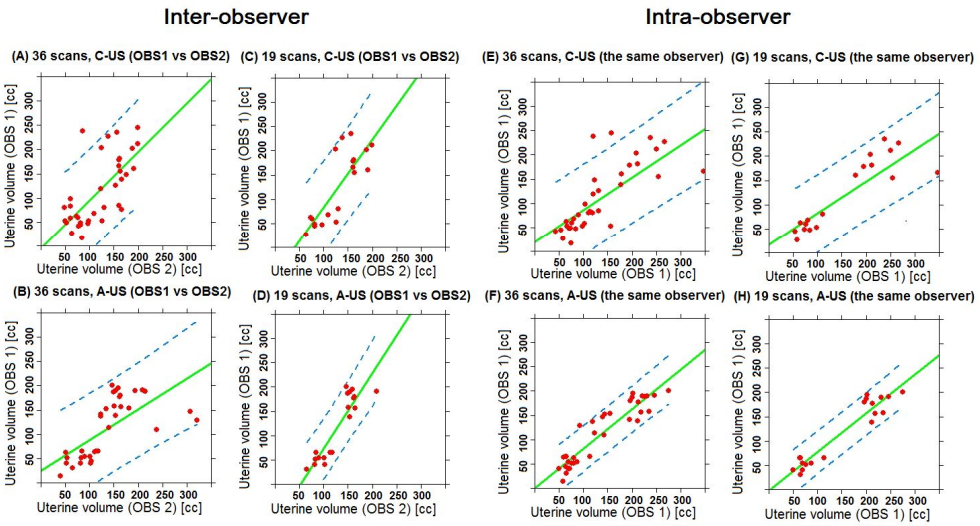

Figure 3. Comparing uterine volume delineated by OBS 1 and OBS 2 (A to D) and two independent delineations by OBS 1 (E to H) using C-US and A-US probes. Left graphs, all 36 scans; right graphs, best 19 scans. Regression (solid lines) and predicted interval (dashed lines) for 95% confidence interval (CI) are indicated.

Figure 4

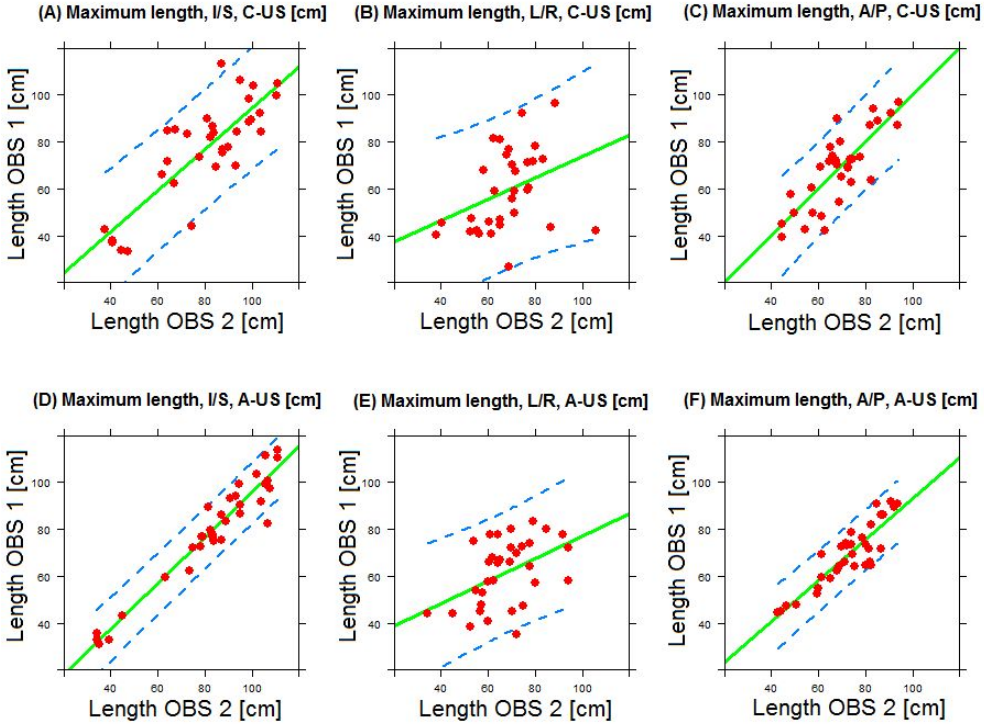

Figure 4. Comparison of the maximum uterine length by OBS 1 and OBS 2 on C-US and A-US scans in Inferior-Superior (I/S); Left-Right (L/R); Anterior-Posterior (A/P)-directions. Regression line fit (solid line) and predicted interval (dashed lines) for 95% confidence interval (CI) are indicated.

Supplemental figure 1

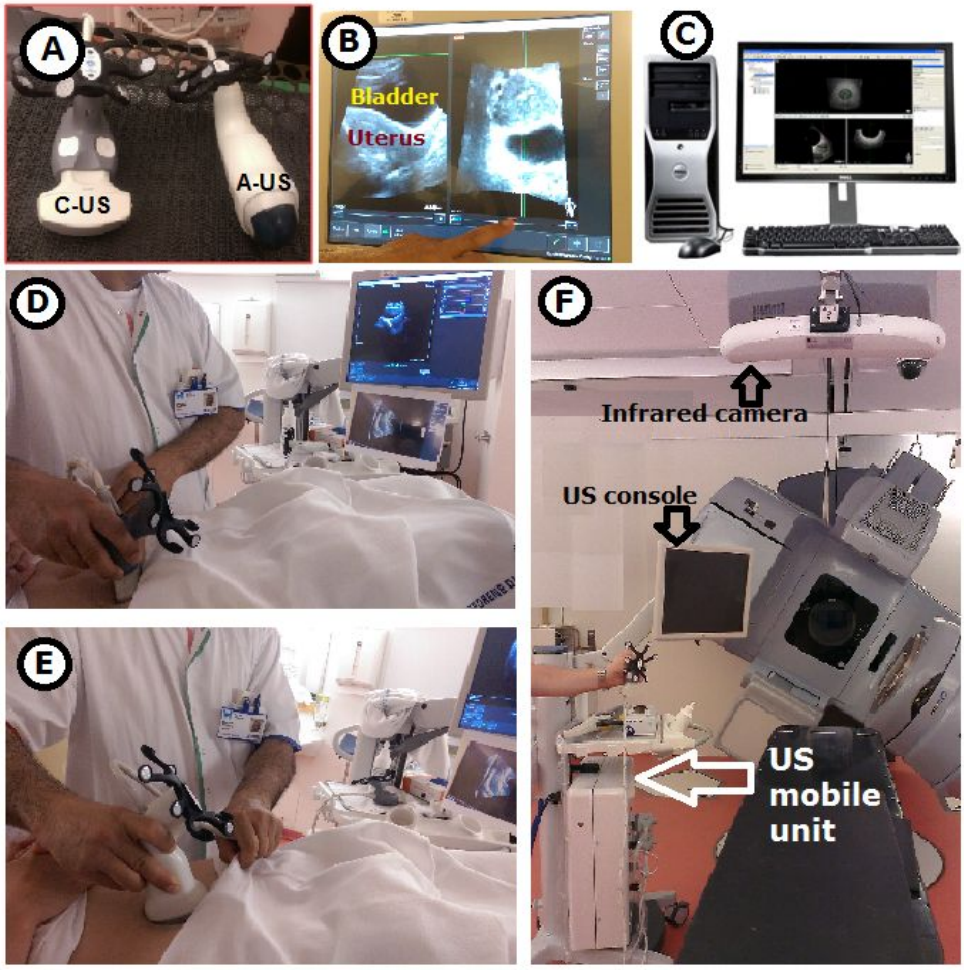

Supplemental Figure 1. Clarity ultrasound (US) system. (A) C-US and A-US probes. **(B)** The ultrasound console. **(C)** The Clarity workstation. **(D)** and **(E)** Volunteer transabdominal **US** scans by means of C-US and A-US probes, respectively. **(F)** The Clarity mobile unit and ceiling-mounted IR camera in the treatment room.

PAPER F

Determining intrafractional prostate motion using four dimensional ultrasound system

Authors: Mariwan Baker, and Calus F. Behrens.

Submitted to: BMC Cancer, September 2015

Abstract

Purpose/Objective: In prostate radiotherapy, it is essential that the prostate position is within the planned volume during the treatment delivery. The aim of this study is to investigate whether intrafractional motion of the prostate is of clinical consequence, using a novel 4D autoscan ultrasound probe.
Methods and Materials: Ten prostate patients were ultrasound (US) scanned at the time of CT imaging and once a week during their course of radiotherapy treatment in an ethics-approved study, using the transperineal Clarity autoscan system (Clarity, Elekta Inc., Stockholm, Sweden). At each US scanning session (fraction) the prostate was monitored for 2 to 2.5 minutes, a typical beam-on time to deliver a RapidArc radiotherapy fraction. The patients were instructed to remain motionless in supine position throughout the US scans. They were also requested to comply with a bladder-filling protocol. In total, 51 monitoring curves were acquired. Data of the prostate motion in three orthogonal directions were analyzed. Finally, the BMI value was calculated to investigate correlation between BMI and the extent of prostate displacement.
Results: The patients were cooperative, despite extra time for applying the TPUS scan. The mean ($\pm$1SD) of the maximal intrafractional displacements were [mm]; I(+)/S: (0.2 $\pm$ 0.9); L(+)/R: (-0.2 $\pm$ 0.8); and A(+)/P: (- 0.2 $\pm$ 1.1), respectively. The largest displacement was 2.8 mm in the posterior direction. The percentage of fractions with displacements larger than 2.0 mm was 4 %, 2 %, and 10 % in the IS, LR, and AP directions, respectively. The mean of the maximal intrafractional Euclidean distance (3D vector) was 0.9 $\pm$ 0.6 mm. For 12 % of the fractions the maximal 3D vector displacements were larger than 2.0 mm. At only two fractions (4 %) displacements larger than 3.0 mm were observed. There was no correlation

between BMI and the extent of the prostate displacement.
Conclusions: The prostate intrafractional displacement is of no clinically consequence for treatment times in the order of 2 to 2.5 minutes, which is typical for a RapidArc radiotherapy fraction. However, prostate motion should be considered for longer treatment times e.g. if applying conventional or IMRT radiotherapy.

Determining intrafractional prostate motion using four dimensional ultrasound system

Mariwan Baker[1,2,3], and Claus F. Behrens[1]

1 Department of Oncology, Radiotherapy Research Unit, Herlev Hospital, University of Copenhagen, Herlev, Denmark
2 Center for Fast Ultrasound Imaging, Dept. of Elec. Eng., Technical University of Denmark, DK-2800 Lyngby, Denmark
3 Center for Nuclear Technologies, Technical University of Denmark, DTU Risø Campus, Roskilde, Denmark

ABSTRACT

Purpose/Objective: In prostate radiotherapy, it is essential that the prostate position is within the planned volume during the treatment delivery. The aim of this study is to investigate whether intrafractional motion of the prostate is of clinical consequence, using a novel 4D autoscan ultrasound probe.
Methods and Materials: Ten prostate patients were ultrasound (US) scanned at the time of CT imaging and once a week during their course of radiotherapy treatment in an ethics-approved study, using the transperineal Clarity autoscan system (Clarity®, Elekta Inc., Stockholm, Sweden). At each US scanning session (fraction) the prostate was monitored for 2 to 2.5 minutes, a typical beam-on time to deliver a RapidArc® radiotherapy fraction. The patients were instructed to remain motionless in supine position throughout the US scans. They were also requested to comply with a bladder-filling protocol. In total, 51 monitoring curves were acquired. Data of the prostate motion in three orthogonal directions were analyzed. Finally, the BMI value was calculated to investigate correlation between BMI and the extent of prostate displacement.
Results: The patients were cooperative, despite extra time for applying the TPUS scan. The mean (±1SD) of the maximal intrafractional displacements were [mm]; I(+)/S: (0.2 ± 0.9); L(+)/R: (-0.2 ± 0.8); and A(+)/P: (-0.2 ± 1.1), respectively. The largest displacement was 2.8 mm in the posterior direction. The percentage of fractions with displacements larger than 2.0 mm was 4 %, 2 %, and 10 % in the IS, LR, and AP directions, respectively. The mean of the maximal intrafractional Euclidean distance (3D vector) was 0.9 ± 0.6 mm. For 12 % of the fractions the maximal 3D vector displacements were larger than 2.0 mm. At only two fractions (4%) displacements larger than 3.0 mm were observed. There was no correlation between BMI and the extent of the prostate displacement.
Conclusions: The prostate intrafractional displacement is of no clinically consequence for treatment times in the order of 2 – 2.5 minutes, which is typical for a RapidArc radiotherapy fraction. However, prostate motion should be considered for longer treatment times e.g. if applying conventional or IMRT radiotherapy.

Introduction

In external beam radiotherapy of the prostate, it is essential that the prescribed dose is precisely delivered to the prostate, while reducing toxicity to rectum and bladder. This can be achieved by daily accurate positional verification of the prostate using image-guided radiation therapy (IGRT) (1,2). Since variation in prostate position during treatment delivery (intrafractional prostate motion) might occur, the target may be underdosed due to a possible prostate shift (3,4). Bladder filling variations, rectal volume changes, and respiratory motion are some of the factors that might lead to intrafractional prostate motion (5–7).

To determine the intrafractional prostate motion, various imaging techniques have been investigated in different studies, such as X-ray imaging, kilovoltage (kV) 3D CBCT and megavoltage (MV) imaging, Cine-MRI, in-room CT, implanted markers and transponders, and ultrasound (8–11). Most of the studies are based on acquiring pre- and post-treatment images (12,13).

Various techniques are developed to enable real-time online prostate localization and monitoring, such as: tracking implanted electromagnetic transponders (Calypso Medical Technologies, Seattle, WA), and tracking fiducial markers (FMs) or implanted radioactive seeds (in Brachytherapy) using real-time X-ray imaging. Recently, transperineal ultrasound (TPUS) autoscan (Clarity®, Elekta Inc., Stockholm, Sweden), a non-ionizing, non-invasive imaging modality, has been developed to allow real-time prostate tracking (14). Various studies have investigated the Calypso system to determine intrafractional prostate motion (15–19), however, to our knowledge, there is only one study (Ballhausen et al.) using the Clarity TPUS system (20). In the study by Ballhausen et al. data from 6 prostate patients are investigated (20). Ballhausen et al. concludes that "intrafraction motion of the prostate is a random walk" and the prostate moves away from the isocenter during treatment delivery. In the present study, the TPUS system was utilized to determine the intrafractional motion of the prostate.

Using advanced radiotherapy techniques, such as volumetric modulated arc therapy (VMAT) or RapidArc® Radiotherapy Technology, the treatment delivery time can be significantly reduced, thus minimizing intrafractional prostate motion (21,22). In our institution, RapidArc radiotherapy is a standard technique for treating prostate cancer patients, and a typical beam-on time for a treatment fraction is approximately 2.5 minutes.

The aim of this study is to investigate whether the intrafractional prostate motion, during a time interval corresponding to the beam-on time for RapidArc, is within 2.0 mm. 2 mm is a tolerance value which is perceived to be clinically irrelevant according to the British Ionization Radiation Medical Exposure Regulations 2000 (IRMER 2000).

Materials and Methods

Patients

Ten prostate cancer patients, with an average age of 68 years (range 58-76 years), were US scanned in the CT room and once a week in the treatment room utilizing the Clarity 4D TPUS monitoring system. All post prostatectomy patients were excluded. The patients received a cumulative dose of 76 Gy in 38 fractions, 2.0 Gy per fraction, 5 fractions per week. The TPUS scans were performed by six radiation therapy technologists (RTTs). The study was approved by the Danish national ethical committee, and voluntary informed consent was obtained for each participant according to the **World Medical Association Declaration of Helsinki (1975/2000)**. The patients were placed in a supine position and instructed to remain motionless throughout the subsequent scans. To ensure better image quality, the patients were requested to comply with a moderate bladder-filling protocol.

Clarity ultrasound system

The Clarity system consists of two mobile units (one in the CT room and the second in the treatment room), which are connected through a workstation/server. The workstation was used for target delineation and retrieving the prostate monitoring curves. Details of US 3D image reconstructions and the precision of the system are explained thoroughly in a previous study (23). In short, a ceiling-mounted infrared (IR)

camera recognizes the US probe by detecting the IR-reflectors affixed to them. This is essential for determining the geographical position of the reconstructed anatomical structures.

To enable superimposition of the reconstructed US images from the 4D autoscan probe on the CT images, the system was calibrated to the same coordinate system as the CT simulation and treatment rooms. The calibration procedure was accomplished by means of a dedicated alignment phantom provided by the vendor.

CT room

All patients underwent a treatment planning CT scan followed by an MRI scan. After the CT-scan the 3D-TPUS scan was acquired. The patient was instructed to remain still during image acquisition and US monitoring. Afterwards, the US-CT fusion was performed, on which the prostate volume was delineated and used as a reference for weekly US imaging in the treatment room.

Autoscan probe

The autoscan-US probe consists of a one dimensional (1D) transducer array of 128 elements, using a central frequency of 5.0 MHz. The probe is provided with IR reflectors fixed in a way that can be detected by the ceiling mounted IR-camera. Initially, the probe is affixed to a TPUS kit, placed over the coach under the patients' knees, and pushed gently to the patient for scanning. The motorized head is capable of real-time online scanning of the prostate.

Prostate monitoring in the treatment room

The patient was prepared for daily treatment by aligning him to the lasers guided by reference marks (tattoos) on the skin, i.e. to reproduce the patient's setup position from the CT-simulation room. Prior to treatment, the inter-fraction patient positioning was corrected for by daily kV images by utilizing three implanted FMs. Once a week and immediately after treatment delivery the TPUS monitoring system was set up for real-time tracking of the prostate. The time dependent prostate displacements (prostate intrafractional motion) were recorded in 2 to 2.5 minutes. The prostate displacements in the three orthogonal directions were recorded for retrospective analysis.

Statistical analysis

The prostate data, showing real-time prostate COM position in the Inferior-Superior (I/S), Left-Right (L/R) and Anterior-Posterior (A/P) directions, were evaluated using the Clarity workstation by one observer (MB). For some fractions, irregular fluctuating data at the beginning of the monitoring curve were discarded. The maximum prostate displacement in each direction was recorded for each fraction. Furthermore, the Euclidean distance (3D vector) was computed and the maximal 3D vector was recorded for each fraction. Finally, the mean (± 1 standard deviation (SD)) of the maximal displacements in each direction and for the 3D vector were calculated. The BMI value for each patient was calculated to investigate correlation between magnitudes of the displacement against the BMI. For the data and statistical analysis the statistical program R (version 2.15.3) was used.

Results

All the patients enrolled in this study were cooperative, despite the extra time of about 10 minutes for each fraction needed for the autoscan setup and prostate monitoring. None of the patients expressed any discomfort during the autoscan setup, nor from the TPUS real-time scanning.

Data analysis of the 51 TPUS scans resulted in mean values (±1SD) of the maximal intrafractional displacements of the prostate [mm]; I(+)/S: (0.2 ± 0.9); L(+)/R: (-0.2 ± 0.8); and A(+)/P: (-0.2 ± 1.1). The largest displacement was 2.8 mm in the posterior direction. The percentage of fractions larger than 2.0 mm was 4 %, 2 %, and 10 % in the IS, LR, and AP directions, respectively. The mean Euclidean distance of the 51 scans was 0.9 ± 0.6 mm. The percentage of fractions with 3D vector displacement larger than 2.0 mm was 12 %, and only 2 scans (4 %) showed displacements larger than 3.0 mm. No correlation was found between BMI-value and the magnitude of the prostate displacement.

The monitoring curves of the prostate show variations in prostate displacement between different fractions (figure 1). A common zero point, start point for the curves, was established by choosing an

arbitrary position-value for each scan/curve, a position immediately after the prostate tracking initiated, and then subtracting that value from the rest. For some fractions, the tendency of larger intrafractional displacement for prolonged observation times can be observed. The figure also indicates that the extent of the prostate intrafractional displacement has its largest dispersal in the A/P direction, and least displacements in the L/R direction.

Figure 2 A-C presents boxplots of the maximal displacements at each fraction for each of the ten patients in I/S, L/R, and A/P directions, respectively. The horizontal band inside the box indicates the second quartile (median), the lower and the upper edges of the box indicate the first (25^{th}) and third (75^{th}) quartiles. Furthermore, the lower and the upper extremes of the whiskers display the minimum and maximum values in the absence of single data point outliers. The individual boxplot of maximal prostate displacements is based on analysis of 4-6 TPUS scans per patient. As can be observed, there are some variations in prostate displacements between the patients and in the different directions. The overall maximal prostate displacement in all three directions and the Euclidean 3D vector were shown to be less than 2.0 mm for most of the fractions (figure 2 D)

Discussion

Intrafractional prostate motion has been investigated previously using pre- and post-treatment imaging. One weakness in applying this method is inter-observer matching uncertainty (24). Despite matching variability, using portal imaging of seeds, there is an additional error associated with the thickness of the CT-slices that may introduce further uncertainty into the determination of the displacement. Another drawback is that the prostate can be displaced and then revert to its initial position, as can be observed in figure 1, which cannot be detected by only a single snapshot pre- and post-treatment image (25). Therefore real-time tracking is a proper monitoring method to accurately detect intrafractional prostate motion. Table 1 tabulates the results of the present study and previously reported data.

In this study the 4D TPUS monitoring system was shown to be able to track the prostate. The operators, with experience from frequently used transabdominal scanning, reported that using the TPUS system, it was easier to acquire images and identify soft tissue structures compared to transabdominal scanning. In a previous phantom study, Abramowitz et al. found good agreement between the TPUS autoscan and Calypso system (Varian Medical Systems, Palo Alto, CA) in tracking the embedded prostate-like sphere (26). The Calypso system has been investigated in different studies, which have confirmed that it is an accurate monitoring method for tracking the prostate gland.

In the current study, prostate monitoring was limited to approximately 2.5 minutes, a typical beam-on time to deliver a RapidArc fraction. We observed that the prostate is not stationary during the tracking time, and displacements tend to increases with the elapsed monitoring time, which is in line with the findings of other published papers (20). Ballhausen et al. found that the intrafractional motion of the prostate tends to “a linear increase of the variance” with the duration of the fraction. Furthermore, we found that the displacement varies for different fractions and also for different patients.

In our study, we noticed that, for most of the fractions, the intrafractional prostate motion was mostly smaller than 2 mm, for a period of 2 to 2.5 minutes. Comparably, Choi et al. (27), using transrectal ultrasound scans to track three implanted fiducial markers (12 patients and 336 fractions), observed that only 11% of the 3D vector displacements were larger than 2 mm during 4-5 minutes of monitoring. Similarly, Li et al. (4), utilizing a Calypso tracking system (35 patients and 1267 fractions), reported that the intrafractional motion of the prostate is mostly less than 2 mm, especially for the first three minutes of tracking. They concluded that a CTV-PTV margin of 2 mm is adequate to ensure covering the target with the planned prescribed dose, despite larger intrafractional uncertainty for some of the patients. Furthermore, Vargas et al. (28), in an Cine-MRI study, calculated the CTV-PTV margin to be 2.1 mm, comparable to Li et al.’s, which would account for the intrafractional motion. They showed also that the prostate motion is smaller in supine than prone patient positioning. On the other hand, Smeenk et al. (29), again using Calypso system (15 patients and 576 fractions), discovered that prostate motion in 3D vector was larger than 3 mm in only 1.4% of the fractions during the first 2.5 minutes, but increased to 18% for a monitoring duration of 10 minutes. Comparably, Tong et al. (8), also using Calypso tracking system (236 patients and 8660 fractions), showed that up to 20% of the prostate shift can be larger than 3 mm when tracking time is 12 minutes. But they ascertained that the prostate motion, for the first three minutes, is very small (< 2 mm) for most patients.

Similarly, Shelton et al. (30) investigated the intrafraction prostate motion, once again using Calypso system (37 patients and 1332 fractions), and found that the overall mean value of the 3D vector displacement is less than 3 mm for the first 3 minutes, but increased with duration time to up to 6.5 mm in the fourteenth minute. Likewise, Kupelian et al. (2), once more using Calypso system (17 patients and 550 fractions) detected that during 10 minutes monitoring in 14% of the fractions the shift was larger than 3 mm. Furthermore, Ng et al. (31), in a study of real-time FM tracking, observed that in 62% of the fractions (10 patients, 268 fractions) the 3D vector displacement of the prostate, during 3-4 minutes tracking was smaller than 1 mm, and corresponded values were 95%, 82%, and 80% in the LR, IS, and AP directions, respectively. They discovered that only 6% of the shifts were larger than 3 mm. Moreover, Langen et al. (18), as well using Calypso system (17 patients and 550 fractions), spotted that only 3% of the shift is larger than 3 mm while tracking the prostate for about 2 minutes. In addition, Lometti et al. (32), using MV fluoroscopy; real-time FM tracking (11 patients and 133 fractions), confirmed that in only 4% of the fractions the displacement is larger than 2 mm while tracking for only one minute. Last, Mayyas et al. (9), in a comparison study of four different systems (27 patients and 1100 fractions), found that the percentage of intrafractional shifts within ±1.5 mm was 76%, 94%, and 82% in the I/S, L/R, and A/P directions. In summary, the published evidence in combination with this study justifies the assertion that the intrafractional motion of the prostate is insignificant during the first 2.5 minutes, thus not of clinical consequence while employing advanced VMAT/ RapidArc.

As all other studies, there are limiting factors in the current study; Firstly, the study does not reveal the magnitude of the intrafractional prostate rotation or form deformation. Second, the number of patients and fractions are limited.

Conclusion

Intrafractional prostate displacement varies between fractions and for different patients. The displacement is insignificant for the first 2-2.5 minutes of the monitoring time, but increases with elapsed time. Consequently, prostate shifts during conventional and IMRT treatment delivery should be taken into consideration, but are clinically inconsequential while employing advanced VMAT/ RapidArc techniques.

Competing interests

The authors declare that they have no competing interests.

Authors' contributions

MB carried out the prostate delineation, participated in designing the study, performed statistical analysis, carried out the sequence alignment and drafted the manuscript. CFB participated in the design of the study, revising the manuscript, and read and approved the final manuscript.

Abbreviations

3D: Three dimensional
4D: Four dimensional
US: Ultrasound
CT: Computed tomography
SD: Standard deviations
IGRT: Image-guided radiation therapy
IMRT: Intensity modulated radiation therapy
kV: Kilo-voltage
MV: Mega-voltage
FM: Fiducial marker
TPUS: Transperineal ultrasound
VMAT: Volumetric modulated arc therapy
RTT: Radiation therapy technologist
MRI: Magnetic resonance imaging
MHz: Mega hertz

I/S: Inferior-superior
A/P: Anterior-posterior
L/R: Left-right
CTV: Clinical target volume
PTV: Planning target volume

Acknowledgements

We would like to thank all our colleagues who helped to conduct this study; Gullander L. (RTT), Pedersen S. K (RTT), Zarp T (RTT), Jacobsson S (RTT), Pazhang S (radiographer) and Lynnerup V. K (radiographer). We would also like to thank Elekta Ltd for their support.

References

1. Scarbrough TJ, Golden NM, Ting JY, Fuller CD, Wong A, Kupelian P a, et al. Comparison of ultrasound and implanted seed marker prostate localization methods: Implications for image-guided radiotherapy. Int J Radiat Oncol Biol Phys. 2006;65(2):378–387.

2. Kupelian P a., Langen KM, Willoughby TR, Zeidan O a., Meeks SL. Image-Guided Radiotherapy for Localized Prostate Cancer: Treating a Moving Target. Semin Radiat Oncol. 2008;18(1):58–66.

3. Kitamura K. Three-dimensional intrafractional movement of prostate measured during real-time tumor-tracking radiotherapy in supine and prone treatment positions. Int J Radiat Oncol Biol Phys. 2002;53(5):1117–1123.

4. Li HS, Chetty IJ, Enke CA, Foster RD, Willoughby TR, Kupellian PA, et al. Dosimetric consequences of intrafraction prostate motion. Int J Radiat Oncol Biol Phys. 2008 ;71(3):801–812.

5. Dawson LA. A comparison of ventilatory prostate movement in four treatment positions. Int J Radiat Oncol Biol Phys. 2000;48(2):319-323.

6. Padhani A. Evaluating the effect of rectal distension and rectal movement on prostate gland position using cine MRI. Int J Radiat Oncol Biol Phys. 1999;44(3):525–533.

7. Van Herk M. Quantification of organ motion during conformal radiotherapy of the prostate by three dimensional image registration. Int J Radiat Oncol Biol Phys. 1995;33(5):1311–1320.

8. Tong X, Chen X, Li J, Xu Q, Lin M, Chen L, et al. Intrafractional prostate motion during external beam radiotherapy monitored by a real-time target localization system. Journal of applied clinical medical physics. 2015;16(2):51–61.

9. Mayyas E, Chetty IJ, Chetvertkov M, Wen N, Neicu T, Nurushev T, et al. Evaluation of multiple image-based modalities for image-guided radiation therapy (IGRT) of prostate carcinoma: a prospective study. Med Phys. 2013;40(4):041707.

10. Chan P, Dinniwell R, Haider M a, Cho Y-B, Jaffray D, Lockwood G, et al. Inter- and intrafractional tumor and organ movement in patients with cervical cancer undergoing radiotherapy: a cinematic-MRI point-of-interest study. Int J Radiat Oncol Biol Phys. 2008;70(5):1507–15.

11. Ghilezan MJ, Jaffray D a, Siewerdsen JH, Van Herk M, Shetty A, Sharpe MB, et al. Prostate gland motion assessed with cine-magnetic resonance imaging (cine-MRI). Int J Radiat Oncol Biol Phys. 2005;62(2):406–17.

12. Kron T, Thomas J, Fox C, Thompson A, Owen R, Herschtal A, et al. Intrafraction prostate displacement in radiotherapy estimated from pre- and post-treatment imaging of patients with implanted fiducial markers. Radiother Oncol. 2010 May;95(2):191–197.

13. Adamson J, Wu Q. Inferences about prostate intrafraction motion from pre- and posttreatment volumetric imaging. Int J Radiat Oncol Biol Phys. 2009;75(1):260–7.

14. Lachaine M, Falco T. Intrafractional prostate motion management with the Clarity Autoscan system. Med Phys Int. 2013;1(1):72–80.

15. Bittner N, Butler WM, Reed JL, Murray BC, Kurko BS, Wallner KE, et al. Electromagnetic tracking of intrafraction prostate displacement in patients externally immobilized in the prone position. Int J Radiat Oncol Biol Phys. 2010;77(2):490–495.

16. Wilbert J, Baier K, Hermann C, Flentje M, Guckenberger M. Accuracy of real-time couch tracking during 3-dimensional conformal radiation therapy, intensity modulated radiation therapy, and volumetric modulated arc therapy for prostate cancer. Int J Radiat Oncol Biol Phys. 2013;85(1):237–242.

17. Curtis W, Khan M, Magnelli A, Stephans K, Tendulkar R, Xia P. Relationship of imaging frequency and planning margin to account for intrafraction prostate motion: analysis based on real-time monitoring data. Int J Radiat Oncol Biol Phys. 2013;85(3):700–706.

18. Langen KM, Willoughby TR, Meeks SL, Santhanam A, Cunningham A, Levine L, et al. Observations on real-time prostate gland motion using electromagnetic tracking. Int J Radiat Oncol Biol Phys. 2008;71(4):1084–1090.

19. Li JS. Observations of prostate intrafractional motion during external beam radiation therapy. Ifmbe Proc. 2009;25(1):499–502.

20. Ballhausen H, Li M, Hegemann N-S, Ganswindt U, Belka C. Intrafraction motion of the prostate is a random walk. Phys Med Biol. 2015;60(2):549–563.

21. Li JS, Lin M-H, Buyyounouski MK, Horwitz EM, Ma C-M. Reduction of prostate intrafractional motion from shortening the treatment time. Phys Med Biol. 2013;58(14):4921–4932.

22. Mutanga TF, de Boer HCJ, Rajan V, Dirkx MLP, Incrocci L, Heijmen BJM. Day-to-day reproducibility of prostate intrafraction motion assessed by multiple kV and MV imaging of implanted markers during treatment. Int J Radiat Oncol Biol Phys. 2012;83(1):400–407.

23. Van der Meer S, Bloemen-van Gurp E, Hermans J, Voncken R, Heuvelmans D, Gubbels C, et al. Critical assessment of intramodality 3D ultrasound imaging for prostate IGRT compared to fiducial markers. Med Phys. 2013;40(2013):071707–1 – 071707–11.

24. Deegan T, Owen R, Holt T, Roberts L, Biggs J, McCarthy A, et al. Interobserver variability of radiation therapists aligning to fiducial markers for prostate radiation therapy. J Med Imaging Radiat Oncol. 2013;57(4):519–523.

25. Kotte ANTJ. Intrafraction motion of the prostate during external-beam radiation therapy: analysis of 427 patients with implanted fiducial markers. Int J Radiat Oncol Biol Phys. 2007;69(2): 419-425.

26. Abramowitz MC, Bossart E, Flook R, Wu X, Brooks R, Lachaine M, et al. Noninvasive Real-time Prostate Tracking Using a Transperineal Ultrasound Approach. Int J Radiat Oncol. 2012;84(3):S133.

27. Choi Y, Kwak D-W, Lee H-S, Hur W-J, Cho W-Y, Sung GT, et al. Effect of rectal enema on intrafraction prostate movement during image-guided radiotherapy. J Med Imaging Radiat Oncol. 2015;59(2):236–242.

28. Vargas C, Saito AI, Hsi WC, Indelicato D, Falchook A, Zengm Q, et al. Cine-magnetic resonance imaging assessment of intrafraction motion for prostate cancer patients supine or prone with and without a rectal balloon. Am J Clin Oncol. 2010;33(1):11–16.

29. Smeenk RJ, Louwe RJW, Langen KM, Shah AP, Kupelian PA, van Lin ENJT, et al. An endorectal balloon reduces intrafraction prostate motion during radiotherapy. Int J Radiat Oncol Biol Phys. 2012;83(2):661–669.

30. Shelton J, Rossi PJ, Chen H, Liu Y, Master V a., Jani AB. Observations on prostate intrafraction motion and the effect of reduced treatment time using volumetric modulated arc therapy. Pract Radiat Oncol. American Society for Radiation Oncology; 2011;1(4):243–250.

31. Ng JA, Booth JT, Poulsen PR, Fledelius W, Worm ES, Eade T, et al. Kilovoltage intrafraction monitoring for prostate intensity modulated arc therapy: first clinical results. Int J Radiat Oncol Biol Phys. 2012;84(5):e655–661.

32. Lometti M. Intrafraction prostate motion using MV fluoroscopy. Int J Radiat Oncol Biol Phys. 2005;63(2).

33. Wang KK-H, Vapiwala N, Deville C, Plastaras JP, Scheuermann R, Lin H, et al. A study to quantify the effectiveness of daily endorectal balloon for prostate intrafraction motion management. Int J Radiat Oncol Biol Phys. 2012;83(3):1055–63.

Table 1. Intrafraction prostate motion in three directions and 3D vector; a comparison of the present study with previously published data using different systems.

				Mean of max prostate shifts (±1SD) [mm]				
Investigator, year	**N (fractions)**	**System**	**Time [min]**	**I(+)/S**	**L(+)/R**	**A(+)/P**	**% 3D vector shift**	**3D-vector [mm]**
Lometti et al., 2005[32]	11 (133)	*MV fluoroscopy: real-time FM tracking*	1				> 2 mm 4%	0.7 ± 0.5
Li HS et al., 2008	35 (1267)	*Calypso*	12	0.3 ± 0.7	0.0 ± 0.3	0.4 ± 0.6		
Kupelian et al., 2008[4]	17 (550)	*Calypso*	10				> 3 mm 14%	
Langen et al., 2008[18]	17 (550)	*Calypso*	2				> 3 mm 3%	
Li et al., 2009[19]	20 (157)	*Calypso*	11.4				> 3 mm 19%	
Vargas et al., 2010[28]	7 (68)	*Cine-MRI*	4					0.41 ±1.2
Wang et al., 2011[33]	29 (1061)	*Calypso*	3				> 3 mm 9%	
Smeenk et al, 2011[29]	15 (576)	*Calypso*	2.5				>3 mm 1.4%	
Ng et al., 2012[31]	10 (268)	*Real-time kilovoltage FM tracking*	3-4				>3 mm 5.6%	
Mayyas et al., 2013[9]	8	*Pre- post-treatment kV images*		0.8 ± 2.7	0.2. ± 2.1	-0.3 ± 2.4		
Mayyas et al., 2013[9]	19	*Calypso*		0.0 ± 1.5	0.0 ± 0.6	0.0 ± 1.3		
Tong et al., 2015[8]	236 (8660)	*Calypso*	2				> 2 mm 13%	
Choi et al., 2015[27]	12 (336)	*Transrectal US/3 FMs*	4-5	0.6 ± 0.6	-0.3 ± 0.3	-0.7 ± 0.6	> 2 mm 11%	1.1 ± 0.8
Present study	**10 (51)**	***Clarity real-time TPUS***	**2-2.5**	**0.2 ± 0.9**	**-0.2 ± 0.8**	**-0.2 ± 1.1**	**> 2 mm 12%**	**0.9 ± 0.6**

Intrafractional motion of prostate patients (N) in 3D vector, I/S, inferior-superior, L/R, left-right, and A/P, anterior-posterior directions, using TPUS, transperineal Clarity ultrasound (US) system, Calypso system, implanted fiducial markers (FMs), CINE-MRI, and endorectal balloon.

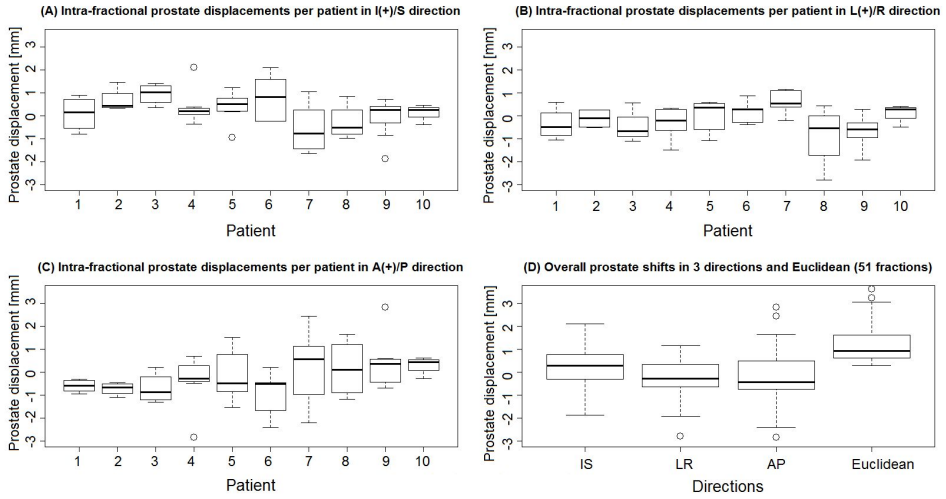

Figure 1. Intrafractional prostate displacement; (A-C) Monitoring graphs show the prostate motion for the total 51 US scans in I/S, L/R, and A/P directions, (D) The 3D vector displacement of the prostate center of mass.

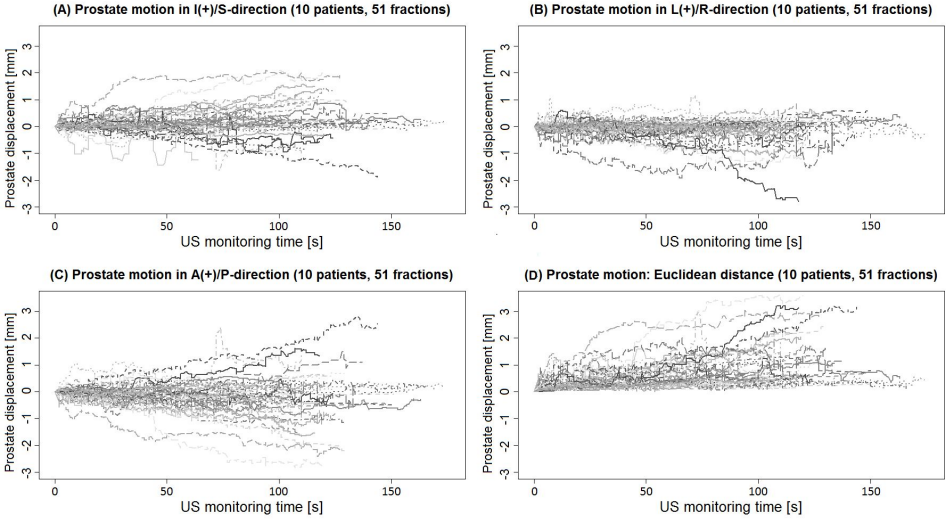

Figure 2. Boxplots of the intrafractional prostate displacements; (A-C) Boxplots of the prostate displacements for ten patients in I/S, L/R, and A/P directions. (D) Boxplot of overall prostate displacements in I/S, L/R, and A/P directions, including Euclidean (3D vector) distance.